Title
Synthesis and Evaluation of Dendritic Polymer Carriers for Chemotherapeutic and Imaging Applications

Author
Floyd, William Clary

Publication Date
2010

Peer reviewed|Thesis/dissertation

Synthesis and Evaluation of Dendritic Polymer Carriers for Chemotherapeutic and Imaging Applications

by

William Clary Floyd, III

A dissertation submitted in partial satisfaction of the

requirements for the degree of

Doctor of Philosophy

in

Chemistry

in the Graduate Division

of the

University of California, Berkeley

Committee in Charge:

Professor Jean M.J. Fréchet, Chair

Professor Dean Toste

Professor Steven Martin

Fall, 2010

Synthesis and Evaluation of Dendritic Polymer Carriers for Chemotherapeutic and Imaging Applications

by

William Clary Floyd, III

Abstract

Synthesis and Evaluation of Dendritic Polymer Carriers for Chemotherapeutic and Imaging Applications

by

William Clary Floyd, III

Doctor of Philosophy in Chemistry

University of California, Berkeley

Professor Jean M.J. Fréchet, Chair

Among the multitude of compounds capable of exerting a potentially therapeutic effect on a diseased biological system, only a very select few happen to possess the stringent pharmacokinetic profile required to be used in practice. In addition to being biologically active, a potential drug candidate must also have good solubility in biological systems, reach its target destination in adequate quantities to bring about the desired effect, and not cause a substantial degree of harm to nontargeted areas of the body through toxicity or side reactions. These requirements also apply to biological agents used in conjunction with treatment, such as molecular diagnostic tools used for disease imaging and marking. Rather than simply discount agents lacking ideal pharmacokinetics, polymeric drug delivery attempts to mask these deficiencies by incorporating these small molecules into their structure, and in doing so create a conjugate structure in which the favorable pharmacokinetic properties of the carrier mask the unfavorable properties of the drug. In this work, the design, synthesis and potential uses and benefits of a specific family of these carriers, pegylated dendrimers, is presented and discussed.
In the first chapter, the general principles of drug and imaging agent delivery via dendrimers and other macromolecules are discussed, as well as the differences found among the various systems commonly employed for this purpose. With a focus on dendrimers, this chapter will go on to address the importance of fidelity to ideal molecular structure, synthetic tailorability, and optimal pharmacokinetic profile in these systems, and how such aspects are installed or maintained with minimal synthetic investment.

In chapter 2, the gradual development of our current dendrimer platform is discussed, as well as several surprising reaction sequences encountered along the way. Starting from promising but synthetically demanding polyester dendrimers, the development of several polyamide structures is discussed, along with their respective advantages and disadvantages, before progressing on to current hybrid structures that offer a highly favorable compromise

between the two systems. Tailorability available within these systems to address several common needs and problems is also discussed.

In chapter 3, an investigation into the feasibility of creating a drug carrier of an elongated shape and its potential benefits in pharmacokinetics is discussed. The platform for such a carrier begins with the living anionic ring opening polymerization of a lysine derived N-carboxyanhydride (NCA) monomer, after which dendronization and elaboration by copper catalyzed "click" chemistry are used to transform this polymer into a biocompatible drug carrier with a predefined aspect ratio. The biodistribution of this elongated carrier and its comparison to other architectures with regards to *in vivo* behavior is also discussed.

In chapter 4, the attachment of an analog of a highly potent potential chemotherapeutic agent, tubulysin, is discussed. This chapter outlines the process for evaluation of potential agents for their use with polymeric drug delivery, and how the native drug can be tailored for the purpose. The synthesis of the new drug analog and its polymer conjugate is then discussed, followed by its preliminary *in vitro* analysis, and finally its *in vivo* performance in tumored mice.

In chapter 5, the delivery of magnetic resonance imaging (MRI) active contrast agents with dendrimers is discussed. This will involve a brief introduction to the field of gadolinium based imaging, what agents are currently in use and how they work, and how these agents can potentially be improved by polymeric delivery systems. The change in performance for several small molecule gadolinium chelators upon binding to an esteramide dendrimer will be presented to support this discussion. Finally, the potential for similar chelates containing different lanthanides to be used in alternate or multimodal imaging polymeric systems will be presented.

In chapter 6, the theme of using polymeric carriers for diagnostics will be continued with discussion of a dendrimer capable of imaging with PET, but the complexity and potential performance of the system will be increased with the addition of a targeting group specific to atherosclerosis markers. The additional synthetic considerations introduced into this system will be discussed, followed by how they may be addressed.

Table of Contents

Acknowledgements

The accomplishment of this work was possible only through the very substantial assistance of many kind people. I'd like to thank first and foremost my parents, Fran and Bill, who at all times made it abundantly clear that their full support was, and is, available towards any pursuit I might choose to overtake. They, along with my sister, Hannah, have also been remarkably patient and tolerant of this long and largely unpunctuated leave far from home, and for this quiet and persistent patience I thank them as well. I would also like to thank Professor Fréchet, who has been a remarkably supportive and insightful advisor during this time, and I have been greatly benefited on more occasions than I could count by his uncanny ability to assess virtually any nature of situation, practical or academic, and immediately give sound and sage advice on the optimal response. I am similarly indebted to Dr. Steve Guillaudeu, my first year mentor, for his advice and counsel during the time I was fortunate enough to share lab space with him. Without his help my first year would have been an extremely difficult introduction to graduate work. I'd like to acknowledge the efforts and effects of Dr. Justin Mynar, who managed to preserve order and cohesion during a time when those of other dispositions would likely have failed. I should go ahead and admit that I owe a big favor to Jeff Young- If he hadn't torn apart my personal essay and practically rewritten it those years ago I never would have made it into Berkeley in the first place. I'd like to thank my suitemates from GSSM- Hank, Cleary and Kantus- whose constant nonsensical and incoherent ramblings and banter throughout hundreds of email correspondences over the past ten years have been a highly valued source of absolutely necessary absurdity. I'd like to thank another good friend from high school, Katie Abole, who was a superb partier in undergrad afterwards, and an excellent roommate here until departing to Germany with the Trauner group. I miss her still. I'd like to thank soon-to-be-Dr Derek van der Poll, who has been an amazing friend here throughout my entire time at Berkeley, from those very first days when we showed up at our first lectures still suffering from the effects of the bars the night before, to this morning, when we showed up at minimeeting, still suffering from the effects of the bars last night. I'd of course also like to thank all of my collaborators and each of the Fréchet group members, who have made this time here pleasant and productive as well. Fortunately for me, this great company of friends and colleagues is also a very large one- much too numerous to be listed in detail here, in fact, but to single out a few I'd like to thank Kyle Broaders, who not only possesses a rare paring of keen scientific intuition and a finely developed sense of humor, but also the kindness to share them both; Heidi Kieler-Ferguson, who has been an excellent neighbor in lab, a great person to speak with, and always made sure the pizza and beer made it to group meetings; Ayano Kohlgruber, who has been an excellent undergraduate researcher, and whose smile and enthusiasm always make the day pass more pleasantly; the rest of my year here in the Fréchet group- Jessica Cohen, Steve Scroggins, and Tom Holcombe, and Seabass, who made this time pass pleasantly as well. Also, Marian Snauko, Dan Poulsen, Eric Bachelder, Megan Fox, Lina Cui, Krystal Chu, Sirisha Grandhe, Tristan Beaudette, Paul Kierstead, Piper Klemm (an excellent collaborator!), Dave Unruh, Sergey Paramonov, and Henry Storms La Pierre (for, among other things, hooking me up with a kickass living arrangement). I'd also like to thank those innumerable friends and acquaintances from other groups, as they have undoubtedly made the time here enjoyable as well. It is true that this work would not have been possible without these individuals' help and support, but much more than that, it would not have been worth it.

"*I never let my schooling interfere with my education.*" -Twain

Chapter 1- Introduction to Polymeric Delivery of Drug and Imaging Agents

Abstract

In order to improve on the efficacy and efficiency of biological agents, polymeric drug delivery may be employed to circumvent many common problems encountered by common therapeutic or imaging moieties. These drawbacks may include low solubility, low blood residence time, low accumulation in targeted areas, inadequate signal or response, and rapid excretion from the body. In this carrier based approach, an agent lacking idealized properties is bound to a large macromolecular carrier exhibiting a more favorable pharmacokinetic profile. Depending on the desired application, the attached agent may be designed for release within a specific environment, or bound in a more permanent way to ensure its eventual excretion commensurate with the carrier molecule. In this chapter, the overall motivations and approaches for this polymer based delivery, and particularly with regard to pegylated dendrimers, are discussed.

Introduction

Drawbacks to Traditional Medicines

For almost as long as medicines have been used for the treatment of ailments, physicians and patients have been burdened with drawbacks common to most medications.[1] As organic compounds, most drugs are sparingly soluble in blood, presenting a daunting obstacle to their being delivered to a patient. Once administered, these drugs are rapidly distributed by the blood throughout the body, reaching diseased and healthy tissues alike. Being small molecules borne in the blood, many of these agents are then cleared rapidly from the body before they can act, wasting a large portion of the dose. Many drugs, particularly many common chemotherapeutic agents (Figure 1), are also highly toxic towards all living tissues and cells, and are effective medicines only by virtue of their being slightly more potent against their intended target. Due to their widespread and predominantly indiscriminate distribution in the body, this leads to extremely dangerous and debilitating side effects at dosages high enough to be of therapeutic use.

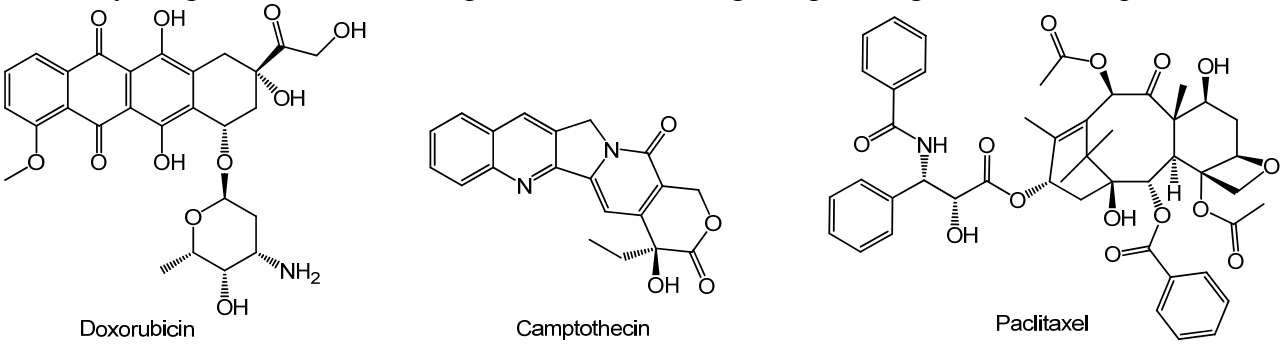

Figure 1. Several common but highly toxic and sparingly soluble chemotherapeutic agents.

The ideal drug would lack these failings in delivery. It would be easily formulated and administered, preferably in a low dose; it would reach the targeted diseased area with adequate degree to induce the desired response, and would have a localized impact.[2] However, the

difficulty of finding a drug of acceptable efficacy against many diseases without regard to these further specifications is already challenging enough.

One common and intuitive method for addressing these concerns is to continue the search for new drugs. This generally involves screening extracts and compounds from various plants, animals, fungi, bacteria, remote sea creatures, and, more currently, vast libraries of randomly generated man-made molecules in search of new compounds exhibiting novel therapeutic properties. This approach is effective in discovering new drugs, but progress is typically slow and the process is highly inefficient.[3] Another common approach is the development of synthetically modified drugs, or drug analogs.[4] This involves the specific synthetic manipulation of a drug to bring about a desired change, such as increased solubility or higher resistance to premature degradation in a biological setting. However, this is commonly accompanied by a significant decrease in drug potency, potential unpredictable changes in drug action or pharmacokinetics. Furthermore, many drugs present a synthetic challenge in their having too many or too few viable synthetic handles with which to craft these improvements. While this immense hunt for the discovery and development of new drugs is underway, many compounds already known to exhibit potential in curing a certain disease are excluded from medical consideration due to their lack of solubility, high toxicity, etc. This delivery problem is not unique to drugs, however, and many imaging and diagnostic agents suffer the same setbacks. Because these agents are generally small molecules designed to accumulate in diseased areas and then elicit a specific response (i.e., an observable signal), their commonly encountered impediments do not significantly diverge from those of drugs, at least with regards to the pharmacokinetic standpoint. For instance, many imaging agents are similarly highly insoluble, toxic, or incapable of accumulating specifically in a region of interest. Because of these similarities, solutions to the setbacks one class of molecule may be easily translated into progress for the other. One attractive route for addressing these concerns is the delivery of the agent as a conjugate to a macromolecule.

Mechanism of Action of Polymeric Conjugates

Simply put, the concept of polymeric drug delivery involves escorting the agent of interest to a desired site of action using a polymeric carrier exhibiting the ideal pharmacokinetic properties sought in a general biological agent. This concept, first put forth by Ringsdorf in the seventies[5], has since advanced to become a clinically realized method for drug improvement.[6]. The carrier used must have high solubility in blood, be nontoxic, exhibit favorable accumulation in areas of interest, evade the immune system, and also carry enough of the active agent to deliver a therapeutic or diagnostic response. To accomplish this, many different carrier systems have been evaluated, including micelles, linear polymers, viral capsids, nanoparticles, polymersomes, antibodies, polyplexes, and others.[7-16] While these systems vary in structure and composition, they share many similarities and pursue the same general purpose. Each carrier is designed to bind a drug or agent of interest, escort it through the body to an intended location, and then release it. Due to their large size, these agents will generally have blood circulation times measured in hours, whereas the agents they deliver are generally excreted with minutes. This additional circulation time enables the conjugate to reach and accumulate in various tissues and organs rather than being eliminated unused. These carriers are also more highly soluble in blood than many common therapeutic and diagnostic agents, allowing formulation and delivery of higher dosages of the drug than otherwise possible. Furthermore, due to a phenomenon known as the Enhanced Permeation and Retention (EPR) Effect[17], (Figure 2), these

macromolecules can potentially accumulate in tumors at substantially higher concentrations than possible with a small molecule.

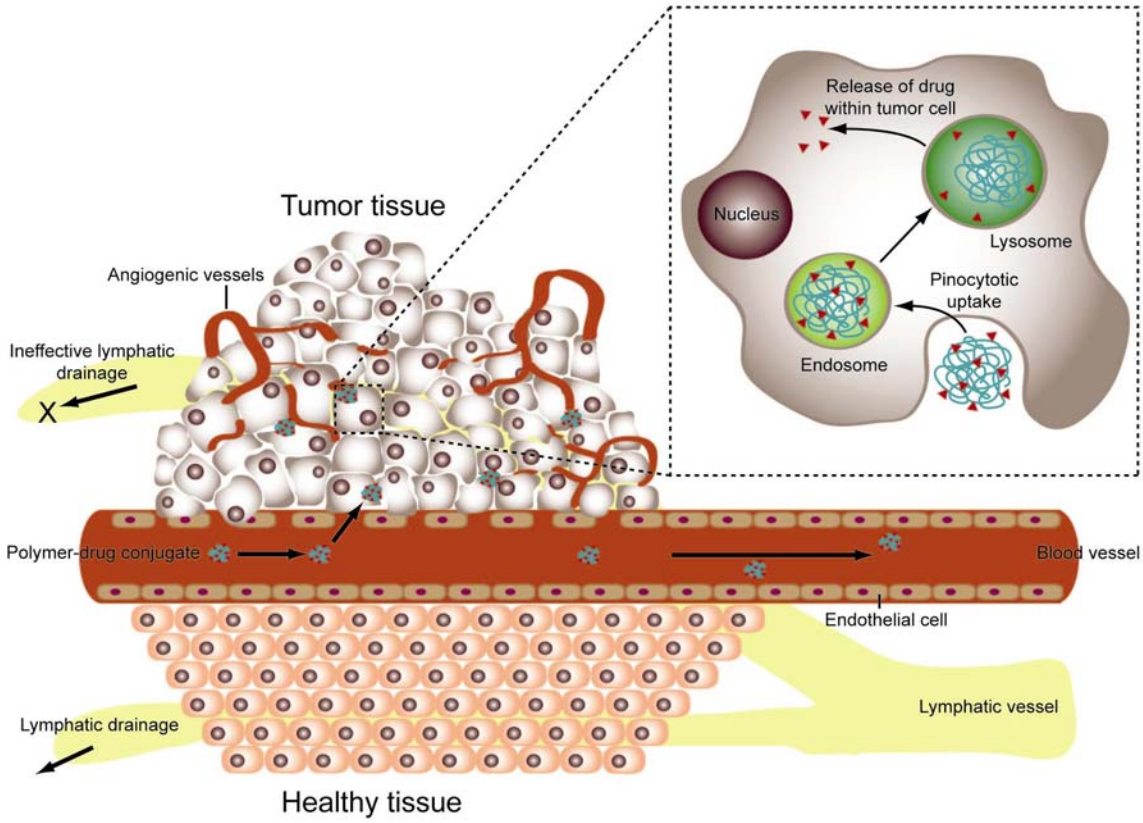

Figure 2. The EPR effect, describing the mechanism of enhanced macromolecule accumulation in tumor tissue. Adapted from reference 15.

This effect comes about by virtue of a combination of the highly permeable vasculature and lack of functional lymphatic drainage commonly found in tumor tissue. Because polymers do not easily cross the endothelial wall of healthy blood vessels, the unusually permeable vasculature of tumor tissue allows the macromolecular conjugate to diffuse from the bloodstream to the extracellular space of tumors at higher rates than elsewhere in the body. To compound this increased permeation into tumor tissue, the decreased drainage of tumor tissue allows the conjugate to reside in tumor tissue longer than elsewhere in the body, where the lymphatic system will typically remove such molecules through a passive cleaning system. Additionally, the high degree of synthetic versatility in many of these systems allows for the introduction of other drugs or agents, reporting molecules or imaging agents, and various targeting groups capable of tuning the biodistribution and eventual localization of the conjugate.

PEGylated Dendrimer Carriers

In this and the following chapters, an emphasis is placed on delivery using polymers functionalized with poly(ethylene glycol), or PEG. These PEGylated dendrimers are highly branched polymers engineered in a specific, stepwise fashion with a high degree of structural control. PEG is well suited as a polymeric carrier, as it shields and protects the agent being carried, imparts high biological solubility, increases blood circulation time, shields the carrier from recognition by the immune system.[18] . Compared to other systems, this platform introduces

an immediate drawback with regards to necessary synthetic investment, as formulations such as micelles or antibody conjugates may require only mixing or a single synthetic step. As compensation for this synthetic investment, however, one obtains a carrier platform of very uniform composition exhibiting potentially highly complex motifs with regard not only to the number and scope of synthetic handles which may be incorporated, but also the specific regions and environments into which they are installed (Figure 3). As shown below, the overall architecture involves a branched core (green and blue) in which the different dendrimer generations may or may not be identical in structure. This core provides the basic framework of the carrier, and contains attachment point for both a molecule of interest such as a drug or imaging agent (red) and the PEG chains (orange).

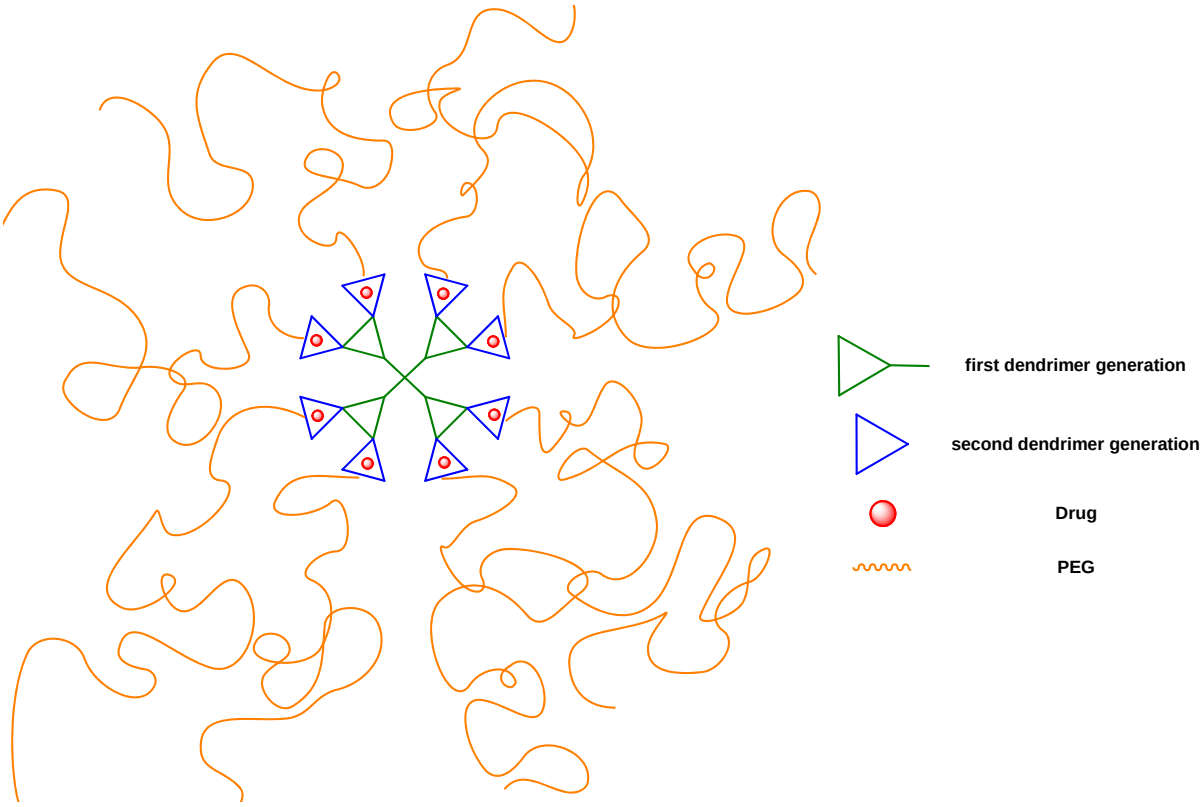

Figure 3. Cartoon of a drug loaded pegylated carrier.

This ability to covalently link a drug or imaging agent in a specific region of the carrier is important, as one of the purposes of the carrier to shield and protect the agent from the surrounding environment. For this reason, it is highly beneficial to attach a fragile or hydrophobic agent near the core of the carrier, as attachment at the periphery may lead to premature agent degradation or low carrier solubility, respectively. However, if the carrier is to be targeted in some specific fashion, such as with a specific ligand, substrate, or binding peptide sequence, then this targeting functionality must be placed at the periphery of the carrier in order for it to achieve its intended biological recognition. The structural uniformity of the carrier, often expressed as its polydispersity, is also of high importance. This is because molecules of different sizes will experience differing biological fates due to the size based selection mechanisms of filter organs such as the liver and kidney. This can be a difficult problem to overcome, as most polymers are synthesized with little control over their molecular weight

distributions. As a result, carriers made from these polymers will also exhibit large variations in their molecular weights and sizes. When administered, differently sized carriers will give differing distribution and excretion profiles, leading to difficulties in repeatability and potential toxicity from carrier populations too large to be excreted. As shown below, the dendritic carriers (where dendritic describes a highly branched dendrimer-like polymer, not to be confused with the immunological term describing certain cells of the immune system) discussed here are synthesized by the coupling of a branched dendrimer core to a predetermined number of PEG chains of precisely controlled molecular weight, giving a carrier of a highly uniform size. Depending on the specific dendrimer core and PEG chain used, various imaging, therapeutic and/or targeting agents can be attached to either the carrier's core or periphery, often using either reversible or specifically irreversible linkages. When properly made, the agent-polymer conjugate thus obtained will contain something on the order of several thousand of atoms, exactly situated and positioned, but with only minor variations in size or chemistry. Of all the carrier platforms under study for agent delivery, dendrimers are among the only ones in which this high degree of structural control, versatility, complexity and precision can be obtained.

Commonly Employed Chemistries

In order to bring about a pharmacokinetic benefit, a polymeric carrier must act as a chaperone to the drug or diagnostic agent being employed. Together this carrier agent conjugate must be stable enough to be synthetically approachable in a realistic setting on a therapeutically relevant scale, and it must also persist in a biological system long enough to reach the agent's intended target. However, for large (>~ 40 kDa) macromolecules excretion by the body may be difficult, leading to bioaccumulation of the conjugate over time. In the delivery of drugs, such as the chemotherapeutic agents discussed below, the cargo must also be released at some point, preferably in a controlled fashion appropriate for timely delivery to the targeted tissue. For these reasons, chemical bonds that are highly unstable are generally undesirable. On the other hand, the carrier should be capable of degrading slowly in order to facilitate excretion. Even more challenging than these, eventual release of a therapeutic agent requires a certain bond to cleave within a very specific time frame, usually in response to specific stimuli. Finally, in order to maintain high fidelity to the ideal carrier structure, any bonds forming the dendrimer scaffold must be capable of being made in very high yields, usually in excess of 99 %. This is due to the compounding effects of defects over multiple steps, as even with a reaction yield of 97 %, a ten step synthesis would lead to a yield only slightly higher than 70%. Since separation of imperfect dendrimers is highly challenging at best, this corresponds to an undesirable high degree of heterogeneity within the sample. While their specific employment will be detailed in Chapter 2, the bonds generally favored for dendrimer scaffold formation are esters and amides. They are both easily formed from many commercial reagents in high yield, and allow a careful tunability with regards to stability and persistence in vivo. For the selective attachment of a drug to the carrier, a more labile bond such as an acyl hydrazone bond is usually favored instead. While this bond is not always formed in the same high yields, it is selectively cleaved by hydrolysis in acidic media, such as that encountered in a lysosome during endocytosis (Figure 3). While not discussed in detail here, other specifically cleavable bonds used in drug delivery include disulfides[19] (cleaved in the cytosol), cis-aconityl linkages[20], and enzymatically cleavable linkages.[21]

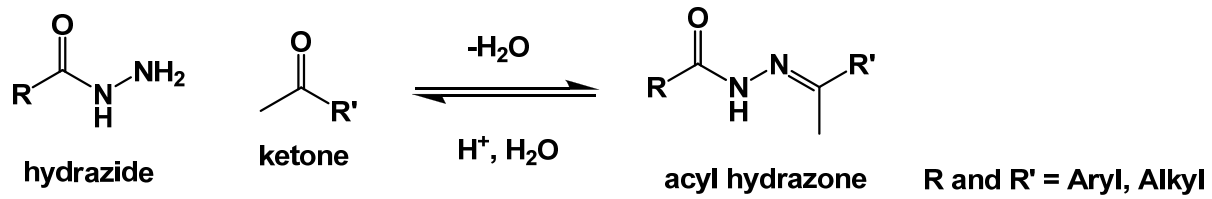

Figure 3. The acid sensitive formation and degradation of the commonly employed acyl hydrazone bond. The bond is highly stable in blood, but is hydrolyzed in mildly acidic media.

As shown in Figure 3, the acyl hydrazone bond employed in our work is formed by the condensation of a hydrazide and a ketone. Because it is desirable to release a drug in its active native form, and because few known drugs are contain hydrazides, this generally requires that any drug delivered contains a ketone. While some drugs such as Doxorubicin naturally contain these, other drugs may have to be modified to include a ketone (see Chapter 4). For imaging agent delivery, however, this difficulty is circumvented, as it is generally not desirable for these agents to be released from the carrier. In this work two drugs are delivered by use of a ketone, Doxorubicin (Chapters 2 and 3) and a synthetic analog of Tubulysin (Chapter 4).

Polymeric drug delivery of Doxorubicin (Dox)

Doxorubicin (Figure 1), an anthracycline which induces apoptosis through DNA intercalation, is a chemotherapeutic agent currently used in the treatment of solid tumors and hematological malignancies, including breast, bile ducts, uterus, ovary, prostate, oesophagus, stomach and liver tumours, childhood solid tumors, Kaposi's sarcoma, osteosarcomas and soft tissue sarcomas, as well as acute myeloblastic and lymphoblastic leukaemia and Wilms Tumor.[22] It is derived from the very similar compound Daunorubicin, which lacks a hydroxyl group on the C-14 carbon of the ketone bearing side chain of the anthracycline. Daunorubicin was discovered by an Italian research group in the 1950's in a soil sample containing a novel strain of *Streptomyces peucetius*. The sample was taken from the grounds surrounding the Castel del Monte in Andria, Italy, which was constructed in 1240 AD by Frederick II as a hunting lodge.[23] The name for the deep red compound is derived from the words *Dauni*, a pre-Roman tribe which had once inhabited the area, and *rubis*, the French word for ruby. Although promising in its activity towards tumor cells, this compound showed exceedingly high cardiotoxicity, and the bacteria were mutated to produce a new compound, Doxorubicin. While high cardiotoxicity remains a primary side effect of Doxorubicin, its higher efficacy against tumors over Daunorubicin results in a higher therapeutic index.

In addition to its high cardiotoxicity, Doxorubicin also shows low aqueous solubility and low tumor accumulation, making it an ideal candidate for polymeric drug delivery. The primary vehicle employed for this purpose is a pegylated liposomal formulation, Doxil.[24] In previous work in this group, it was shown that when delivered to mice bearing C-26 colon carcinomas, Dox attached to a pegylated polyester dendrimer was as effective in treatment as Doxil.[25] Having shown that dendrimers are promising agents for Doxorubicin's delivery, we proceeded to delivery it using dendrimers more synthetically accessible as described in chapter 2 and using a dendrimer of a more linear and rodlike conformation, as discussed in chapter 3.

A second drug for which effective polymeric delivery was pursued is a synthetic analog of a class of potential chemotherapeutic agents, the tubulysins (Figure 4). These compounds, first isolated from myxobacteria by the Reichenbach and Höfle research groups at the

Gesellschaft für Biotechnologische Forschung (GBF), are highly apoptosis inducing agents, with IC_{50} values in the nM to low pM range.[26]

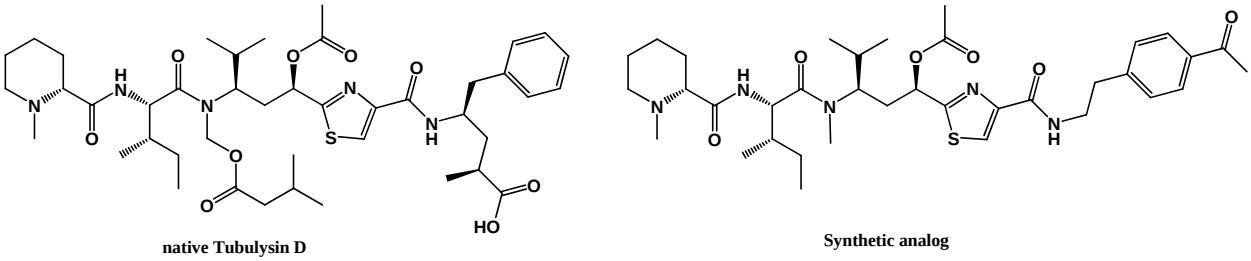

Figure 4. The structure of native tubulysin A (left) and a synthetic analog designed for polymeric drug delivery (right).

The tubulysins act upon cells by depolymerizing tubulin, which allows it to specifically target cells with increased rates of replication, a common feature of cancer cells. This mechanism of action is directly opposed to many other chemotherapeutic agents such as Taxol (paclitaxel) (Figure 1), which works by inhibiting the depolymerization of tubulin. These opposing mechanisms allow for the pitting of these compounds against each other in a tubulin binding assay. Tubulysin has been observed to depolymerize tubulin in the presence of equimolar concentration Taxol,[27] augmenting its low IC_{50} as an indicator of potency. Due to this high potency, clinical use of the tubulysins has been challenging. Furthermore, their total synthesis is difficult and their isolation from their parent bacteria is limited to quantities inadequate for clinical use.[26] To circumvent these challenges, we have collaborated with the Ellman group to achieve a practical and effective delivery of a potent synthetic analog of native tubulysin (Figure 4), as discussed in Chapter 4.

Because early detection of diseases is a crucial parameter to their effective treatment, the effective delivery of imaging and diagnostic agents is also of high importance. Current clinical techniques such as Magnetic Resonance Imaging (MRI) are capable of imaging small changes in biological environments, enabling the identification of diseased tissues and other abnormalities. To aid in producing these images, paramagnetic contrast agents (CA's) will commonly be utilized. These agents accelerate the rate at which water protons relax when pulsed with the radio frequencies utilized in MRI, allowing for increased image contrast. These agents commonly employ chelated gadolinium(III) ions, as their seven unpaired electrons make it the most paramagnetic ion known, giving it the highest potential image contrast. The ability to provide this contrast, or relaxivity, is one of the primary aspects of these agents, although others such as solubility, osmolality and viscosity are also of clinical interest. Further parameters affecting the relaxivity of the agent include the number of water molecules chelated to the Gd(III) ion, how fast these exchange with other water molecules, and the rate of molecular tumbling of the ion.[28] These agents may also present toxicity concerns, as free (uncomplexed) Gd ions displace calcium *in vivo*, and can lead to Nephrogenic Systemic Fibrosis (NSF), an incurable and debilitating condition characterized by the thickening of the skin and tissues.[29] To optimize these parameters and diminish these potential toxicity concerns, high performance MRI agents synthesized by the Raymond group have also been bound to dendrimers to increase their relaxivities and biocompatibilities, as discussed in Chapter 5. In a similar vein of research, in Chapter 6 we also investigate a dendrimer endowed with the ability to image by the mode of Positron Emission Tomography, or PET, to become competent in diagnostic services. In order to direct this dendrimer, its periphery is decorated with an atherosclerosis targeting peptide known

as C-ANF. If successful, this dendrimer, when injected, will selectively accumulate in diseased vasculature tissues by binding to plaques in the walls of the arteries. When subjected to a PET scan, this should allow for *in vivo* imaging and early detection of cardiovascular diseases.

Conclusions

In order to increase the efficacy and biocompatibility of biologically active agents, it is commonly advantageous to modify the agent. This can be done through conjugation to a well selected macromolecule that possesses the pharmacokinetic properties desired in the molecule of interest. In this work, attention is particularly focused on accomplishing this through PEGylated dendrimers, as these highly versatile structures can be used to escort a wide variety of compounds and agents through biological environments. Their design and synthesis is concerned, as well as architectural effects, delivery of a novel drug analog, and their use in the delivery of imaging agents and targeted diagnostics.

References

1) Allen, T.M., Cullis, P.R. Drug Delivery Systems: Entering the mainstream, *Science*, **2004**, *303*, 1818-1822.

2) Henry, C.M., Drug Delivery, Chemical and Engineering News, 2002, 80, 39-47.

3) Paul, S.M., Mytelka, D.S., Dunwiddie, C.T., Persinger, C.C., Munos, B.H., Lindborg, S.R., Schacht, A.L. How to Improve R&D Productivity, The Pharmaceutical Industry's Grand Challenge, *Nature Reviews, Drug Discovery*. **2010**, *9*, 203-214.

4) Müller, C. E., Prodrug Approaches for Enhancing the Bioavailability of Drugs with Low Solubility, *Chemistry and Biodiversity*, **2009**, *6*, 2071-2083.

5) Ringsdorf, H. *J. Polym. Sci. Polym. Symp.* **1975**, *51*, 135-153.

6) HO, R. J. Y. and CHIEN, J, Y., Clinical Trials and Translational Medicine Commentary, Drug Delivery Trends in Clinical Trials and Translational Medicine: Updated Analysis of ClinicalTrials.gov Database, *Journal of Pharmaceutical Sciences*, **2009**, *98*, 1928-1934.)

7) Liu, S., Maheshwari, R., and Kiick, K. L., Polymer-Based Therapeutics. *Macromolecules*, **2009**, *42*, 3-13.

8) Kataoka, K., Harada, A., and Nagasaki, Y., Block copolymer micelles for drug delivery: design, characterization and biological significance. *Advanced Drug Delivery Reviews*, **2001**, *47*, 113-131.

9) Guo, X., and Szoka, F. C., Chemical approaches to triggerable lipid vesicles for drug and gene delivery. *Accounts of Chemical Research*, **2003**, *36*, 335-341.

10) Christian, D. A., Cai, S., Bowen, D. M., Kim, Y., Pajerowski, J. D., and Discher, D. E., Polymersome carriers: From self-assembly to siRNA and protein therapeutics. *European Journal of Pharmaceutics and Biopharmaceutics*, **2009**, *71*, 463-474.

11) Fox, M. E., Szoka, F. C., and Fréchet, J. M. J., Soluble Polymer Carriers for the Treatment of Cancer: The Importance of Molecular Architecture. *Accounts of Chemical Research*, **2009**, *42*, 1141-1151.

12) Li, M. H., and Keller, P., Stimuli-responsive polymer vesicles. *Soft Matter*, **2009**, *5*, 927-937.

13) Green, J. J., Langer, R., and Anderson, D. G., A combinatorial polymer library approach yields insight into nonviral gene delivery. *Accounts of Chemical Research*, **2008**, *41*, 749-759.

14) Haag, R., and Kratz, F., Polymer therapeutics: Concepts and applications. *Angewandte Chemie-International Edition*, **2006**, *45*, 1198-1215.

15) Peer, D., Karp, J. M., Hong, S., FaroKHzad, O. C., Margalit, R., and Langer, R., Nanocarriers as an emerging platform for cancer therapy. *Nature Nanotechnology*, **2007**, *2*, 751-760.
16) Medina, S. H., and El-Sayed, M. E. H., Dendrimers as Carriers for Delivery of Chemotherapeutic Agents. *Chemical Reviews*, **2009**, *109*, 3141-3157.
17) Matsumura, Y., Maeda, H., A New Concept for Macromolecular Therapeutics in Cancer Chemotherapy: Mechanism of Tumoritropic Accumulation of Proteins and the Antitumor Agent Smancs1Cancer Res, **1986**, *46*, 6387-6392.
18) Greenwald, R.B., Conover, C.D., Choe, Y.H. *Crit. Rev. Ther. Drug. Carrier. Syst*. **2000**, *17*, 101-161.
19) Satyam, A., Design and synthesis of releasable folate–drug conjugates using a novel heterobifunctional disulfide-containing linker, *Bioorganic & Medicinal Chemistry Letters*, **2008**, *18*, 3196–3199.
20) Zhu, S., Hong, M., Zhang, L., Tang, G., Jiang, Y., Pei, Y., PEGylated PAMAM Dendrimer-Doxorubicin Conjugates: In Vitro Evaluation and In Vivo Tumor Accumulation, Pharmaceutical Research, **2010**, 27, 161-174.
21) Kratz, F., Müller, A.I., Ryppa,C. and Warnecke, A., Prodrug Strategies in Anticancer Chemotherapy, *Chem Med Chem*, **2008**, *3*, 20-53.
22) Carvalho, C., Santos, X. R., Cardoso, S., Correia, S., Oliveira, P. J., Santos, M. S., and Moreira, P. I., Doxorubicin: The Good, the Bad and the Ugly Effect. *Current Medicinal Chemistry,* **2009**, *16,* 3267-3285.
23) Castles of the Western World, Armin Tuulse, **2002**, Anton Schroll and Co, New York, p 60-61.
24) Ferrandina, G., Corrado, G., Licameli, A., Lorusso, D., Fuoco, G., Pisconti, S., Scambia, G., Pegylated liposomal doxorubicin in the management of ovarian cancer, *Therapeutics and Clinical Risk Management,* **2010**, *6*, 463–483.
25) Lee, C. C., Gillies, E. R., Fox, M. E., Guillaudeu, S. J., Fréchet, J. M. J., Dy, E. E., and Szoka, F. C. A single dose of doxorubicin-functionalized bow-tie dendrimer cures mice bearing C-26 colon carcinomas. *Proceedings of the National Academy of Sciences of the United States of America*, **2006**, *103*, 16649-16654.
26) Domling, A.; Richeter, W., Myxobacterial epothilones and tubulysins as promising anticancer agents. *Molecular Diversity*, **2005**, *9*, 141-147.
27) Khalil, M.W.; Sasse, F.; Heinrich Lünsdorf, H.; Yasser A; Elnakady, Y.A.; Reichenbach, A. Mechanism of Action of Tubulysin, an Antimitotic Peptide from Myxobacteria. *Chem Bio Chem*, **2006**, *7*, 678-683.
28) *Bloembergen N*, *Morgan L. O*., Proton relaxation times in paramagnetic solutions effects of electron spin relaxation, *J. Chem. Phys*., ***1961***, *34*, 842-850.
29) Caravan, P. Strategies for increasing the sensitivity of gadolinium based MRI contrast agents, *Chem. Soc. Rev*. **2006**, *35*, 512-523.

Chapter 2: Dendrimer Synthesis, Directions and General Considerations

Introduction

The use of macromolecular carries for the delivery of chemotherapeutics originated from the hypothesis that polymers may be used to improve both the solubility and the blood circulation time of small molecule drugs.[1,2] It was later discovered that macromolecules have the additional benefit of increased accumulation in tumor tissue as a result of the highly permeable vasculature surrounding rapidly growing neoplasm—a concept known as the enhanced permeation and retention (EPR) effect.[3,4] Thus, macromolecular carriers can provide both enhanced pharmacokinetics and a passive targeting mechanism, characteristics that may be used to increase the efficacy of small molecule drugs. To this end, carrier systems such as linear polymers, micellar assemblies, liposomes, polymersomes and dendrimers have been studied in an effort to identify an ideal drug carrier.[5-14] Important design features[9] include a long blood circulation time, high tumor-accumulation, high drug-loading, low toxicity, low polydispersity index and simple preparation. Considering the above criteria, PEGylated dendrimers[15,16] constitute an attractive platform because their size and degree of branching can be precisely controlled and they possess multiple functional appendages for the attachment of both drugs and solubilizing groups. Dendritic drug carriers based on polyesters[17-19], polyamines[20,21], melamines or triazines[22-24], PAMAM[25-30], and other polyamides[31-33] have all been explored and recently reviewed.[14] Polyesters constitute a very attractive class of materials because they are biodegradable; however, the hydrolytic susceptibility of the ester bond can make the synthesis of drug conjugates somewhat challenging. The hydrolysis rates of polyesters can vary dramatically depending on the hydrophobicity of the monomer, steric environment, and the reactivity of functional groups located within the dendrimer[34]. In contrast, polyamide and polyamine dendrimers can withstand a much wider selection of synthetic manipulations, but they do not degrade as easily in the body and thus they may be more prone to long-term accumulation *in vivo*.[35] Currently, challenges facing the biological application of dendrimers are their lengthy syntheses and the need to develop nontoxic, biodegradable dendrimers that are still resilient to the reaction conditions encountered during their synthesis and modification. As a result, accessing a universal, biodegradable, highly soluble, unimolecular carrier capable of achieving a high drug loading and low polydispersity has remained a challenge.

In recent studies, we have determined that a family of polyester-core dendrimer based on a 2,2-bis(hydroxymethyl) propanoic acid (bis-HMPA) monomer unit, typically functionalized with eight 5 kDa poly(ethylene glycol) (PEG) chains[18] is biocompatible and that it is capable of high drug loading while facilitating high tumor accumulation through its long circulation half-life. An asymmetric bis-HMPA PEGylated dendrimer functionalized with doxorubicin via a pH sensitive acyl hydrazone bond demonstrated outstanding antitumor activity in mice bearing murine C26 colon carcinoma.[17] Despite these promising *in vivo* results, further evaluation of this asymmetric carrier in biological models was slowed by its lengthy synthesis.[37] Therefore we sought to transpose the beneficial features[9] of this PEGylated dendrimer onto a simpler and more readily prepared carrier. Initial approaches involved simplified multifunctional dendrimers based on bis-HMPA[38,39]; however, some issues still remained as undesired degradation of the polyester backbone was observed during the attachment of certain drugs.

Herein, the design evolution of three dendrimers that resulted in the creation of a new PEGylated dendrimer is described, which circumvented the synthetic and biological limitations uncovered in previous studies. This involves discussion of a dendronized linear poly-L-lysine carrier, followed by PEGylated branched lysine dendrimers, ultimately cumulating in an efficient synthesis for a mixed peptide dendrimer with the robustness of polyamide dendrimers and degradability of ester dendrimers, yielding a hybrid scaffold capable of translation into clinical studies.

Materials and Methods

Materials. Materials were used as obtained from commercial sources unless otherwise noted. Poly(ethylene glycol) was purchased from Laysan Biosciences Inc. Amino acid derivatives were purchased from Bachem. Dimethylformamide (DMF), pyridine, and CH_2Cl_2 for syntheses were purged 1 h with nitrogen and further dried by passing them through commercially available push stills (Glass Contour). Solvents were removed under reduced pressure using a rotary evaporator or by vacuum pump evacuation. Compounds **2, 3, 4**[19], **6**, **8**, **9**[39], **10**[40], **15**, **17**, **18, 19**[41] were synthesized according to published procedures.

Characterization. NMR spectra were recorded on Bruker AV 300, AVB 400, AVQ 400, or DRX 500 MHz instruments. Spectra were recorded in $CDCl_3$ or D_2O solutions and were referenced to TMS or the solvent residual peak and taken at ambient temperature. Elemental analyses were performed at the UC Berkeley Mass Spectrometry Facility. MALDI-TOF MS was performed on a PerSeptive Biosystems Voyager-DE using the following matrices: *trans*-3-indoleacrylic acid (IAA) for *tert*-butyloxycarbonyl (Boc) protected dendrimers; or 2,5-dihyroxybenzoic acid (DHB) for amine-terminated dendrimers. Samples were prepared by diluting dendrimer solutions (~1 M) 40-fold in 100 mM matrix solutions in tetrahydrofuran and spotting 0.5 μL on the sample plate. Size exclusion chromatography (SEC) was performed using one of three systems:

SEC System A: a Waters 515 pump, a Waters 717 autosampler, a Waters 996 Photodiode Array detector (210-600 nm), and a Waters 2414 differential refractive index (RI) detector. SEC was performed at 1.0 mL/min in a PLgel Mixed B (10 μm) and a PLgel Mixed C (5 μm) column (Polymer Laboratories, both 300 x 7.5 mm), in that order, using DMF with 0.2% LiBr as the mobile phase and linear PEO (4,200-478,000 MW) as the calibration standards. The columns were thermostated at 70 °C.

SEC System B: The same equipment as System A, but performed at 1.0 mL/min in two SDV Linear S (5 μm) columns (Polymer Standards Service, 300 x 8 mm) using DMF with 0.2% LiBr as the mobile phase.

SEC System C: A Waters Alliance separation module 2695 (sample compartment maintained at 37.0 ± 3.0 ^{o}C), a Waters 410 differential RI detector, a Waters 996 photodiode array detector (λ = 486 nm), and a Shodex OHpak SB-804 HQ SEC column. An isocratic flow rate of 0.7 mL/min was used with a mobile phase composed of 70%/30%/0.05% water/acetonitrile/formic acid.

Doxorubicin loading was quantified using a Lambda 35 UV-vis spectrometer (PerkinElmer, Wellesley, MA). Measurements were performed in sealed, standard 1-cm quartz cells in millipore water at room temperature.

EA-G_1-Lys(Boc)$_8$ (22). Pentaerythritol (353mg, 2.6 mmol), BocLys(Boc)-ONp (5.500 g, 11.8 mmol) and DMAP (125 mg, 1.0 mmol) were added to a 20 ml reaction vial. Under a nitrogen atmosphere, DMF (5.5 mL) and triethylamine (1.6 mL, 11.5 mmol) were added and the reaction

stirred for 48 h. MALDI-ToF analysis confirmed the reaction had gone to completion. *N,N*-dimethylethylene diamine (300 µL, 4.1 mmol) was added to quench excess PNP esters. After 10 min, the mixture was diluted with ether (200 mL) and washed with three 100 mL portions of 1M NaOH, three 100 mL portions of 1M $NaHSO_4$, 100 mL DI water, and 100 mL of brine. The organic layer was dried over Na_2SO_4 and evaporated to dryness to give **22** (3.455 g, 93% yield) as a white foam. ^{1}H NMR (400 MHz, $CDCl_3$): δ 1.26-1.49 (m, 88H), 1.58-1.83 (m, 8H), 3.09-3.11 (m, 8H), 4.08-4.18 (m, 12H), 4.80 (s, 4H), 5.3-5.6 (br d, 4H). ^{13}C NMR (100 MHz, $CDCl_3$): δ 22.5, 28.3, 28.4, 29.6, 31.5, 39.9, 53.4, 62.2, 79.0, 79.8, 155.7, 156.1. Calc $[M]^+$ ($C_{69}H_{124}N_8O_{24}$) *m/z* = 1448.87. Found MALDI-ToF $[M+Na]^+$ *m/z* = 1470.0.

EA-G$_1$-Lys(NH$_3$TFA)$_8$ (22a). Compound **22** (209 mg, 144 µmol) was dissolved in 1:1 TFA:DCM for 1 h. Quantitative deprotection was confirmed by MALDI-ToF analysis. The solvents were removed under reduced pressure to give **22a** as a gummy solid in quantitative yield. ^{1}H NMR (400 MHz, MeOD): δ 1.40-1.60 (m, 8H), 1.67-1.75 (m, 8H), 1.87-2.10 (m, 8H), 2.99 (t, *J* = 8 Hz, 8H), 4.21 (t, *J* = 6 Hz, 4H), 4.40 (s, 8H). ^{13}C NMR (100 MHz, MeOD): δ 21.8, 26.5, 29.5, 38.7, 42.5, 52.3, 62.9, 161.4, 161.7, 168.6. Calc $[M]^+$ ($C_{29}H_{60}N_8O_8$) *m/z* = 648.45. Found MALDI-ToF $[M+H]^+$ *m/z* = 649.6.

EA-G$_1$-Lys(Glu(Bn)Boc)$_8$ (24). Compound **22a** (89 mg, 63 µmol) and BocGlu(OBz)-ONp (290 mg, 632 µmol) were added to a 20 ml reaction vial. Under a nitrogen atmosphere, DMF (1 mL) and triethylamine (140 µL, 1.0 mmol) were added and the reaction was allowed to stir for 4 h. MALDI-ToF analysis showed a single peak corresponding to the fully functionalized dendrimer. *N,N*-dimethylethylene diamine (50 µl, 690 µmol) was added to quench excess PNP esters. The reaction was diluted with ethyl acetate (100 mL) and washed with three 50 mL portions of 1M $NaHSO_4$, three 50 mL portions of saturated K_2CO_3, 50 mL of DI water, and 50 mL brine. The organic layer was dried over Na_2SO_4 and evaporated to dryness to give **24** (171 mg, 87% yield) as a white foam. ^{1}H NMR (400 MHz, MeOD): δ 1.41-1.56 (bm, 96H), 1.60-1.75 (m, 4H), 1.70-2.13 (m, 16H), 2.25-2.40 (m, 4H), 2.44-2.51 (m, 12H), 2.58-2.61 (m, 4H), 3.10-3.20 (m, 8H), 4.09-4.25 (m, 12H), 4.35-4.40 (m, 4H) 5.08-5.09 (2s, 16H), 7.28-7.38 (m, 40H). ^{13}C NMR (100 MHz, MeOD): δ 23.8, 28.6, 31.5, 40.8, 44.6, 49.0, 54.4, 64.9, 163.4, 163.8, 170.7. Calc $[M]^+$ ($C_{165}H_{228}N_{16}O_{48}$) *m/z* = 3201.59. Found MALDI-ToF $[M+Na]^+$ *m/z* = 3223.3.

EA-G$_1$-Lys(Glu(Bn)NH$_3$TFA)$_8$ (24a). Compound **24** (100 mg, 31 µmol) was dissolved in 1:1 TFA:DCM for 1 h. Quantitative deprotection was confirmed by MALDI-ToF analysis. The solvents were removed under reduced pressure to give **24a** as a gummy solid in quantitative yield. ^{1}H NMR (400 MHz, MeOD): δ 1.19-1.35 (m, 16H), 1.45-1.65 (m, 8H), 2.04-2.20 (m, 16H), 2.38-2.46 (m, 8H), 2.51-2.63 (m, 8H), 2.89-2.93 (m, 4H), 3.09-3.12 (m, 4H), 3.89-3.96 (m, 12H), 4.11 (t, *J* = 4.4 Hz, 4H), 4.30-4.33 (m, 4H), 4.80-5.00 (m, 16H), 7.17-7.26 (m, 40H). ^{13}C NMR (100 MHz, MeOD): δ = 24.1, 27.7, 29.7, 30.3, 30.5, 31.6, 40.2, 53.5, 53.9, 54.1, 63.9, 67.8, 116.7, 119.6, 129.2, 129.3, 129.6, 137.3, 162.8, 163.2, 169.8, 170.3, 172.7, 173.6, 173.8. Calc $[M]^+$ ($C_{125}H_{164}N_{16}O_{32}$) *m/z* = 2402.73. Found MALDI-ToF $[M+Na]^+$ *m/z* = 2424.8.

EA-G$_1$-Lys(Glu(Bn)PEO)$_8$ (25). PNP-PEG carbonate (986 mg, 192 µmol) and **24a** (81 mg, 25 µmol NH_3) were added to a 20 ml reaction vial. Under a nitrogen atmosphere, DMF (3 mL) was added. After using a warm water bath to dissolve the starting material, triethylamine (120 µL, 0.863 mmol) was added. After stirring for 48 h (reaction monitored by SEC analysis), no further increase in the molecular weight was observed and the reaction was considered complete. Piperidine (50 µL, 0.506 mmol) was added to quench remaining PNP carbonate. After 1 h, acetic anhydride (400 µL, 4.24 mmol) was added to acylate any remaining primary amines on the dendrimer that had not reacted with the PNP-PEG carbonate. After stirring an additional hour,

the reaction mixture was precipitated into ether (300 mL) and **25** (999 mg) was collected by filtration as a fluffy white solid. In some cases residual 5kDa PEG was observed after the PEGylation was considered complete. This could be removed by dialysis using 100,000 MWCO tubing against water for 24 hours. ^{1}H NMR (500 MHz, D_2O): δ 1.20-1.80 (br m, 24H), 1.80-2.10 (br d, 16H), 2.35-2.55 (br s, 16H), 3.05-3.20 (br s, 8H), 3.38 (s, 24H), 3.40-3.90 (br m, ~3,900H), 4.00-4.40 (br m, 36H), 5.09-5.15 (br s, 16H), 7.25-7.40 (br m, 40H). DMF SEC: Mn: 32,000 Da, Mw: 35,000 Da, PDI: 1.09.

EA-G_1-Lys(GluPEO)$_8$ (25a). Compound **25** (402 mg, 10.1 μmol) was added to a 20 ml reaction vial and dissolved in MeOH (9 mL). Activated Pd/C (10 wt%, 50 mg) was added and the reaction put under hydrogen atmosphere. The reaction was stirred overnight, then filtered and solvent removed via rotary evaporation to give **25a** (387 mg) as a white solid. ^{1}H NMR (500 MHz, D_2O): δ 1.20-1.80 (br m, 24H), 1.80-2.1 (br d, 16H), 2.40-2.51 (m, 16H), 3.15-3.25 (br s, 8H), 3.38 (s, 24H), 3.40-3.90 (br m, ~3,900H), 4.00-4.40 (br m, ~36H).

EA-G_1-Lys(Glu(NNBoc)PEO)$_8$ (26). Compound **25a** (710 mg, 142 μmol COOH), *t*-butyl carbazate (94 mg, 711 μmol), and DMAP (10 mg, 81 μmol) was added to a 20 ml reaction vial. Under a nitrogen atmosphere, DCM (8 mL) was added dropwise. The solution was cooled to 0 ^{o}C followed by the addition of EDC (136 mg, 709 μmol). The reaction was allowed to warm to room temperature and stirred over night. The reaction was dialyzed against MeOH in 12kDa-14kDa MWCO dialysis with 3 solvent changes over 18 h. Concentration of the bag contents *in vacuo* gave **26** (660 mg) as a white solid. ^{1}H NMR (500 MHz, D_2O): δ 1.30-1.60 (br m, 100H), 1.65-2.20 (br m, 20H), 2.30-2.45 (br s, 16H), 3.15-3.25 (br s, 8H), 3.38 (s, 24H), 3.50-3.90 (br m, ~3,900H), 4.00-4.45 (br m, 40H).

EA-G_1-Lys(Glu(NNH$_3$TFA)PEO)$_8$ (26a). Compound **26** (102 mg) was dissolved in 1:1 TFA:DCM for 1 h. The solvents were removed under reduced pressure to give **26a** as a gummy solid. Quantitative deprotection confirmed by ^{1}H NMR.

EA-G_1-Lys(Glu(NNDox)PEO)$_8$ (27). Compound **26a** (72 mg, 14 μmol NNBoc) and doxorubicin (50 mg, 92 μmol) were added to a 20 ml reaction vial and were dissolved in MeOH (3 mL), pyridine (100 μL), and acetic acid (100 μL). The reaction was purged with nitrogen and stirred at 60 ^{o}C in the dark for 18 h. The reaction mixture was loaded directly onto a Sephadex LH-20 column and eluted with methanol. The first dark red band was collected and the solvent removed by rotary evaporation. The solid material was further purified using a Biorad PD-10 column with water as the eluent. After lyophilization 67.2 mg of red powder remained. The Dox loading was quantified using the absorbance at 486 nm (ε = 11,500) (*42*) to be 9.6%.

Polymer Degradation Study. Compound **26** (20 mg) was dissolved in 1.5 ml of 1X PBS buffer and incubated at 37 ^{o}C. At t = 0, 1, 2, 3, 6, 15, 20 days, 100 μl aliquots were taken out and immediately frozen followed by lyophilization. At the end of the experiment, each sample was dissolved in 0.5 ml DMF from the System A mobile phase, filtered though a 0.2 μm PVTF filter and measured by the RI detector on system A.

Hydrolysis of Dox from Compound 27 at pH 7.4 and pH 5. Drug release rates were determined by a modified published procedure.(*43*) Compound **27** was dissolved in either 1X PBS or pH 5 acetate buffer (30 mM with 70 mM $NaNO_3$), at 1 mg/mL. Buffers were preheated to 37 ^{o}C before dissolving polymer and maintained at this temperature throughout the experiment. At each time point, 25 μL was injected onto SEC system C for analysis.

Cytotoxicity Studies in Cells. The cytotoxicities of free Dox, **26**, and **27** were determined by using the MTT assay with C26 cells. Cells were seeded onto a 96-well plate at a density of 5.0 × 10^3 cells per well in 100 μl of medium and incubated overnight (37°C, 5% CO_2, and 80%

humidity). An additional 100 µl of new medium (RPMI medium 1640, 10% FBS, 1% penicillin-streptomycin, 1% Glutamax) containing varying concentrations of DOX, **26**, or **27** were added to each well. After incubation for 72 h, 40 µl of media containing thiazolyl blue tetrazolium bromide (5 mg/ml) was added. The cells were incubated for 3 h, after which time the medium was carefully removed. To the resulting purple crystals were added 200 µl of DMSO and 25 µl of pH 10.5 glycine buffer (0.1 M glycine/0.1 M NaCl). Optical densities were measure at 570 nm by a SpectraMAX 190 microplate reader (Molecular Devices, Sunnyvale, CA). Optical densities measured for wells containing cells that received neither dendrimer nor drug were considered to represent 100% viability. IC_{50} values were obtained from sigmoidal fits of the data using Origin 7 SR4 8.0552 software (OriginLab, Northhampton, MA).

Results and Discussion

Exploring Polyester-Core Dendrimers

Polyester dendrimers based on bis(HMPA) monomer units are an attractive scaffold for biological applications because they are non-immunogenic, biodegradable, and non-toxic.[36] Scheme 1 outlines the synthesis of a core-functionalized PEGylated dendrimer we have developed earlier.[39] Briefly, the tetrafunctional pentaerythritol core **1** was modified with a benzylidene-protected bis(HMPA) monomer **2** to afford the first generation dendrimer **3**. After removal of the protecting groups via hydrogenolysis, the eight peripheral hydroxyl groups were functionalized with orthogonally protected aspartic acid to give **6**. Subsequent deprotection of the amino groups of **6** followed by PEGylation with the 5 kDa PEG electrophiles gives dendrimer **8**.

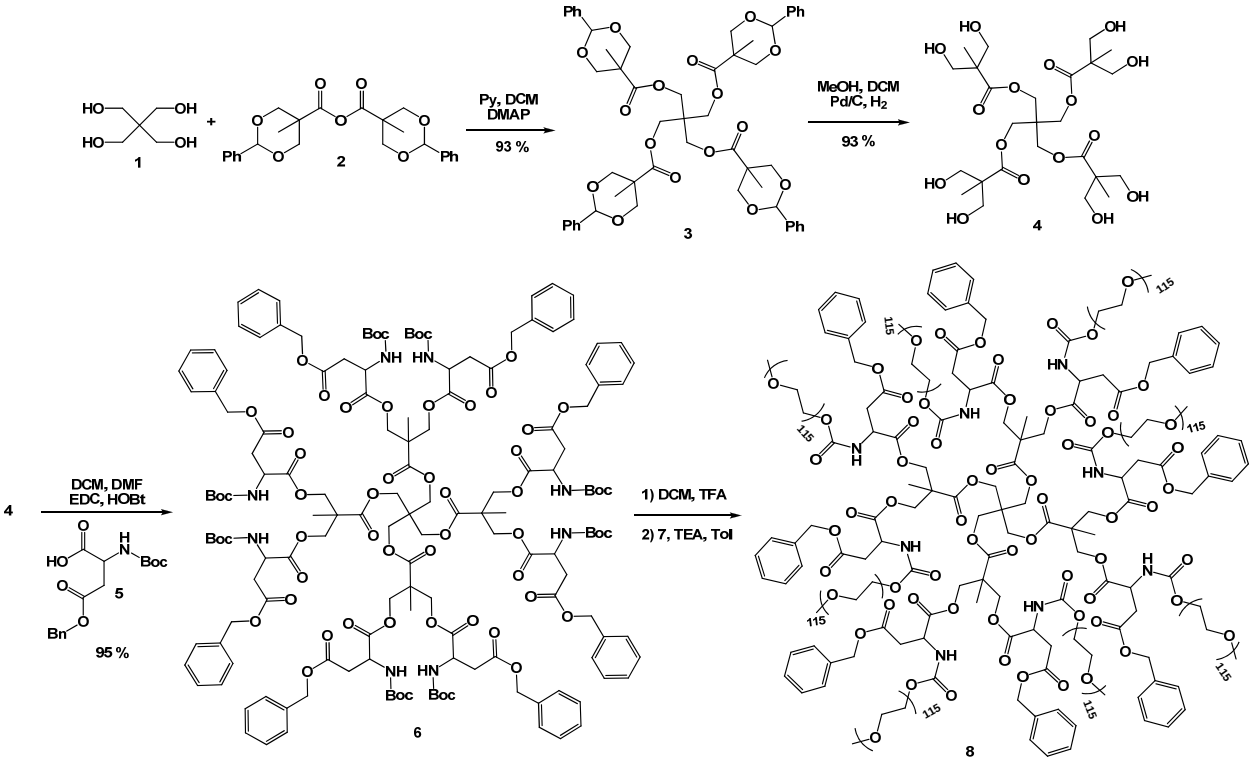

Scheme 1. Synthesis of a symmetrical PEGylated dendrimer.

Removal of the benzyl ester protecting groups of **8** via hydrogenolysis afforded dendrimer **9** with eight carboxylic acids moieties available for potential drug attachment (Scheme 2). However,

early attempts at the functionalization of this dendrimer with *t*-butyl carbazate or glutamic acid derivative **10** were unsuccessful as degradation of the dendrimer was observed during this reaction.

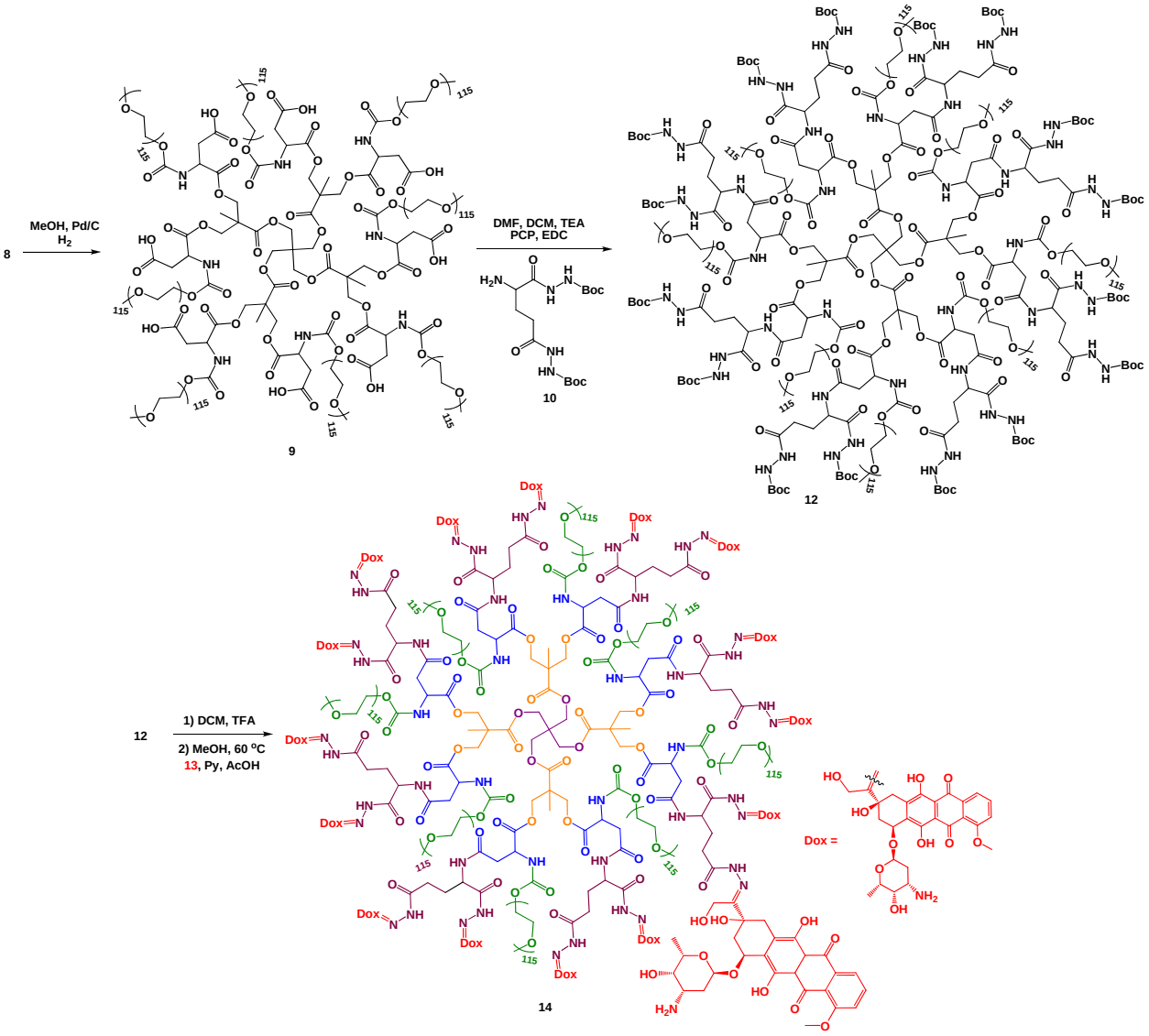

Scheme 2. Linker attachment and Dox loading.

In order to gain insight into the degradation pathway, we prepared the dendrimer probe **11** and attempted to functionalize its aspartic acid chain-ends with *t*-butyl carbazate. Probe molecule **11** was selected instead of PEGylated dendrimer **9** as progress of its reaction could be more easily monitored by MALDI-ToF since it does not contain PEG chains (Figure 1).

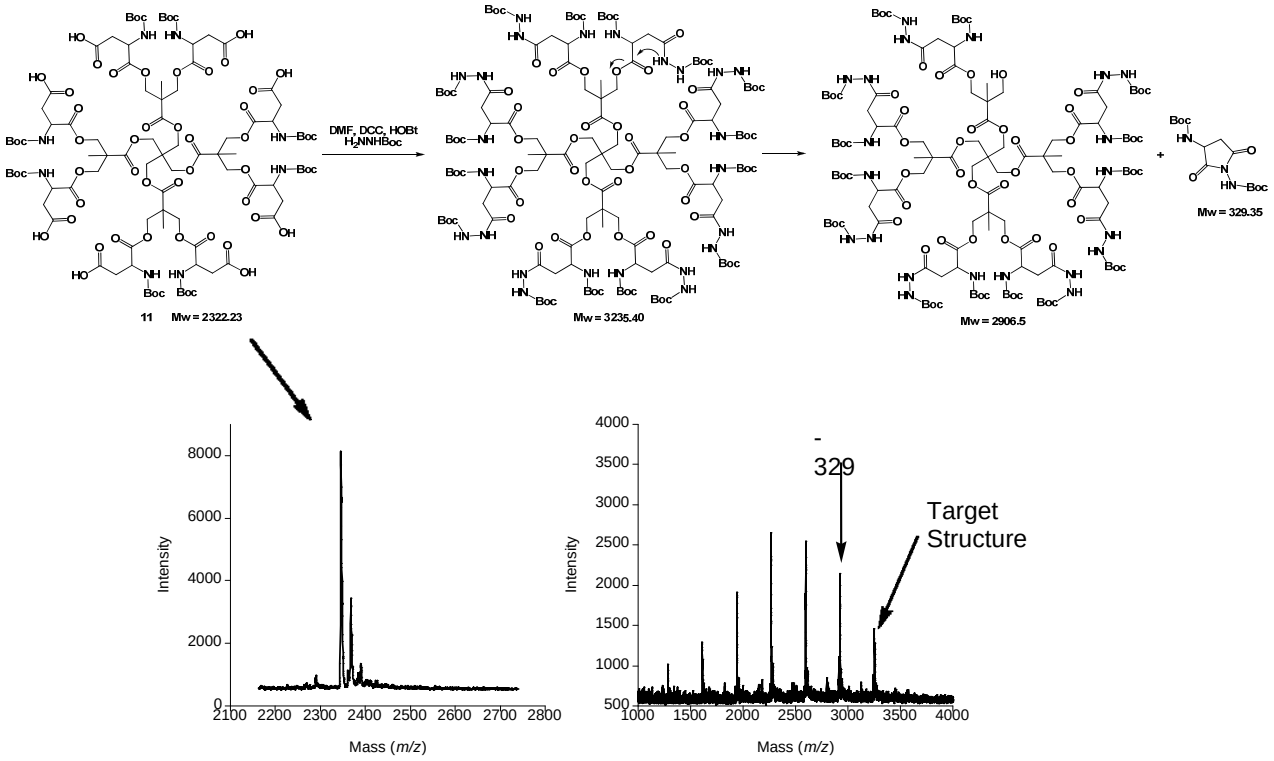

Figure 1. Proposed degradation pathway for the polyester dendrimer.

As a result of a degradation side reaction, only a small amount of the target product was formed, leading to the appearance of lower molecular weight products with molecular weights that decreased in increments of 329 amu, likely as a result of intramolecular cyclization reactions as proposed in Figure 1. This type of cyclization reaction on benzyl ester-protected aspartic acid residues is documented in the peptide literature and additives have been developed to suppress such reactions.[44] For example, pentachlorophenol (PCP) has been used to decrease the production of the aminosuccinyl by-product by inhibiting amide deprotonation. Under these buffered conditions, the primary amines are still available to react with *p*-nitrophenyl (PNP) carbonates and other electrophiles. The use of PCP as an additive proved beneficial in our hands as it allowed the functionalization of the carboxylic acid side chains of dendrimer **9** with protected nucleophile **10** to give dendrimer **12**. Finally, doxorubicin hydrazone conjugate **14** was obtained after removal of the Boc groups from the hydrazide linkers in **12** and condensation of the resulting amines with the ketone group of doxorubicin **13** (scheme 2). In order to determine how rapidly this polyester architecture breaks down under physiological conditions, **12** was incubated in PBS buffer at 37 ^{o}C and the evolution of its molecular weight with time was monitored by SEC. This revealed that the α-amino esters located did not survive long enough for use of **12** *in vivo* as significant degradation was observed after only 10 hours. For this reason, we began exploring alternative dendrimer scaffolds based on more robust polyamide cores.

Exploring Polylysine-Core Dendrimers

In contrast to polyester dendrimers, polyamide dendrimers are less susceptible to hydrolysis, but this increased stability may hamper their break down *in vivo*. Recently, Fox *et al.* functionalized a PEGylated polylysine with camptothecin and observed complete tumor

remission in transgenic mice with HT-29 human colon carcinoma.[41] While the degradation of amide bonds in linear peptides *in vivo* is well established, the fate of branched, acylated, and PEGylated polyamide dendrimers is less certain as proteases may not be able to access amide bonds near the core of the structure. However, even slow or incomplete degradation of the carrier may be permissible for drug delivery applications if the by-products are non-toxic and small in size.[45-46] In order to apply the polylysine carrier used by Fox[41] to the delivery of doxorubicin, dendrimer **18** with a protected hydrazide had to be prepared.

Lysine dendrimer **15**, first described by Denkewalter[47] in 1982 was used as the starting material. Its peripheral amines were acylated with PNP-Asp(Bn)Boc to afford dendrimer **17** (Scheme 3). It is worth noting that the PCP additive was also needed when attaching aspartic acid to the G_2 lysine periphery. Otherwise, a 5-membered amino succinyl byproduct can form via amidolysis of the benzyl ester protected side chain. Deprotection of the amino groups of the aspartate termini and PEGylation with PEG-*p*-nitrophenyl carbonate afforded **18**.

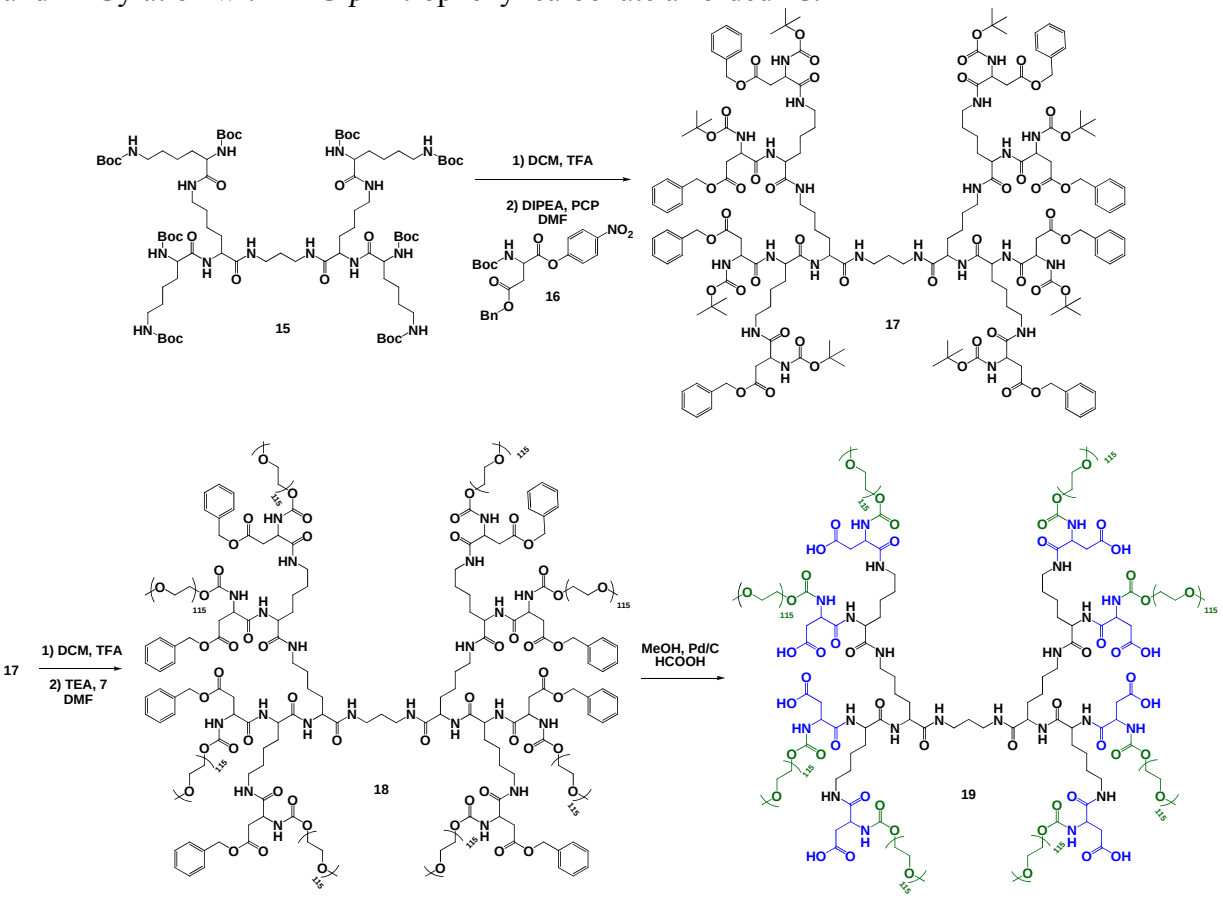

Scheme 3. PEGylated polylysine synthesis.

Unfortunately, the coupling of *t*-butyl carbazate to the deprotected side chain carboxylic acid terminal moieties (**19**) led to the appearance of degradation byproducts such as **20** as shown in Figure 2. Monitoring of the reaction by size exclusion chromatography showed the formation of lower molecular weight by products - presumably formed as a result of attack of the hydrazide nitrogens onto the carbamate linkers to PEG, thus forming a six-membered cyclic by-product and releasing PEG.

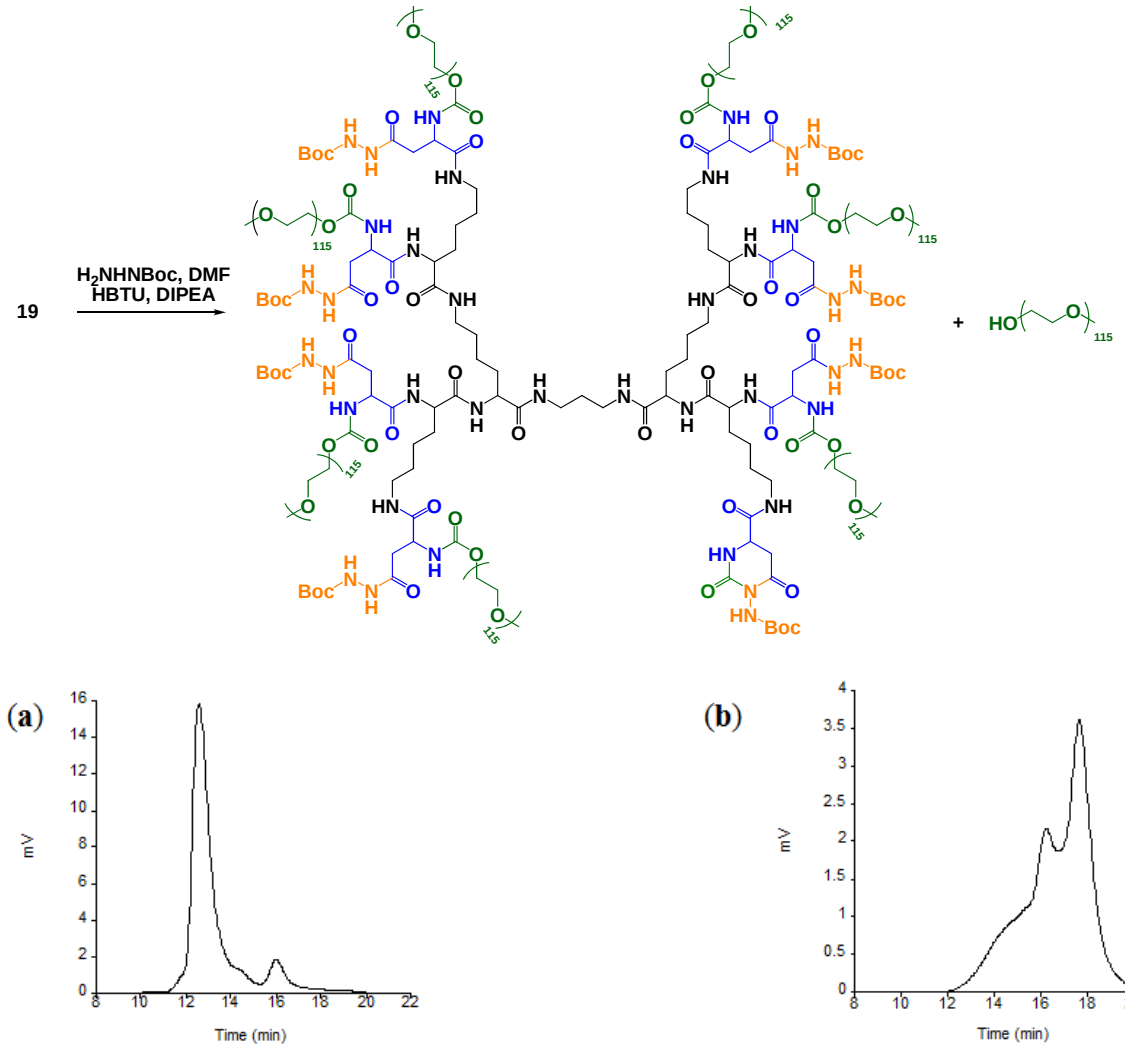

Figure 2. PEGylated polylysine degradation: (a) SEC of compound **19**, (b) SEC of reaction mixture with byproduct **20**.

This side reaction could be circumvented in two ways: (i) replacement of the carbamate in **18** with a more stable amide linkage by using carboxymethyl terminated PEG instead of a PNP carbamate; or (ii) use of a glutamic acid spacer between the nucleophilic hydrazides and the relatively labile carbamate linkages to PEG. The latter route requires more synthetic operations, but has the added benefit of doubling the number of hydrazides through which drug molecules can be attached. Overall, while feasible, this route did not fully meet our criteria for an optimized dendritic drug carrier.

Exploring Hybrid Ester-Amide-Core Dendrimers

The important lessons learned from the synthesis of both the polyester and polyamide carriers ultimately led us to consider a hybrid approach that combines their separate virtues in one scaffold. It appears that the combination of a hydrolytically degradable ester core and a more chemically resistant amide periphery might be ideal for the construction of PEGylated drug conjugates. Furthermore, the early designs we tested (*vide supra*) also underscored the importance of avoiding the positioning nucleophilic sites at a 5- or 6-atom distance from potential leaving groups.[43] Hybrid dendrimer **24** (Scheme 4), representing such an architecture

was obtained in three simple steps and 81% overall yield without any chromatographic purification.

Synthesis of the hybrid carrier began by treatment of pentaerythritol **1** with the *p*-nitrophenyl ester of lysine **21** (Scheme 4). The amine protecting groups of the resulting dendrimer **22** were then removed and the molecule was provided with "differentiated end functionalities" by reacting each of its eight primary amino groups with orthogonally protected PNP-glutamic acid **23**.

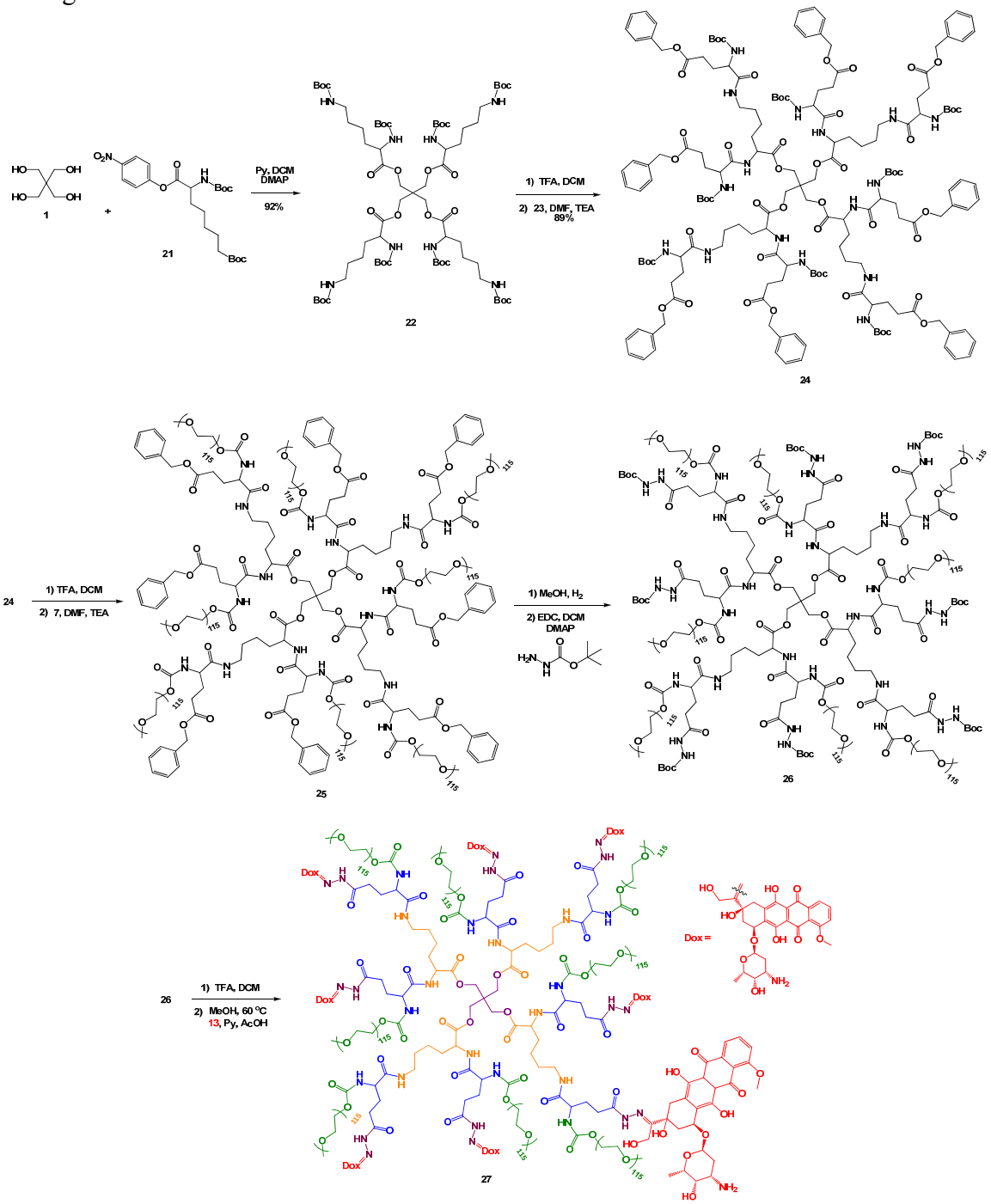

Scheme 4. Synthesis of drug loaded PEGylated ester-amide dendrimer.

In this synthesis glutamic acid was selected over aspartic acid for the following reasons: (i) pentachlorophenol was no longer needed to prevent amidolysis of the benzyl ester group, since formation of the 6-membered amino succinyl byproduct was not observed; and (ii) *t*-butyl carbazate could be attached directly to the glutamic acid side chain without any degradation as cyclization of the acyl hydrazide onto the carbamate to form a 7-membered ring was not an issue. Eight 5 kDa PEG chain were then installed on the dendrimer periphery via a carbamate linkage. This was accomplished by quantitative removal of the Boc protecting groups and subsequent PEGylation with one equivalent (per amine) of PNP-PEG (Scheme 4). The PEGylation reaction was extended over two days, at which time, piperidine was added to quench any unreacted PNP-PEG, and then acetic anhydride was added to acylate any remaining primary amines on the dendrimer scaffold. The resulting PEGylated dendrimer **25** was purified via precipitation into ether to give a polymer with MW ~40,000 Da and PDI < 1.1, with an average particle size of 12 nm as determined by dynamic light scattering (DLS). Finally, residual linear PEG could be removed by dialysis using 100,000 MW cut-off dialysis tubing in water.

The benzyl ester protected side chains of the glutamic acid moieties in **25** were removed via hydrogenolysis, and the resultant carboxylic acids were treated with *t*-butyl carbazate and 1-ethyl-3-(3-dimethylaminopropyl)carbodiimide (EDC) to give dendrimer **26** with eight protected hydrazides available for drug attachment. Finally, target drug conjugate **27** was successfully obtained from the protected precursor **26** by removal of the Boc groups and subsequent condensation with doxorubicin in 5% pyridine/acetic acid solution of methanol at 60 ^{o}C.

The degradation profile of the ester-amide dendrimer hybrid was evaluated under physiological conditions. Polymer **26** was incubated at 37 ^{o}C in phosphate buffer at physiological pH and the molecular weight was monitored over 20 days by size exclusion chromatography (Figure 3a). As expected, the polymer degraded into 10 kDa and 5 kDa fragments as a result of the slow hydrolysis of both ester and carbamate moieties. Given that the threshold for renal clearance for linear polymers is estimated to be near 45,000 Daltons[48], cleavage of the 40,000 Dalton branched polymer following delivery of its payload contributes to prevent its long-term accumulation. The observed degradation profile is promising as it suggests that hybrid dendrimer **26** is sufficiently stable to allow for selective tumor uptake, yet can be eventually broken down and cleared.[9] It is also noteworthy that the drug is attached to a narrow population of polymeric material and that no significant amount of free drug is present as confirmed by the absence of a peak corresponding to free drug at 590 nm in the UV-vis trace of the conjugate (Figure 3b).

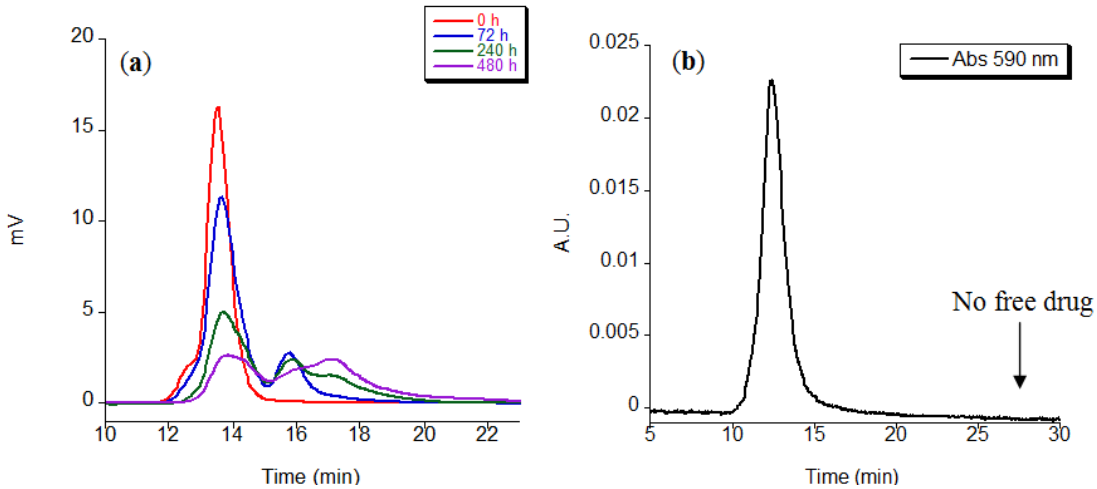

Figure 3. a) Size exclusion chromatographs of **26** in pH 7.4 PBS buffer at 37°C showing degradation over 20 days. b) UV-vis size exclusion chromatograph of **27** at 590 nm showing only polymeric UV active species.

Carrier drug loading was determined via UV-vis spectroscopy and could be varied from 6-10 wt/wt% depending on how many equivalents of doxorubicin were used in the loading step. Doxorubicin was chosen for attachment because it is a well-established and highly effective chemotherapeutic agent[49] that can benefit from conjugation to a carrier to decrease its innate cardiotoxicity. It is important to note that a variety of drugs, prodrugs, or other biological agents may potentially be attached to dendritic carriers based on **25** through its latent carboxylic acid side chains. The pH-dependence for the rate of hydrolysis of the hydrazone bond we formed is well studied[43,50,51], and we could confirm that the drug would be selectively released under acidic conditions similar to those found in the lysosome.[43] At pH 7.4, less than 5% of drug was released over 48 hours while the half-life of hydrolysis at pH 5 was 22 hours.

***In Vitro* Toxicity of Ester-Amide Dendrimer.**

The *in vitro* cytotoxicity tests showed that **26** remained non-toxic toward C26 cells at a concentration of 5 mg/mL. When Dox was conjugated to the carrier, a ten fold decrease in toxicity was observed over the free Dox ($IC_{50(\mathbf{27})}$ = 529.6 +/- 3.8 nM; $IC_{50(Dox)}$ = 52.4 +/- 12.7 nM). The decrease in toxicity may be attributed to the slower rate of uptake of the ester-amide carrier compared to free Dox and the slow hydrolysis of the drug from the carrier.

Conclusion

In conclusion, the attractive features of polyester and polyamide dendrimers have been combined to form a robust yet degradable polyvalent macromolecular scaffold that can be prepared in a scalable fashion. The final drug loaded dendrimer is made entirely from commercial starting materials in nine high-yielding steps, four of which are near quantitative deprotection steps. No chromatographic steps are required during the dendrimer preparation.

References

(1) Kopecek, J. (1977) Soluble Biomedical Polymers. *Polymers in Medicine 7*, 191-221.
(2) Bader, H., Ringsdorf, H., and Schmidt, B. (1984) Water soluble Polymers in Medicine. *Angewandte Makromolekulare Chemie 123*, 457-485.
(3) Seymour, L. W. (1992) Passive Tumor Targeting of Soluble Macromolecules and Drug Conjugates. *Critical Reviews in Therapeutic Drug Carrier Systems 9*, 135-187.
(4) Matsumura, Y., and Maeda, H. (1986) A New Concept for Macromolecular Therapeutics in Cancer-Chemotherapy - Mechanism of Tumoritropic Accumulation of Proteins and the Antitumor Agent Smancs. *Cancer Research 46*, 6387-6392.
(5) Liu, S., Maheshwari, R., and Kiick, K. L. (2009) Polymer-Based Therapeutics. *Macromolecules 42*, 3-13.
(6) Kataoka, K., Harada, A., and Nagasaki, Y. (2001) Block copolymer micelles for drug delivery: design, characterization and biological significance. *Advanced Drug Delivery Reviews 47*, 113-131.
(7) Guo, X., and Szoka, F. C. (2003) Chemical approaches to triggerable lipid vesicles for drug and gene delivery. *Accounts of Chemical Research 36*, 335-341.

(8) Christian, D. A., Cai, S., Bowen, D. M., Kim, Y., Pajerowski, J. D., and Discher, D. E. (2009) Polymersome carriers: From self-assembly to siRNA and protein therapeutics. *European Journal of Pharmaceutics and Biopharmaceutics 71*, 463-474.
(9) Fox, M. E., Szoka, F. C., and Fréchet, J. M. J. (2009) Soluble Polymer Carriers for the Treatment of Cancer: The Importance of Molecular Architecture. *Accounts of Chemical Research 42*, 1141-1151.
(10) Li, M. H., and Keller, P. (2009) Stimuli-responsive polymer vesicles. *Soft Matter 5*, 927-937.
(11) Green, J. J., Langer, R., and Anderson, D. G. (2008) A combinatorial polymer library approach yields insight into nonviral gene delivery. *Accounts of Chemical Research 41*, 749-759.
(12) Haag, R., and Kratz, F. (2006) Polymer therapeutics: Concepts and applications. *Angewandte Chemie-International Edition 45*, 1198-1215.
(13) Peer, D., Karp, J. M., Hong, S., FaroKHzad, O. C., Margalit, R., and Langer, R. (2007) Nanocarriers as an emerging platform for cancer therapy. *Nature Nanotechnology 2*, 751-760.
(14) Medina, S. H., and El-Sayed, M. E. H. (2009) Dendrimers as Carriers for Delivery of Chemotherapeutic Agents. *Chemical Reviews 109*, 3141-3157.
(15) Gillies, E. R., and Fréchet, J. M. J. (2005) Dendrimers and dendritic polymers in drug delivery. *Drug Discovery Today 10*, 35-43.
(16) Lee, C. C., MacKay, J. A., Fréchet, J. M. J., and Szoka, F. C. (2005) Designing dendrimers for biological applications. *Nature Biotechnology 23*, 1517-1526.
(17) Lee, C. C., Gillies, E. R., Fox, M. E., Guillaudeu, S. J., Fréchet, J. M. J., Dy, E. E., and Szoka, F. C. (2006) A single dose of doxorubicin-functionalized bow-tie dendrimer cures mice bearing C-26 colon carcinomas. *Proceedings of the National Academy of Sciences of the United States of America 103*, 16649-16654.
(18) De Jesus, O. L. P., Ihre, H. R., Gagne, L., Fréchet, J. M. J., and Szoka, F. C. (2002) Polyester dendritic systems for drug delivery applications: In vitro and in vivo evaluation. *Bioconjugate Chemistry 13*, 453-461.
(19) Parrott, M. C., Marchington, E. B., Valliant, J. F., and Adronov, A. (2005) Synthesis and properties of carborane-functionalized aliphatic polyester dendrimers. *Journal of the American Chemical Society 127*, 12081-12089.
(20) Bellis, E., Hajba, L., Kovacs, B., Sandor, K., Kollar, L., and Kokotos, G. (2006) Three generations of alpha,gamma-diaminobutyric acid modified poly(propyleneimine) dendrimers and their cisplatin-type platinum complexes. *Journal of Biochemical and Biophysical Methods 69*, 151-161.
(21) Krishna, T. R., Jain, S., Tatu, U. S., and Jayaraman, N. (2005) Synthesis and biological evaluation of 3-amino-propan-1-ol based poly(ether imine) dendrimers. *Tetrahedron 61*, 4281-4288.
(22) Chen, H. T., Neerman, M. F., Parrish, A. R., and Simanek, E. E. (2004) Cytotoxicity, hemolysis, and acute in vivo toxicity of dendrimers based on melamine, candidate vehicles for drug delivery. *Journal of the American Chemical Society 126*, 10044-10048.
(23) Lim, J. D., and Simanek, E. E. (2008) Synthesis of water-soluble dendrimers based on melamine bearing 16 paclitaxel groups. *Organic Letters 10*, 201-204.
(24) Lim, J., Guo, Y., Rostollan, C. L., Stanfield, J., Hsieh, J. T., Sun, X. K., and Simanek, E. E. (2008) The role of the size and number of polyethylene glycol chains in the biodistribution and tumor localization of triazine dendrimers. *Molecular Pharmaceutics 5*, 540-547.

(25) Esfand, R., and Tomalia, D. a. (2001) Poly(amidoamine) (PAMAM) dendrimers: from biomimicry to drug delivery and biomedical applications. *Drug Discovery Today 6*, 427-436.
(26) Khandare, J. J., Jayant, S., Singh, A., Chandna, P., Wang, Y., Vorsa, N., and Minko, T. (2006) Dendrimer versus linear conjugate: Influence of polymeric architecture on the delivery and anticancer effect of paclitaxel. *Bioconjugate Chemistry 17*, 1464-1472.
(27) Kono, K., Kojima, C., Hayashi, N., Nishisaka, E., Kiura, K., Wataral, S., and Harada, A. (2008) Preparation and cytotoxic activity of poly(ethylene glycol)-modified poly(amidoamine) dendrimers bearing adriamycin. *Biomaterials 29*, 1664-1675.
(28) Bhadra, D., Bhadra, S., Jain, S., and Jain, N. K. (2003) A PEGylated dendritic nanoparticulate carrier of fluorouracil. *International Journal of Pharmaceutics 257*, 111-124.
(29) Patri, A. K., Myc, A., Beals, J., Thomas, T. P., Bander, N. H., and Baker, J. R. (2004) Synthesis and in vitro testing of J591 antibody-dendrimer conjugates for targeted prostate cancer therapy. *Bioconjugate Chemistry 15*, 1174-1181.
(30) Malik, N., Evagorou, E. G., and Duncan, R. (1999) Dendrimer-platinate: a novel approach to cancer chemotherapy. *Anti-Cancer Drugs 10*, 767-776.
(31) Kaminskas, L. M., Kelly, B. D., McLeod, V. M., Boyd, B. J., Krippner, G. Y., Williams, E. D., and Porter, C. J. H. (2009) Pharmacokinetics and Tumor Disposition of PEGylated, Methotrexate Conjugated Poly-L-lysine Dendrimers. *Molecular Pharmaceutics 6*, 1190-1204.
(32) Kaneshiro, T. L., Wang, X., and Lu, Z. R. (2007) Synthesis, characterization, and gene delivery of Poly-L-lysine octa(3-aminopropyl)silsesquioxane dendrimers: nanoglobular drug carriers with precisely defined molecular Architectures. *Molecular Pharmaceutics 4*, 759-768.
(33) Okuda, T., Kawakami, S., Akimoto, N., Niidome, T., Yamashita, F., and Hashida, M. (2006) PEGylated lysine dendrimers for tumor-selective targeting after intravenous injection in tumor-bearing mice. *Journal of Controlled Release 116*, 330-336.
(34) Grinstaff, M. W. (2002) Biodendrimers: New polymeric biomaterials for tissues engineering. *Chemistry-a European Journal 8*, 2838-2846.
(35) Malik, N., Wiwattanapatapee, R., Klopsch, R., Lorenz, K., Frey, H., Weener, J. W., Meijer, E. W., Paulus, W., and Duncan, R. (2000) Dendrimers: Relationship between structure and biocompatibility in vitro, and preliminary studies on the biodistribution of I-125-labelled polyamidoamine dendrimers in vivo (vol 65, pg 133, 2000). *Journal of Controlled Release 68*, 299-302.
(36) Gillies, E. R., Dy, E., Fréchet, J. M. J., and Szoka, F. C. (2005) Biological evaluation of polyester dendrimer: Poly(ethylene oxide) "Bow-Tie" hybrids with tunable molecular weight and architecture. *Molecular Pharmaceutics 2*, 129-138.
(37) Gillies, E. R., and Fréchet, J. M. J. (2002) Designing macromolecules for therapeutic applications: Polyester dendrimer-poly(ethylene oxide) "bow-tie" hybrids with tunable molecular weight and architecture. *Journal of the American Chemical Society 124*, 14137-14146.
(38) Goodwin, a. P., Lam, S. S., and Fréchet, J. M. J. (2007) Rapid, efficient synthesis of heterobifunctional biodegradable dendrimers. *Journal of the American Chemical Society 129*, 6994-6995.
(39) Guillaudeu, S. J., Fox, M. E., Haidar, Y. M., Dy, E. E., Szoka, F. C., and Fréchet, J. M. J. (2008) PEGylated dendrimers with core functionality for biological applications. *Bioconjugate Chemistry 19*, 461-469.
(40) King, H. D., Yurgaitis, D., Willner, D., Firestone, R. A., Yang, M. B., Lasch, S. J., Hellstrom, K. E., and Trail, P. A. (1999) Monoclonal antibody conjugates of doxorubicin

prepared with branched linkers: A novel method for increasing the potency of doxorubicin immunoconjugates. *Bioconjugate Chemistry 10*, 279-288.
(41) Fox, M. E., Guillaudeu, S., Fréchet, J. M. J., Jerger, K., Macaraeg, N., and Szoka, F. C. (2009) Synthesis and In Vivo Antitumor Efficacy of PEGylated Poly(L-lysine) Dendrimer-Camptothecin Conjugates. *Molecular Pharmaceutics 6*, 1562-1572.
(42) Gabbay, E. J., Grier, D., Fingerle, R. E., Reimer, R., Levy, R., Pearce, S. W., and Wilson, W. D. (1976) Interaction Specificity of Anthracyclines with Deoxyribonucleic-Acid. *Biochemistry 15*, 2062-2070.
(43) Lee, C. C., Cramer, A. T., Szoka, F. C., and Fréchet, J. M. J. (2006) An intramolecular cyclization reaction is responsible for the in vivo inefficacy and apparent pH insensitive hydrolysis kinetics of hydrazone carboxylate derivatives of doxorubicin. *Bioconjugate Chemistry 17*, 1364-1368.
(44) Martinez, J., and Bodanszky, M. (1978) Side Reactions in Peptide-Synthesis.9. Suppression of the Formation of Aminosuccinyl Peptides with Additives. *International Journal of Peptide and Protein Research 12*, 277-283.
(45) Tekade, R. K., Kumar, P. V., and Jain, N. K. (2009) Dendrimers in Oncology: An Expanding Horizon. *Chemical Reviews 109*, 49-87.
(46) Kaminskas, L. M., Boyd, B. J., Karellas, P., Krippner, G. Y., Lessene, R., Kelly, B., and Porter, C. J. H. (2008) The impact of molecular weight and PEG chain length on the systemic pharmacokinetics of PEGylated poly L-lysine dendrimers. *Molecular Pharmaceutics 5*, 449-463.
(47) Denkewalter. (1982) *U.S. Patent*, 4,360,646.
(48) Seymour, L. W., Duncan, R., Strohalm, J., and Kopecek, J. (1987) Effect of Molecular-Weight (Mbarw) of N-(2-Hydroxypropyl)Methacrylamide Copolymers on Body Distribution and Rate of Excretion after Subcutaneous, Intraperitoneal, and Intravenous Administration to Rats. *Journal of Biomedical Materials Research 21*, 1341-1358.
(49) Kratz, F., Warnecke, A., Schmid, B., Chung, D. E., and Gitzel, M. (2006) Prodrugs of anthracyclines in cancer chemotherapy. *Current Medicinal Chemistry 13*, 477-523.
(50) Bae, Y., Nishiyama, N., Fukushima, S., Koyama, H., Yasuhiro, M., and Kataoka, K. (2005) Preparation and biological characterization of polymeric micelle drug carriers with intracellular pH-triggered drug release property: Tumor permeability, controlled subcellular drug distribution, and enhanced in vivo antitumor efficacy. *Bioconjugate Chemistry 16*, 122-130.
(51) Ulbrich, K., Etrych, T., Chytil, P., Jelinkova, M., and Rihova, B. (2003) HPMA copolymers with pH-controlled release of doxorubicin - In vitro cytotoxicity and in vivo antitumor activity. *Journal of Controlled Release 87*, 33-47.

Chapter 3: Influence of Carrier Architecture on *In Vivo* Behavior

Introduction

Polymeric drug delivery has enhanced the therapeutic profiles of multiple chemotherapeutic agents over the past few decades, with several polymer-drug conjugates in clinical use today.[1] This improved activity is brought about through several mechanisms, including increased aqueous solubility, an extension of the blood residence time of the conjugate compared to the small molecule drug, and elevated levels of drug delivered to the tumor site. However, these carriers still distribute highly toxic agents to nontargeted regions of a patient, and a major limitation of chemotherapy remains systemic toxicity resulting from high percentages of drug reaching undesired destinations *in vivo*. The bulk of recent efforts aimed at increasing drug accumulation in tumor tissue have pursued decoration of a polymeric drug carrier with targeting agents that can distinguish between tumorous and healthy cells, tissue or vasculature. However, because tumors chemically and physiologically resemble healthy tissue or cells in many respects, identification of a universal and highly selective cancer targeting agent has proven difficult when coupled with polymeric drug delivery.[2] A more commonplace approach to increasing the delivery of agents to tumors involves passive targeting achieved by exploiting the macroscopic and structural differences between tumorous and healthy tissues. One of these differences is the unusually permeable vasculature found in the vicinity of tumors. As described by the Enhanced Permeation and Retention (EPR) effect[3], this permeability allows macromolecules direct access to tumorous tissue by diffusion through the discontinuous endothelial lining of nearby blood vessels. Because this lining is more structurally competent in healthy tissues, permeation by macromolecules is more prohibited in these areas, leading to an overall enhanced delivery of polymeric agent to tumorous tissue. However, this effect does not result in a complete selectivity for macromolecular carriers, allowing room for improved exploitation of this tumor feature to achieve a more favorable biodistribution. One possible route of affecting this is to optimize the carrier's shape to achieve an architecture which is more sensitive to the differing vasculatures encountered *in vivo*. It has been established that a particle or polymer's shape bears influence on its ability to diffuse through different tissues, and hence its biodistribution. For instance, work by Uzgiris *et al* has shown that elongated polymers more readily cross the compromised endothelia membrane found in tumor vasculature.[4] Previous work in this area by our own group suggests that tumor tissue accumulates unusually high dose percentages of elongated polymers (up to 18% ID/g) compared to those generally seen for drug delivery vehicles of globular or nonspecific architectures. To build on these promising results, we report herein on an elongated dendronized linear polymer bearing Dox attached at the interior of the polymeric carrier through an acid-labile acylhydrazone bond (Figure 1). At its core is a poly-L-lysine (PLL) backbone (red), chosen because of its potential biodegradability, high water solubility, low polydispersity and functionalizable amine side chain. Near this backbone is the drug attachment site (black) binding Dox (green), and outside of this a fourth generation polyester dendrimer (blue) terminated with solublizing oligoglycol chains (orange). With this conjugate we intend to induce and utilize the elongation of the carrier to selectively deliver high levels of drug payload to cancerous cells in tumor tissue, thereby increasing the therapeutic efficiency of the chemotherapeutic agent.

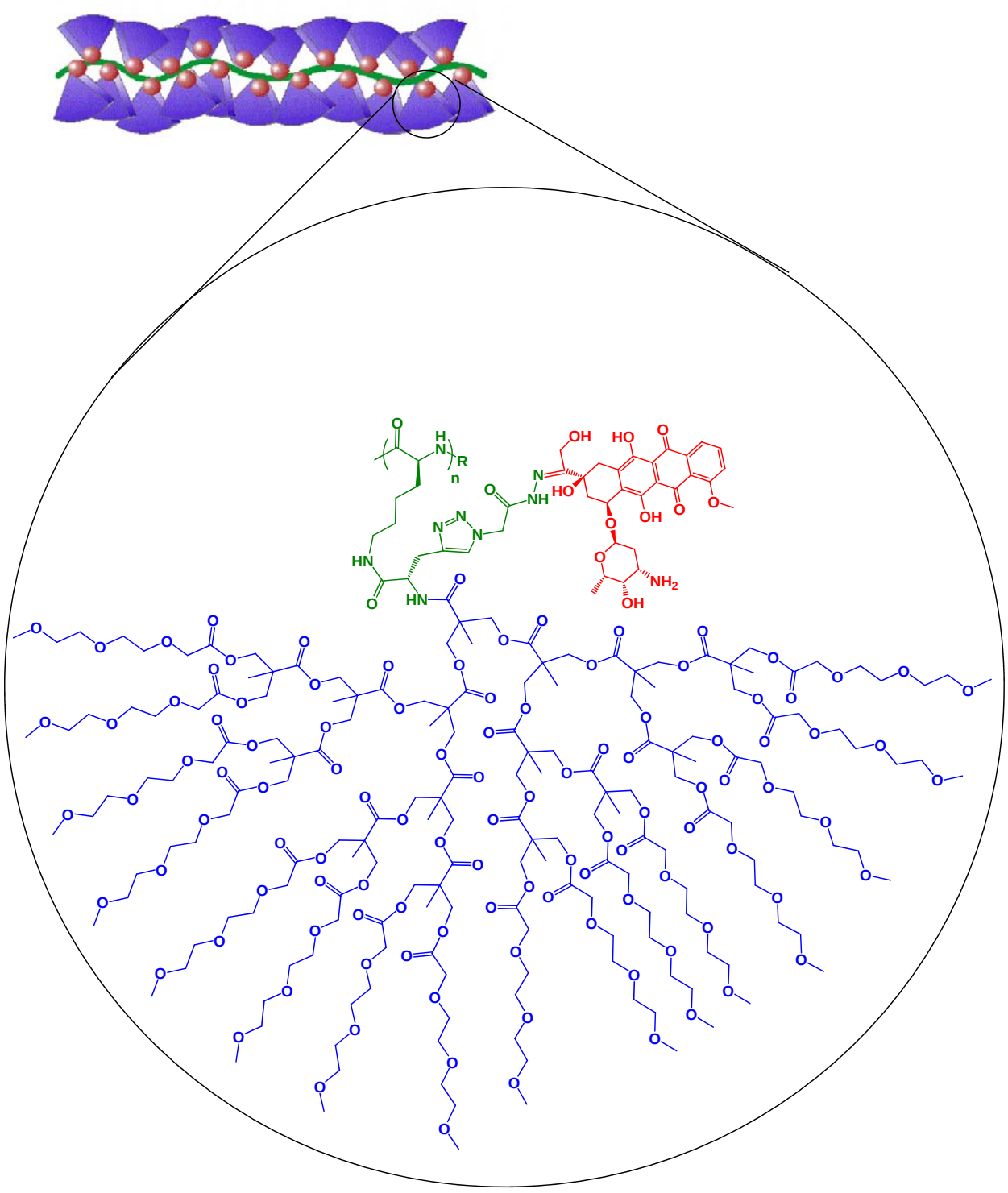

Figure 1. The target dendronized linear polymer.

Results and Discussion

Synthesis

Because polymer chains of differing lengths have different biological activities, polymeric drug conjugates must have a low (preferably < 1.2) polydispersity index (PDI, M_w/M_n) in order to have consistent and controlled therapeutic activity. As a result, the polymer chains comprising the backbone of the dendronized polymer must be of a uniform length. This excludes many common routes of polymerization such as condensation and standard radical polymerizations, as these yield polymers with wide and often uncontrollable distributions of molecular weight. One route for obtaining polymers of uniform and predictable molecular weight is the anionic ring opening polymerization of the N-carboxyanhydride (NCA) of amino acids (Scheme 1).[5] The desired mechanism of polymerization of NCA monomers involves ring opening by attack from a nucleophilic initiator, followed by decarboxylation to regenerate a nucleophilic chain end for propagation. However, side reactions are common. The NCA monomer must be of extremely high purity for a living polymerization to be obtained, as acidic impurities will protonate or poison the initiator and inhibit polymerization. Basic or nucleophilic impurities such as water lead to either a premature initiation of the polymerization via nucleophilic attach of the NCA, or removal of the amide proton of the NCA ring, giving rise to a monomer unit capable of initiating chain.

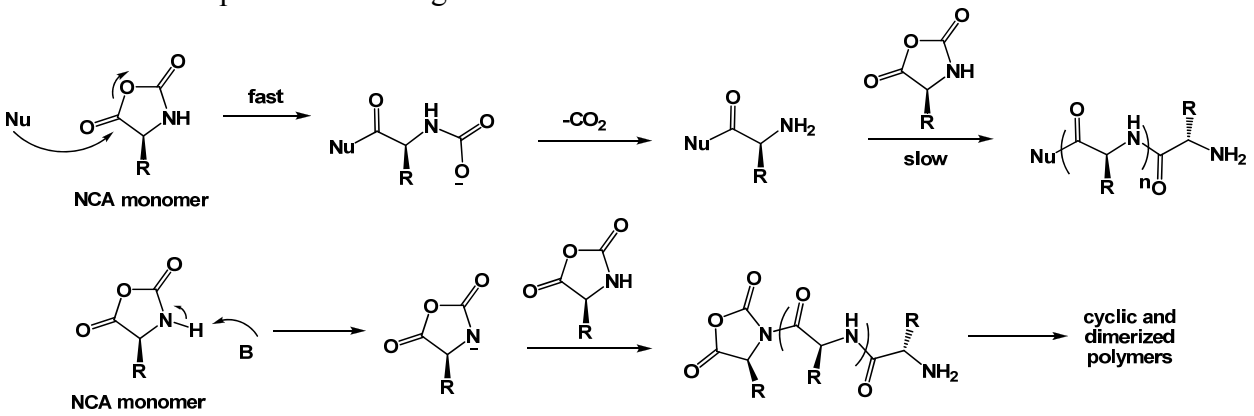

Scheme 1. The intended mechanism for NCA polymerization (top) and the base induced side reaction for monomer deprotonation and activation (bottom).

In order for the polymerization to meet the requirements for a living polymerization (ie, minimal chain transfer or termination and uniform growth of polymer chains), the initiation step must be fast relative to chain propagation. For this reason, the initiating nucleophile must have a higher nucleophilicity than the amine of the propagating polymer chain. However, many highly nucleophilic initiators such as hydroxide or alkoxides will also deprotonate the monomer, leading to side reactions. As a result, optimal initiators for this polymerization will have very high nucleophilicity to basicity ratios, a requirement met by primary amines.

In addition to a controlled molecular weight, the backbone for the dendronized linear polymer must also contain a synthetic handle for later functionalization and, preferably, be biodegradable in order to prevent accumulation *in vivo*. For these reasons, poly-$_L$-lysine (PLL) of a uniform and predictable molecular weight was pursued. PLL is biodegradable due to its amide backbone, and contains a primary amine side chain for synthetic elaboration. This controlled

polymerization was accomplished by the anionic ring opening polymerization of the NCA of commercial ε-CBZ protected lysine (**1**) using n-butylamine as an initiator (Scheme 2).

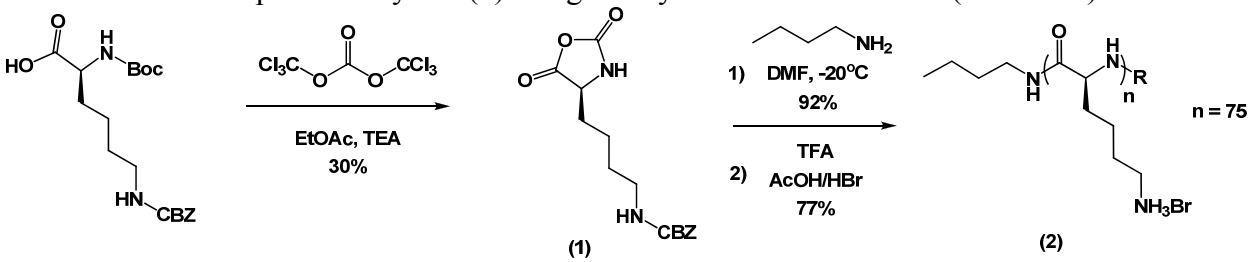

Scheme 2. Formation of the lysine NCA monomer (1) and its polymerization using n-butylamine.

Monomer **1** is synthesized by reaction of triphosgene in the presence of base. While the crude product is generally obtained in > 80% yield, multiple recrystallizations are required before material appropriate for a living polymerization can be obtained, as traces of water, HCl, TEA, decomposed NCA or triphosgene are each highly problematic for polymerization. After purification, **1** was polymerized using *n*-butylamine to yield ε-CBZ protected PLL (**2**). While similar polymerizations have been successfully carried out at elevated temperatures using the HCl salt of the amine initiator, superior polymers were obtained in this case using the free base at low temperatures, presumably due either to a higher selectivity between the initiation and propagation steps or a slowing of the decarboxylation of the carbamic acid intermediate. A chain length of 75 monomer units was pursued (Mn = 19,700), as this gives a theoretical molecular weight of approximately 80 kDa at the third generation of dendronization, which is the point at which previously investigated dendronized polylysines have transitioned to a rodlike conformation.[6] This molecular weight was pursued because it was expected to be of an optimal size for a favorable distribution in tumors, as polymers below ~40 kDa can be rapidly excreted from the blood and polymers over ~100 kDa tend to be removed by the renal system. Deprotection of the PLL's CBZ group by TFA and HBr in acetic acid yield PLL as the hydrogen bromide salt.

In order to elaborate the amine side chain of the PLL, a molecule was needed which would be capable of both dendronization and drug attachment. For this we chose a propargyl glycine derivative (**7**, Scheme 3) containing both an acetonide protected first generation polyester dendrimer and an alkyne for an eventual Cu(I) mediated Huisgen 1,3-dipolar cycloaddition, or "click reaction." In this case, click chemistry was attractive for two reasons. First, the alkyne is inert to the conditions to which the polymer will be subjected throughout the synthesis, allowing it to serve as a protected functional group but circumventing actual protection and deprotection steps. Secondly, because the Doxorubicin, a chemically fragile and reactive chemotherapeutic, would be introduced at a late stage of the synthesis after dendronization, it is important that a chemical route capable of obtaining high yields in sterically demanding environments such as this cycloaddition be used. Synthesis of **7** began with the previously described anhydride **4**, obtained from the reaction of acetonide protected 2,2-bis-(hydroxymethyl)propionic acid (**3**) with DCC. In order to facilitate the crystallization of anhydride **4**, it was found beneficial to add one half of an equivalent of DCC slowly to **3** at lowered temperature in order to prevent the intermolecular cyclization of the activated intermediate to give the N-acyl urea side product (not shown). Anhydride **4** was then used to acylate the methyl ester of propargyl glycine (**5**), which was obtained in high yield from the reaction of propargyl glycine with thionyl chloride in methanol. This yielded methyl ester **6**,

which was deprotected under mild conditions and reacidified to give the multifunctional molecule **7**. This compound contains three separate synthetic functional handles: a carboxylic acid for coupling to the PLL backbone, a protected first generation dendrimer, and an alkyne for eventual drug attachment.

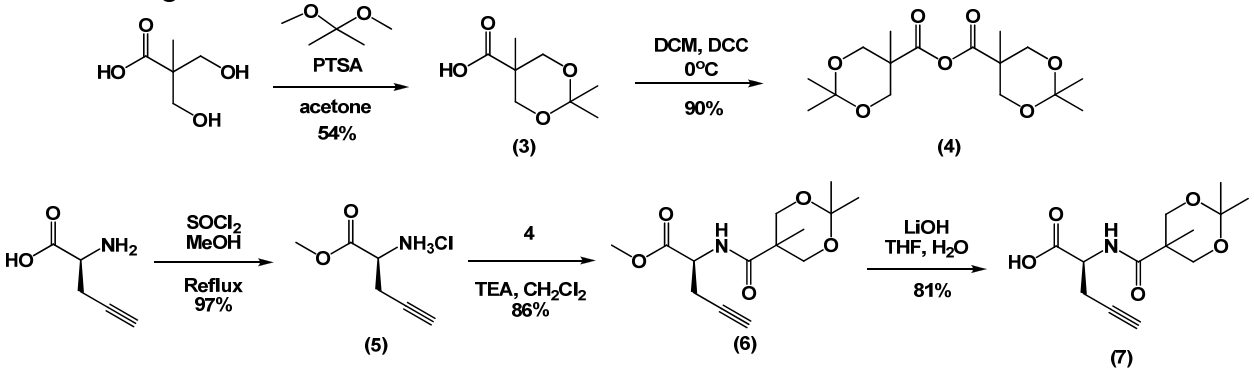

Scheme 3. Synthesis of a multifunctional molecule for a drug, dendrimer and polymer backbone attachment point.

Attachment of **7** to polymer **2** was carried out with DCC under standard peptide bond forming conditions (Scheme 4). Because the polymer obtained contains a first generation dendrimer protected as an acetonide, it is denoted as **G1An**. This coupling installed the desired drug attachment and dendronization locales onto the polymer backbone.

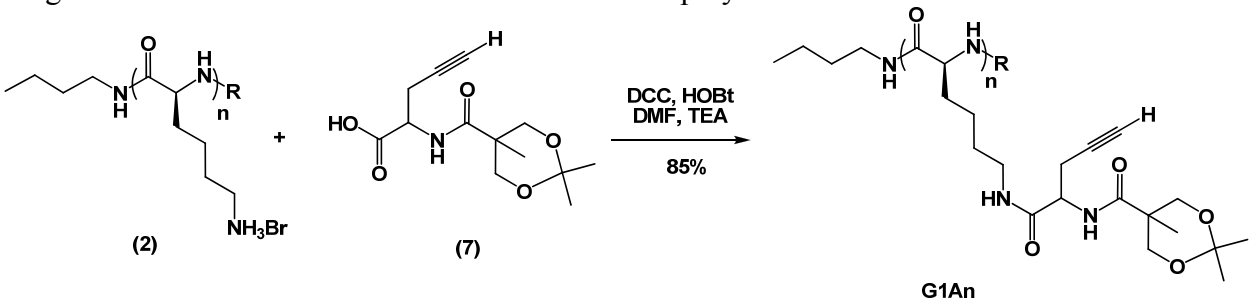

Scheme 4. Synthesis of a side chain functionalized poly-$_L$-lysine (PLL) containing an alkyne for eventual drug attachment and an acetonide protected first generation dendrimer. n = 75.

Dendronization of **G1An** was carried out by an iterative process of deprotection of the acetonide group with catalytic acid followed by introduction of the next generation by reaction with anhydride **4** (Scheme 5). In order to maintain fidelity to the theoretical structure of the polymer, it is imperative that these reactions go to completion (lower yields in schemes arise from nonquantitative recoveries from dialysis and precipitation purification steps), as separation of perfectly and imperfectly formed polymers is extremely difficult. To accomplish this, concentrated conditions, resubjections, and/or large excesses of reagents were employed at each step. Maintaining the polymer notation used for **G1An**, polymers of *x* dendrimer generations with an acetonide protected periphery are labeled as G*x*An, and polymers with a hydroxyl periphery are labeled as G*x*OH (Scheme 5).

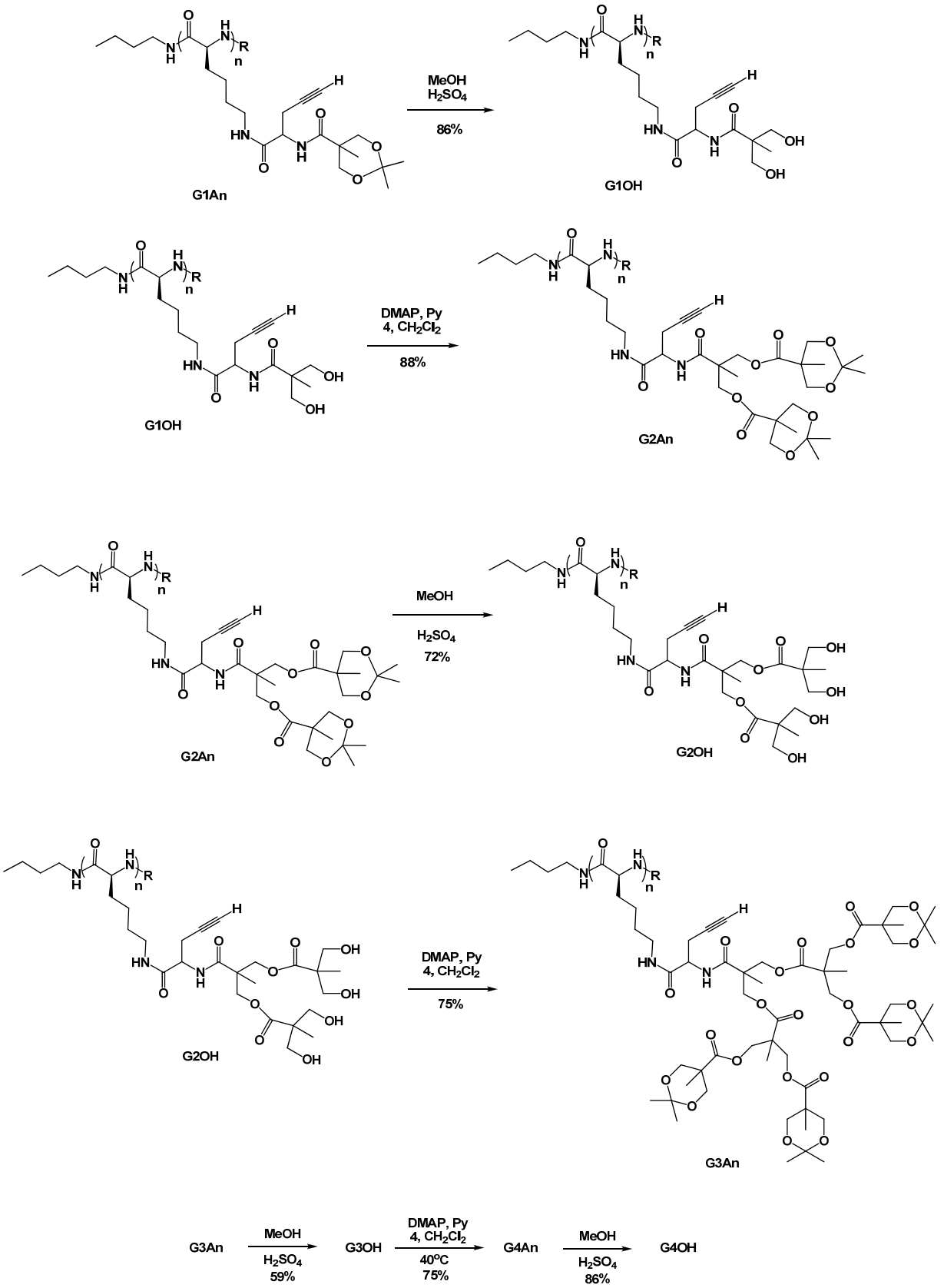

Scheme 5. Iterative dendronization of PLL.

While previous studies investigating dendronized PLL found linearization of the backbone at the third generation, circular dichroism experiments (Figure 2) showed that in this case the third generation of dendronized polymer still possessed the α-helix conformation, indicating that elongation of the polymer had not occurred. This may be because upon inserting the drug linkage site between the lysine backbone and dendrimers, the dendrons were positioned further from the backbone and each other, diminishing their ability to sterically force the backbone into a linear conformation. To overcome this we proceeded to a fourth generation alcohol terminated dendrimer, **G4OH**, which provided sufficient steric strain to bring about the necessary conformation change.

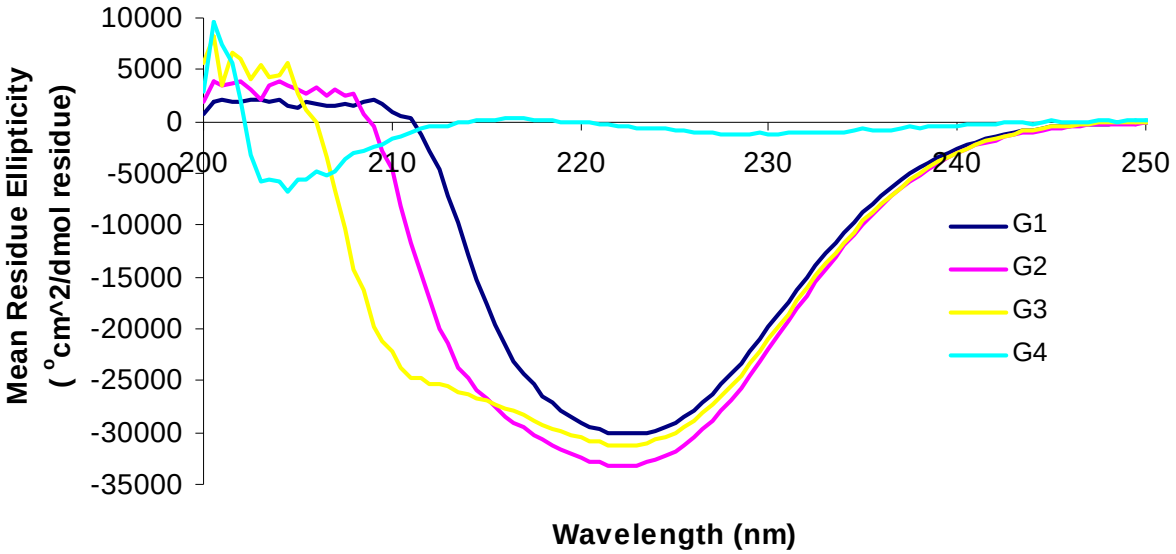

Figure 2. Circular Dichroism (CD) traces showing transition between α helix and linear conformations upon adding the fourth generation of dendrimer.

As shown in Table 1, the PLL backbone was synthesized with a low polydispersity and has a molecular weight in good agreement with the target molecular weight. Furthermore, dendronized polymers derived from this backbone gave molecular weights agreeing well with the theoretical weight throughout the dendronization process, indicating good fidelity to the theoretical polymer structure. As expected from previous results, molecular weights obtained by DMF SEC using linear polyethylene glycol standards are artificially lowered.[7] This is due to the highly branched and dense nature of the dendronized polymers, which have a lower hydrodynamic volume than the linear PEG standards of similar molecular weights. While SEC is a capable mode of characterization for polydispersity, for more accurate determination of molecular weight MALS (multiangle light scattering) was employed, as this measurement is independent of polymer branching effects. The SEC traces of the alcohol terminated polymers also show polymer peaks that are monomodal, symmetrical and of low polydispersity throughout the dendronization process (Figure 3).

Polymer	Mn (SEC)	PDI (SEC)	Mn (MALS)	St Dev	Theoretical Mn (n = 75)
PLL-CBZ	8,000	1.13	19,700	1,100	19,700
G1An	11,000	1.11	-	-	28,400
G1OH	600	3	27,500	800	25,600
G2An	15,000	1.12	48,200	4,900	48,800
G2OH	12,000	1.09	42,200	1,600	43,000
G3An	27,000	1.18	83,500	3,500	89,700
G3OH	23,000	1.14	76,600	2,600	77,600
G4An	38,000	1.16	160,000	5,000	170,000
G4OH	19,000	1.16	141,000	7,600	146,000

Table 1. Molecular weights and polydispersities (Mn/Mw) of PLL and its dendronized derivatives, as well as their theoretical molecular weighs for a degree of polymerization of 75 monomer units.

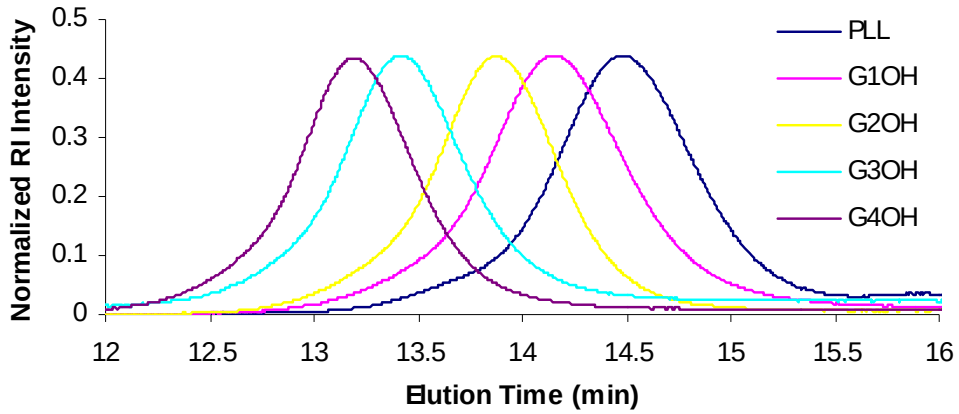

Figure 3. DMF SEC overlay of the PLL backbone and its dendronized derivatives.

In order for Doxorubicin to be delivered selectively to intracellular environments rather than released in the blood stream, an acid labile acyl hydrazone bond was used to bind the Dox to the polymer carrier (see Chapter 1, scheme 1). This bond has been shown to be stable in neutral media such as the blood serum, but is cleaved in slightly acidic environments such as the endosomes of cells. In order to attach Dox to the fourth generation polymer in this way, a linker molecule (**9**) was synthesized containing both an azide for coupling to the alkyne of the polymer and a *tert*-butoxycarbonyl (Boc) protected hydrazide for eventual reversible binding to Dox. This accomplished by the reaction of Boc protected hydrazine with chloroacetyl chloride to give chloride **8**. Displacement of the chloride using sodium azide yields **9**, which can then be installed into the dendronized polymer **G4OH** using the commonly employed copper catalyzed Huisgen cycloaddition (Scheme 6). Because the alkyne has been changed to a Boc protected hydrazide, the polymer is labeled as **G4(Boc)OH** after linkage to **9**.

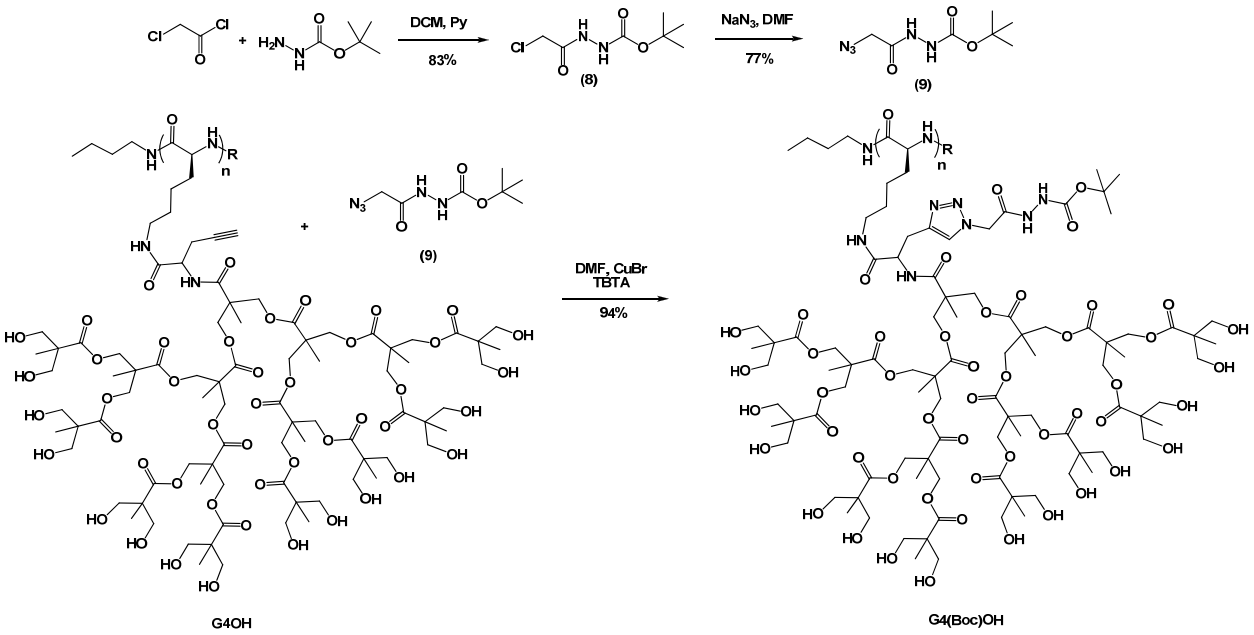

Scheme 6. Synthesis of a linker molecule for drug attachment through an acid sensitive acyl hydrazone bond, and its attachment to the polymer using click chemistry.

However, dynamic light scattering (DLS) data and casual observations of warmed aqueous solutions of polymer **G4OH** and **G4(Boc)OH** indicated that upon adding the fourth generation of dendrimer the carrier obtains a lower critical solution temperature (LCST) of approximately 39 ^{o}C (Figure 4), although clouding and precipitation were observed by eye at slightly lower temperatures. This would cause aggregation of the conjugate in biological systems, and to regain solubility at physiological temperatures the alcohol periphery of the dendrimer was esterified with short oligogylcol chains (Scheme 7). After this the polymer was found to dissolve well in warm aqueous solutions, and DLS data shows a lack of aggregation for the glycol coated polymer, **G4(Boc)Gly**, upon heating.

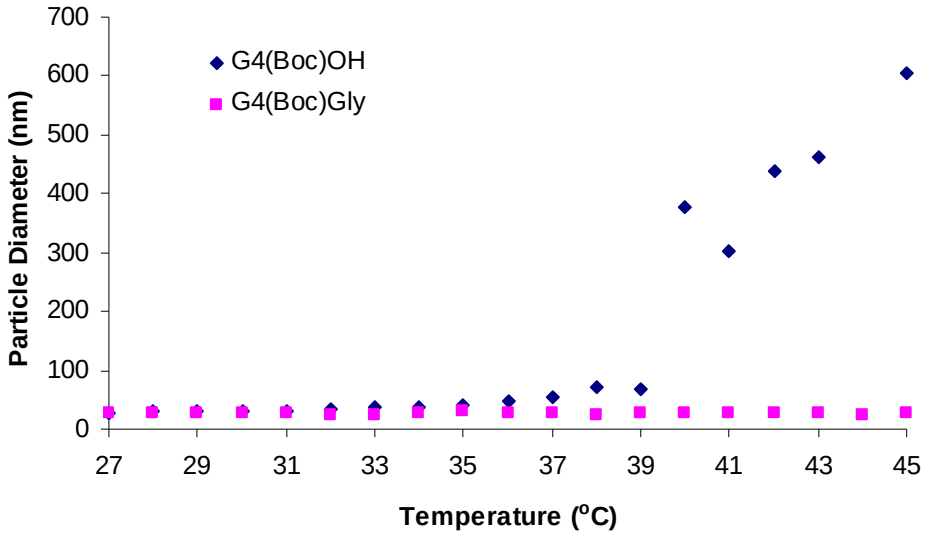

Figure 4. Aggregation of **G4(Boc)OH** in water above ~37°C. The **G4(Boc)Gly** polymer remains soluble at higher temperatures.

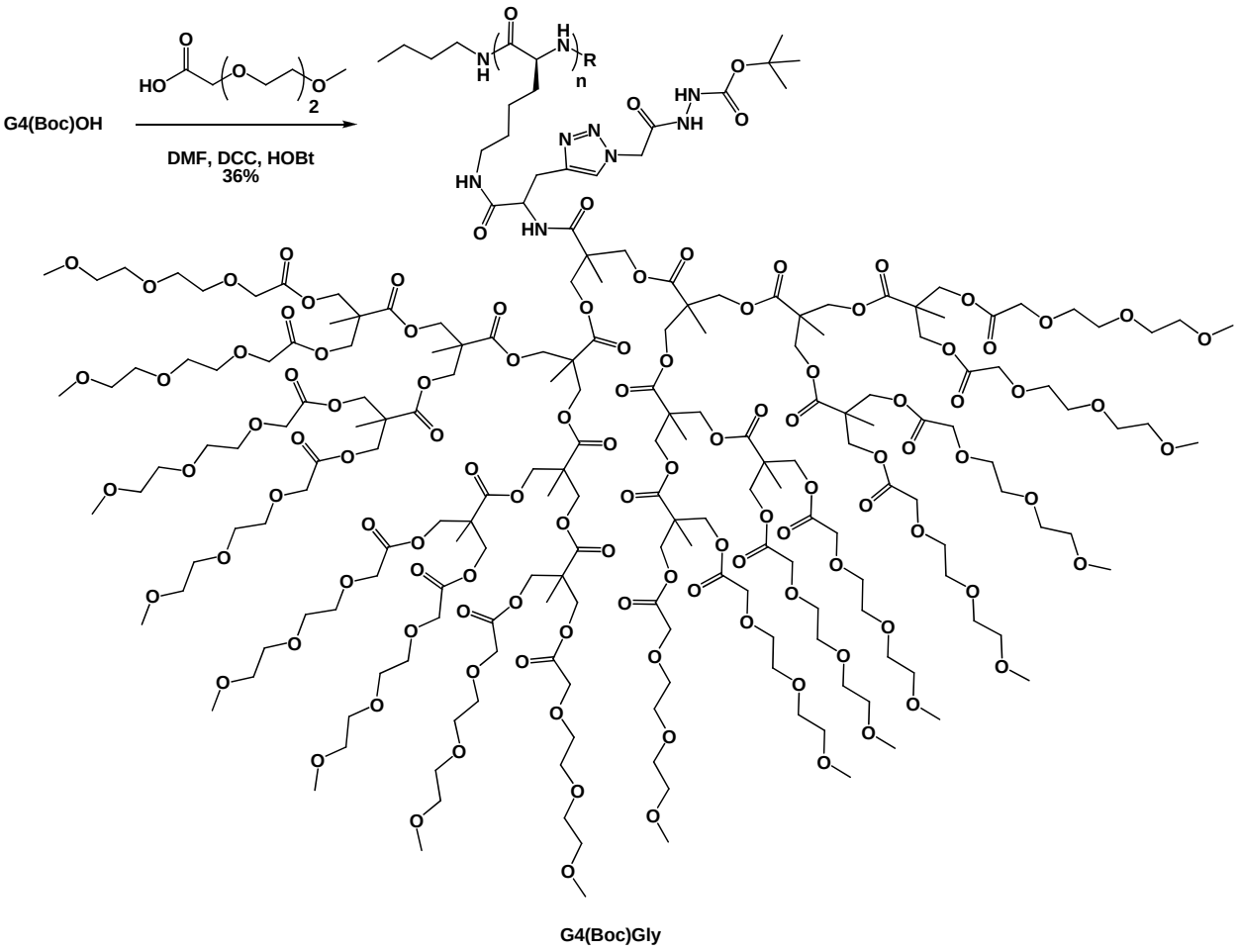

Scheme 7. Addition of short glycol chains to the periphery of **G4(Boc)OH** to overcome limited aqueous solubility at physiological temperatures.

To complete the synthesis, Dox was attached by Boc deprotection of the hydrazide followed by condensation to the ketone of Dox in methanol buffered to pH using acetic acid and pyridine (Scheme 8). Dox loading of the polymer formed, **G4(Dox)Gly**, indicated a nearly quantitative loading of 10% Dox by weight. The Doxorubicin (**red**) sits near the linearized lysine backbone (**black**), attached through a propargyl glycine derived linker containing an acyl hydrazone bond (**green**) and situated underneath a fourth generation polyester dendrimer (**blue**) solubilized by short oligoglycol chains (**orange**). The steric repulsions are expected to be considerable.

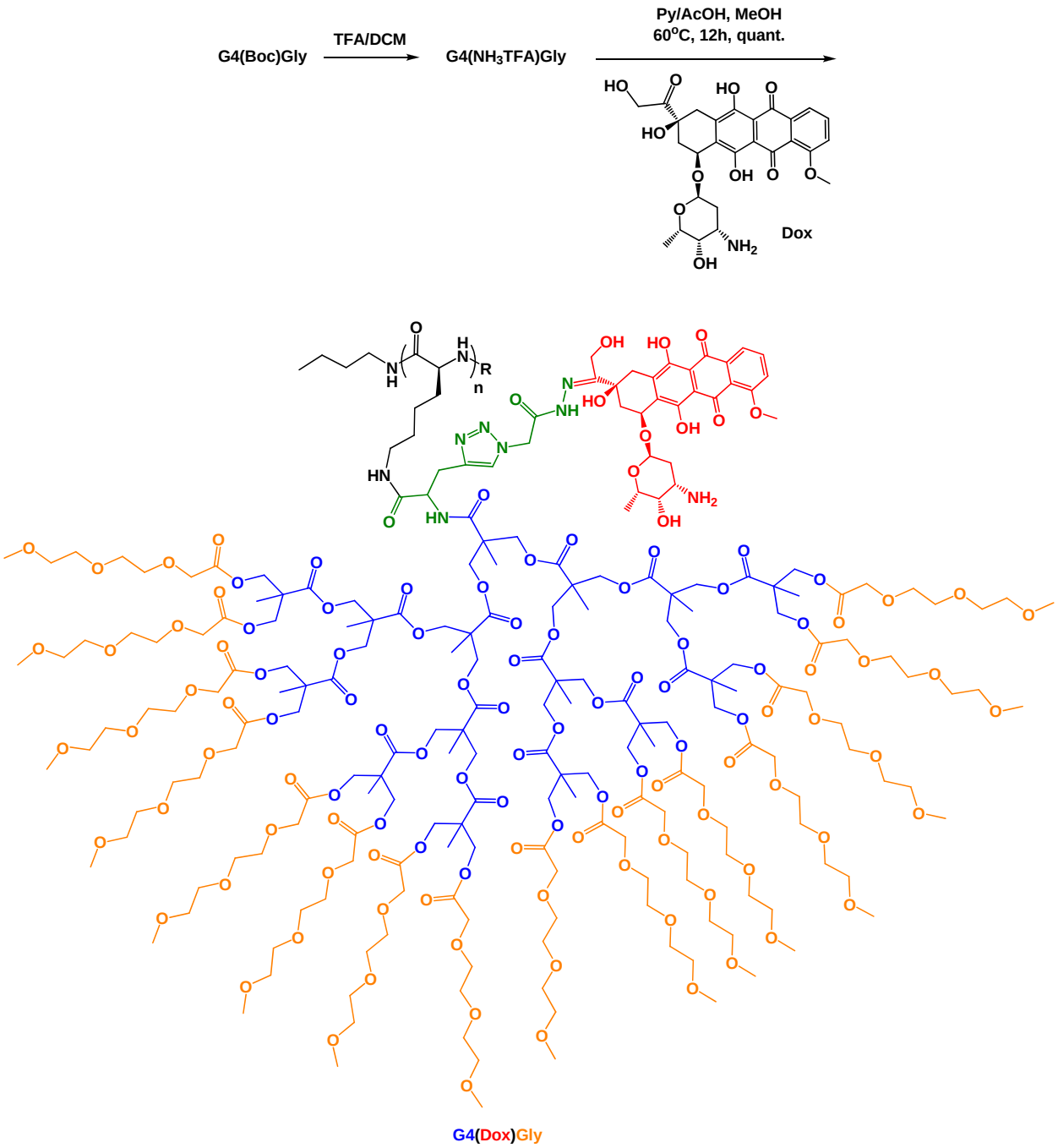

Scheme 8. Formation of the final drug loaded dendronized linear polymer, **G4(Dox)Gly**.

Evaluation *in Vivo*

To test whether this polymer is capable of accumulating at high levels in tumor tissue, the biodistribution of **G4(Dox)Gly** in tumored mice was determined for time points corresponding to one half hour, eight hours and twenty four hours (Figure 5). The distribution for free doxorubicin was also determined over twenty four hours as a control. When administered to mice, in twenty

four hours about six percent of the injected dose of the polymeric carrier accumulated per gram of tumor tissue, whereas negligible levels of free doxorubicin accumulation were observed. While the polymer's tumor accumulation of 6% was significantly below that obtained in pervious work with non-drug loaded dendronized linear polymers[8], the tumor accumulation is 150% higher than the accumulation in the organ showing the second highest accumulation, and we observe very low or negligible accumulation of the polymer in many organs, including the spleen and kidneys.

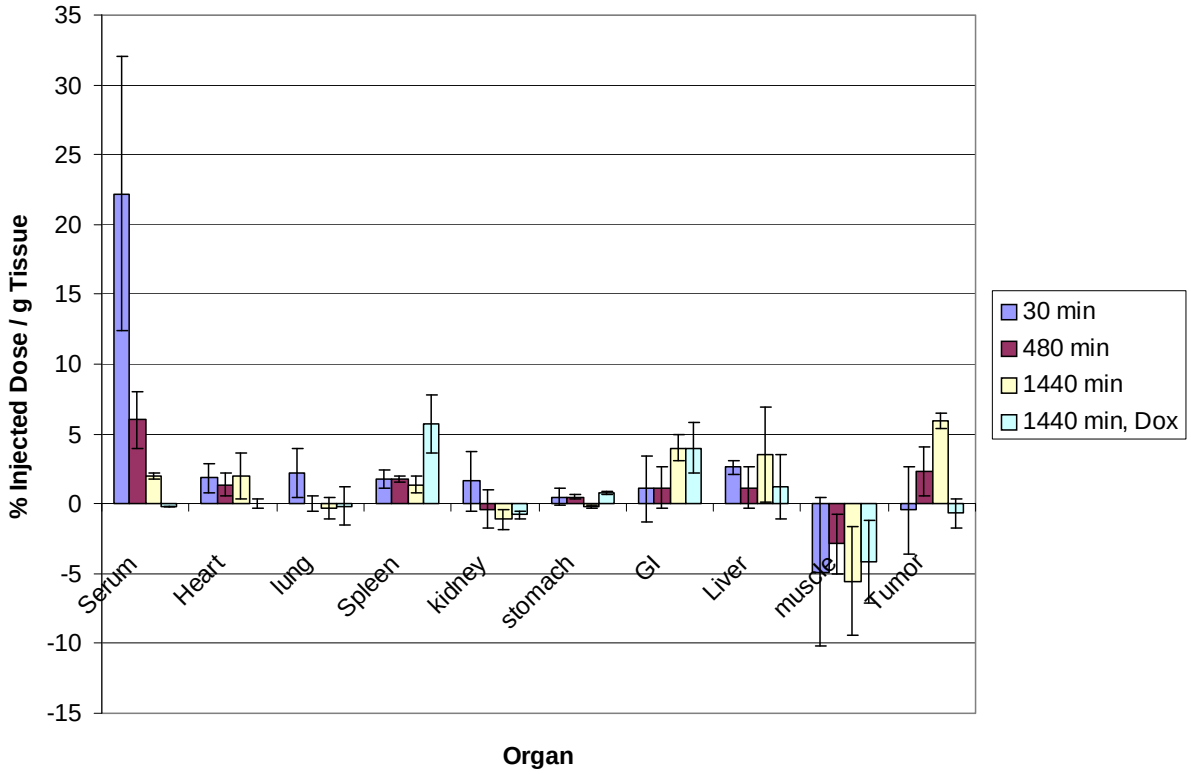

Figure 5. Biodistribution of free Dox ad **G4(Dox)Gly** in tumored mice over 24 hours.

A likely cause for a tumor accumulation lower than previously evaluated dendronized linear polymers is indicated in the AFM of our current polymer carrier as shown in Figure 6. On the left is a representative SFM image of a G3 steroylated linear dendronized polymer which was shown to have high tumor accumulation in mice.[7]

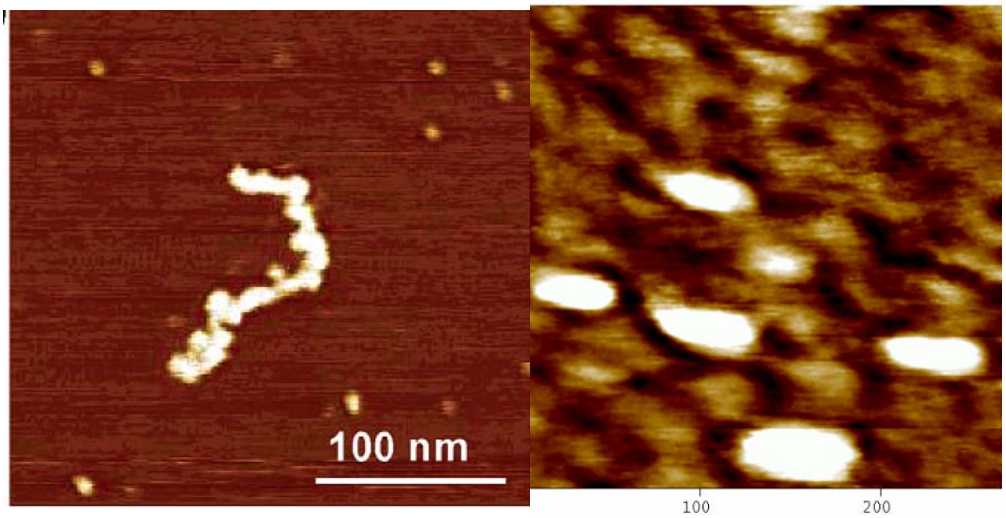

Figure 6 AFM of a previously synthesized dendronized polymer (left) and the currently investigated polymer (right).

The degree of polymerization is approximately 1300, and a high aspect ratio is expected assuming an extended conformation in vivo. However, for the dendrimer studied here the aspect ratio is estimated to be as low as five or six.[9]

Conclusion

In this work we have synthesized a water soluble fourth generation dendronized linear polymer bearing doxorubicin for investigation of the influence of carrier rigidity and elongation on tumor accumulation. Due to the introduction of a spacer between the backbone and pendant dendrimers for a drug attachment location, the PLL backbone transitions from an α-helix to an extended randomly coiled chain upon adding the fourth generation of the polyester dendrimer, rather than the third dendrimer generation as reported for directly dendronized PLL. The adding of this dendrimer generation also results in a LCST in water at approximately physiological temperature, which may have potential for targeted hyperthermic treatment strategies. For the current investigation, complete aqueous solubility at physiological temperatures was restored by acylating the alcohol periphery with short oligoglycol chains. The drug bearing polymer shows an accumulation of 6 weight percent of the initial dose per gram of tumor tissue after twenty four hours, which is a higher accumulation than that seen in other tissues, but less than that observed in tumors by previously investigated linear dendronized polymers possessing higher aspect ratios. It is possible that due to the unanticipated addition of the large fourth generation dendrimer and glycol periphery, the aspect ratio obtained for the polymer may be insufficient to realize the effects of a linearized architecture as described elsewhere.[11] However, the dendrimer also shows at least a 150% selectivity over other tissues, indicating that selectivity for tumorous tissue has been retained. This finding may have impact on considerations for future polymeric carriers relying on architecture and shape for targeting ability.

Experimental Procedures

Materials and Methods

General

Unless otherwise noted, all reagents were used as received and without further purification, or were prepared according to literature procedure. Unless otherwise specified, organic extracts were dried over anhydrous $MgSO_4$ and solvents were removed with a rotary evaporator under reduced pressure. Methylene chloride, tetrahydrofuran (THF), toluene, pyridine, *N,N*-dimethylformamide (DMF), and triethylamine were purchased from Fisher and vigorously purged with nitrogen for 1 h. The solvents were further purified by passing them under nitrogen pressure through two packed columns (Glass Contour) of neutral alumina (for THF and methylene chloride), neutral alumina and copper (II) oxide (for toluene), or activated molecular sieves (for DMF). All glassware was flame dried under vacuum or nitrogen purge prior to use and reactions were conducted under a nitrogen atmosphere. Unless otherwise noted, liquid reagents were introduced to the reaction flask via syringe or cannula. Unless otherwise noted, all NMR spectra were measured in $CDCl_3$ with TMS or solvent signals as the standards. Shifts are reported in ppm and coupling constants are reported in Hz. Elemental analyses were performed by the University of California, Berkeley Mass Spectrometry Facility. IR spectroscopy was performed on a Mattson Genesis II FTIR in KBr. Unless otherwise noted, purifications using dialysis were carried out in water using regenerated cellulose dialysis membranes with a 3,500 molecular weight cutoff. Previously prepared compounds were determined to be pure within the limits of NMR analysis, except where otherwise noted. Size exclusion chromatography (SEC) was carried out at 1.0 mL/min in two PL gel mixed-bed C columns (7.5 x 300 mm) with a particle size of 5 microns using DMF with .2% lithium bromide as a solvent and PMMA or PEO as standards. The SEC system consisted of a Waters 510 pump, a Waters U6K injector, a Waters 486 UV-Vis detector, and a Waters 410 differential refractive index (RI) detector. Multiangle light scattering (MALS) experiments were performed using DMF with 0.2% LiBr as a solvent on a chromatography line containing two 7.5 x 300 mm PLgel mixed-bed C columns with a 5 micron particle size fitted with a Waters 510 pump, a 7125 Rheodyne injector, a Wyatt Optilab differential refractive index detector and a Wyatt DAWN-EOS MALS detector. Absolute molecular weights determined from light scattering data were calculated using Astra software from Wyatt assuming a quantitative mass recovery (online method). Columns used in MALS and SEC experiments were thermostatted at 70^{o}C. Dynamic light scattering (DLS) was performed using a Zetasizer Nano ZS (Malvern Instruments) equipped with a 4 mW He-Ne laser at 633 nm. Circular Dichroism (CD) spectroscopy was performed using an AVIV 62DS circular dichroism spectrometer. Measurements were recorded at 25 ^{o}C with sampling every .5 nm with a 5 s averaging time over the range of 180-270 nm (bandwidth = 1.5 nm). Solutions were made in 1 M PBS buffer with polymer concentrations between 100 and 500 μg/mL. AFM was performed using a Digital Instruments (Veeco) Multimode Atomic Force Micrometer with a Nanoscope IIIa controller and tap 300 tips in tapping mode. Samples were cast from a 1 μg/mL solution in chloroform onto silica surface at 3200 rpm. Biodistribution studies were carried out with as reported previously.[10]

ε-carboxybenzoyl (CBZ) lysine N-carboxyanhydride (NCA) (1). To a 1-L flask was added ε-carboxybenzyloxy-N-*tert*-butoxycarbonyl-$_L$-lysine (21.0 grams, 55.2 mmol) followed by ethyl

acetate (900 mL) and stirred. To this was added triphosgene (7.09 g, 23.9 mmol). The reaction was then stoppered using a rubber septum and a purge needle was added to allow for the escape of residual air and gaseous byproducts. For approximately 2 min the triphosgene was allowed to dissolve, and then triethylamine (8.4 mL, 60.7 mmol) was added in one portion. A white slurry quickly formed, and the reaction was allowed to stir for 24 h. The viscous liquid was then quickly filtered under a nitrogen flow to remove the salts formed, and the filtrate was concentrated to yield a hard white solid. A nitrogen atmosphere was reintroduced, and the crude product was dissolved at room temperature in methylene chloride (ca. 150 mL). An equal portion of hexanes was then added slowly with stirring, causing the precipitation of white solids. This solution was stored at –20 ^{o}C overnight under positive nitrogen pressure to complete the precipitation. This slurry was then again filtered under a nitrogen flow, and the crude solid obtained was then further purified by iterative recrystallizations carried out under a nitrogen atmosphere at room temperature in methylene chloride/hexanes and ethyl acetate/hexanes until aqueous washings of the filtrate were neutral by litmus paper. When recrystallizing in methylene chloride and hexanes, it was found to be beneficial to employ a 2-fold excess of the required volume of methylene chloride for complete dissolution in order to avoid a complete solidification of the recrystallizing solution upon the addition of hexanes. By this method 5.62 g (33%) of **2** was obtained as a white crystalline solid. Spectroscopic data was consistent with that reported in literature for compounds prepared by different means.[27;28]

ε-CBZ Poly-L-lysine To a flask charged with freshly recrystallized **1** (5.50 g, 18.0 mmol) was added DMF (100 mL) that had been degassed by three freeze-pump-thaw cycles. In a separate flask, *n*-butylamine (0.095 mL, 0.961 mmol) freshly distilled from calcium hydride was dissolved in similarly degassed DMF (4.0 mL). With vigorous stirring, the monomer solution was heated to 50 ^{o}C and 1.0 mL of the initiator stock solution containing 23.8 μL (0.24 mmol) of *n*-butylamine was added in one portion. After stirring 12 h the mixture was precipitated in cold ether (ca. 100 mL) to give a white oil. The product was then dissolved in methylene chloride (ca. 25 mL) and precipitated in hexanes (ca. 200 mL) to give ε-CBZ protected poly-$_{L}$-lysine (4.61 g, 98%) as a white solid. Spectroscopic characterization was consistent with the literature. SEC: PEO: M_n=8,000 Da, PDI= 1.13.

Poly-L-Lysine hydrogen bromide (2). In a typical experiment, trifluoroacetic acid (180 mL) was added to protected polylysine (8.6 g, 32.8 mmol) in a 250 mL flask and stirred. To this was added of HBr as a 33% wt solution in acetic acid (10 mL, 115 mmol). The solution was then stirred for 5 h at RT and precipitated into cold ether (400 mL). In the cases that product was observed to oil out of the reaction, methanol was added to aid solvation prior to the precipitation. After collecting the polymer by filtration and washing with ether, it was redissolved in methanol and precipitated again in ether. After isolating by filtration **2** (5.3 g, 77 %) was obtained as an orange solid. Spectroscopic characterization was consistent with the literature.[29]

D,L-Propargylglycine methyl ester hydrogen chloride (**5**). ThiTo a flask containing propargyl glycine (3.00 g, 26.5 mmol) was added methanol (100 mL). With vigorous stirring, thionyl chloride (6.5 g, 55 mmol) was added. The solution was heated at reflux for 6 h, and was then concentrated to give **5** (4.14 g, 96%) as a hard white solid which was used without further purification. ^{1}H NMR (400 MHz, $CDCl_3$): δ 2.30 (s, 1), 3.00-3.25 (q, 2, *J* = 16.4, 38.8), 3.88 (s, 3), 4.44 (s, 1), 8.85 (s, 1).

D,L-Propargylglycine methyl ester G1 acetonide (**6**). To a flask charged with **5** (4.1 g, 25 mmol) was added **4** [30] (9.2 g, 28 mmol) and methylene chloride (50 mL). To this solution was added triethylamine (4.0 mL, 29 mmol) and the reaction was stirred 12 h. The excess **4** was quenched at 0 ^{o}C with asymmetric dimethylethylene diamine (0.5 mL), and stirred 10 min. The reaction was diluted with methylene chloride (ca. 50 mL), cooled to 0 ^{o}C and washed with 1 M $NaHSO_4$ (2 x 20 mL), 5% $NaHCO_3$ (2 x 20 mL), water (2 x 20 mL), and brine (20 mL). The organic layer was dried, filtered, and concentrated to an oil. Recrystallizations in methylene chloride/hexanes gave **6** (3.70 g, 52%) as fine needles. Mp: 105-107 ^{o}C. ^{1}H NMR (400 MHz, $CDCl_3$): δ 1.02 (s, 3), 1.47 (d, 6, *J* = 24), 2.03 (t, 1, *J* = 2.8), 2.81 (s, 2), 3.73 (d, 2, *J* = 10.5), 3.76 (s, 3), 3.92 (d, 2, *J* = 11), 4.76 (m, 1), 8.01 (br s, 1). ^{13}C NMR (400 MHz, $CDCl_3$) δ 17.8, 18.5, 22.6, 26.3, 28.8, 40.4, 51.0, 52.8, 67.1, 67.3, 78.9, 98.8, 171.0, 174.9. FTIR: 3356 (m), 3285 (m), 2293 (m), 2954 (m), 2874 (m), 1747 (s), 1665 (s), 1523 (s), 1439 (m), 1375 (m), 1202 (s), 1081 (s). Anal. Calcd. for $C_{14}H_{21}NO_5$: C, 59.35; H, 7.47; N, 4.94. Found: C, 59.67; H, 7.78; N, 5.02.

D,L-Propargylglycine acid G1 acetonide (**7**). To a flask containing **6** (3.70 g, 13.07 mmol) was added THF (50 mL). In a separate flask, lithium bromide (0.63 g, 26 mmol) was dissolved in H_2O (20 mL). The two solutions were combined and stirred 30 min. The reaction was then diluted with water (ca. 50 mL) and methylene chloride (ca. 50 mL) and transferred to a 200 mL separation funnel, and the pH was adjusted to approximately 7 using 1M $NaHSO_4$. The solution was then shaken and the organic layer removed. The aqueous layer was reacidified using additional $NaHSO_4$, and extracted with methylene chloride (2 x 20 mL). The combined organic extracts were dried and concentrated to a viscous oil. Recrystallization in methylene chloride/hexanes produced an oil which crystallized upon freezing. Washing with hexane and drying gave **7** (2.85 g, 81%) as a white crystalline solid. Mp: 124-127 ^{o}C. ^{1}H NMR (400 MHz, $CDCl_3$): δ 1.02 (s, 3), 1.50 (d, 6, *J* = 6), 2.06 (t, 1, *J* = 3.2), 2.86 (q, 2, *J* = 3.6, 2.4), 3.89 (q, 4, *J* = 16.4, 51.6), 4.84 (dt, 1, *J* = 6.4, 10), 8.12 (d, 1, *J* = 10). ^{13}C NMR (500 MHz $CDCl_3$): δ 17.7, 18.5, 22.3, 28.6, 40.4, 51.0, 67.00, 67.0, 71.9, 78.7, 99.0, 173.79, 175.5. FTIR: 3307 (s), 2993 (s), 2936 (s), 2877 (s), 2603 (m), 2251 (w), 1742 (s), 1628 (s), 1534 (s), 1376 (m), 1202 (s), 1081 (s). Anal. Calcd. for $C_{13}H_{19}NO_5$: C, 57.98; H, 7.11; N, 5.20. Found: C, 58.28; H, 7.40; N, 5.15.

Poly-L-lysine-G1 acetonide (**G1An**). To a flask containing **2** (1.3 g, 6.2 mmol) was added **7** (2.9 g, 11 mmol), HOBt (83 mg, 0.62 mmol) and DMF (30 mL). After 5 min DCC (2.9 g, 14 mmol) was added, resulting in a cloudy solution. To this was added triethylamine (5.0 mL, 36 mmol), and the reaction was stirred for 4 d at RT. Upon completion of the reaction the polymer was precipitated into cold ether (20 mL) and centrifuged, then washed with ether (2 x 15mL). The polymer was then dissolved in methylene chloride (0.7 mL) and reprecipitated into ether (ca. 30 mL). The solution was centrifuged and the solid dried to yield **G1An** (1.8 g, 75%) as a pale yellow solid. ^{1}H NMR (300 MHz, $CDCl_3$): δ 1.03 (s, 3), 1.48 (s, 10), 1.90 (s, 1), 2.20 (s, 1), 2.62 (s, 1), 2.80 (s, 1), 3.21 (br s, 2), 3.82 (s, 4), 3.98 (s, 1), 4.66 (s, 1), 7.38 (s, 1), 8.03 (s, 1), 8.17 (s, 1). ^{13}C NMR (400 MHz, CD_3OD): δ 17.4, 19.1, 22.3, 23.7, 28.2, 29.0, 30.0, 39.6, 40.4, 51.6, 57.7, 66.5, 67.5, 72.0, 79.6, 169.90, 174.6, 175.6. FTIR: 3304 (s), 3084 (m), 2992 (m), 2940 (s), 2874 (m), 2119 (w), 1646 (s), 1539 (s), 1377 (s), 1202 (s), 1077 (s), 936 (m), 660 (m). SEC: PMMA: M_n= 21,900, M_w= 25,500, PDI= 1.16. PEO: M_n= 14,300, M_w= 16,700, PDI= 1.17. MALS: M_n= 35,400, M_w= 38,100, PDI= 1.07.

Deprotection of acetonide-terminated dendrimers G1An, G2An, and G3An. In a typical experiment, **G1An** (1.50 g 3.95 mmol) was dissolved in methanol (ca. 50 mL) and stirred. To this was added sulfuric acid (5 drops) dissolved in methanol (10 mL). The reaction solution turned from turbid to clear within 5-10 min, and was allowed to proceed for 2 h. The solvent and 2,2-dimethoxypropane formed were then removed *in vacuo*, and additional methanol (ca. 50 mL) was added and the reaction was allowed to continue for 4 h. After this process was repeated three times the reaction was concentrated to one-fifth the original volume and neutralized with 7 N ammonia in methanol (0.7 mL). This cloudy suspension was then dialyzed against water (1 L) for 24 h. The solution was concentrated and the oil produced was redissolved in methanol (5 mL) and filtered over glass wool into cold ether (ca. 50 mL). The solid formed was washed with cold ether (2 x 20 mL) and dried to give **G1OH** (0.81 g, 60%) as a pale yellow solid. **G1OH:** ^{1}H NMR (300 MHz, CD_3OD): δ 1.18 (s, 3), 1.57 (m, 4), 1.95 (m, 2), 2.46 (s, 1), 2.73 (s, 2), 3.21 (s, 2), 3.69 (q, 4, *J* = 11.7, 12.9), 3.92 (s, 1), 4.55 (s, 1), 8.31 (br s, 1). ^{13}C NMR (400 MHz CD_3OD): δ 14.8, 19.9, 21.8, 27.0, 28.2, 37.5, 46.9, 47.2, 50.4, 56.0, 63.2, 70.0, 77.6, 169.2, 174.3, 174.9. FTIR: 3300 (s), 2943 (s), 2873 (m), 1650 (s), 1536 (s), 1425 (m), 1251 (m), 1105 (m), 1047 (m), 911 (w), 622 (m). SEC: M_n= 600 Da, PDI= 3. MALS: M_n=27,500 Da. **G2OH:** ^{1}H NMR (300 MHz, CD_3OD): δ 1.17 (s, 6), 1.34 (s, 3), 1.58 (br s, 4), 1.90 (br s, 2), 2.46 (s, 1), 2.70 (br s, 2), 3.15 (br s, 1), 3.67 (q, 10, *J* = 10.2, 17.7), 3.92 (s, 1), 4.27 (br s, 4), 4.60 (s, 1). ^{13}C NMR (400 MHz, CD_3OD): δ 17.1, 21.6, 23.4, 28.6, 29.3, 39.2, 46.3, 48.4, 52.1, 57.6, 65.6, 71.7, 79.5, 170.6, 173.7, 174.7, 175.9. FTIR: 3289 (s), 2943 (s), 2883 (m), 1724 (s), 1653 (s), 1460 (s), 1377 (m), 1227 (s), 1042 (s), 663 (m). SEC: M_n= 12,000 Da, PDI= 1.12. MALS: M_n= 42,000 Da. **G3OH:** ^{1}H NMR (400 MHz, CD_3OD): δ 1.16 (s, 14), 1.32 (s, 9), 2.49 (br s, 2), 3.65 (d, 18, *J* = 24.8), 4.33 (br m, 8), 4.60 (s, 2), 4.95 (m, 1). ^{13}C NMR (400 MHz, CD_3OD): δ 23.5, 30.2, 40.8, 47.7, 47.9, 50.2, 73.7, 80.8, 171.8, 173.9, 176.0, 177.2. FTIR: 3406 (s), 2944 (m), 2886 (m), 1732 (s), 1650 (s), 1466 (m), 1223 (s), 1129 (s), 1045 (s), 910 (w), 657 (w). DMF SEC: M_n= 23,000 Da PDI= 1.12. MALS: M_n= 76,000 Da. **G4OH**: ^{1}H NMR (400 MHz, CD_3OD): δ 1.16 (s, 24), 1.32 (s, 16), 1.5 (br s, 4) 2.49 (br s, 1), 2.7 (br s, 2), 3.65 (q, 28, *J* = 24.8), 4.33 (br m, 22), 4.60 (br s, 2). SEC: M_n= 19,000 Da, PDI= 1.16. MALS: M_n= 141,000

Dendronization of polymers G1OH, G2OH and G3OH. In a typical experiment, DMAP (0.43 g, 3.5 mmol) and **7** (1.98 g, 6 mmol) were dissolved in pyridine (0.9 mL) and stirred for 30 min. In a separate flask, **G1OH** (.634 g, 1.87 mmol) was dissolved in methylene chloride (3 mL) and pyridine (6 mL). The polymer solution was then added to the solution containing DMAP and **7** and the mixture was stirred for 12 h. The reaction was then precipitated into cold ether (ca. 50 mL) to give a yellow oil. The oil was then taken into methylene chloride (5 mL) and reprecipitated into cold ether (ca. 50 mL). The oil obtained from this precipitation was redissolved in methylene chloride (5 mL) and precipitated into hexane (ca. 50 mL) to give **G2An** (770 mg, 63%) as a white solid. **G2An**: ^{1}H NMR (300 MHz, $CDCl_3$): δ 1.15 (s, 6), 1.34 (s, 8), 1.40 (s, 6), 1.92 (s, 2), 2.14 (s, 2), 2.63 (s, 1), 3.63 (s, 4), 3.87 (s, 1), 4.16 (s, 4), 4.36 (s, 2), 4.82 (s, 1), 7.80 (br m, 2) SEC: M_n= 15,000 Da, PDI= 1.12. MALS: 48,200 Da. **G3An**: ^{1}H NMR (300 MHz, $CDCl_3$): δ 1.32 (m, 54), 2.13 (s, 1), 2.60 (br s, 2), 3.60 (m, 16), 4.25 (m, 12). SEC: 27,000 Da, PDI= 1.18. MALS: 83,500 Da. **G4An**: ^{1}H NMR (400 MHz, $CDCl_3$): δ 1.32 (s, 12), 1.27 (s, 8), 1.32 (s, 12), 1.39 (s, 12), 2.2 (br s, 1), 3.6 (d, 8, J = 6.7), 4.13 (d, 8, J = 6.7), 4.3 (br s, 10). SEC: 19,000 Da, PDI = 1.16 MALS: 141,000 Da.

Azide hydrazone linker (9). To a flask containing chloroacetyl chloride (1.32 g, 6.94 mmol) dissolved in methylene chloride (6 mL) at 0 ^{o}C was added a solution of *t*-butyl carbazate (.916 g, 6.93 mmol) and pyridine (0.566 g, 7.16 mmol) in methylene chloride (5 mL). After 30 min the reaction was filtered into a 50-mL separatory funnel and extracted with 5% citric acid (20 mL), 5% $NaHCO_3$ (20 mL), and brine (20 mL). In cases in which this produced an emulsion, solvents were separated by centrifugation. The organic phase was then dried, filtered and evaporated to give **8** (1.24 g, 63%) as an off-white solid. Without further purification, a portion of **8** (294 mg, 1.03 mmol) was dissolved in DMF (8 mL) and sodium azide (80 mg, 1.23 mmol) was added. The reaction flask was wrapped in aluminum foil and after 6 h the reaction was diluted with ether (ca. 15 mL) and transferred to a 50-mL separatory funnel. The solution was then washed with cold water (2 x 20 mL). A precipitate formed in the organic layer at this stage, and ethyl acetate (20 mL) was added to redissolve the solid. This solution was then washed with 5% citric acid (2 x 20 mL) followed by cold water (20 mL). The organic phase was then dried, filtered and evaporated to give a white solid (235 mg). A portion of this crude product (100 mg, 0.34 mmol) was recrystallized in ethyl acetate and hexanes to give **9** (54 mg, 18%) as a white crystalline solid. Mp: 164-166 ^{o}C. ^{1}H NMR (300 MHz, $CDCl_3$): δ 1.50 (s, 9), 4.40 (s, 2), 6.75 (br s, 1), 7.38 (d, 2, *J* = 6), 7.82 (d, 2, *J* = 6), 8.09 (br s, 1). ^{13}C NMR (400 MHz, CD_3OD): δ 28.5, 45.6, 79.6, 128.1, 128.9, 132.7, 141.4, 155.9, 166.0. Due to the potentially explosive nature of this compound, elemental analysis was not pursued.

G4(Boc)OH: In a typical experiment, to a 25 mL flask containing 356 mg (0.182 mmol) **G4OH** polymer, was added a solution containing 210 mg (0.98 mmol, 5.4 eq) **9**, 15.5 mg (0.029 mmol, .16 eq) TBTA, and 60 μL (.34 mmol, 1.9 eq) DIPEA in 1.0 mL acetonitrile. The solution was stirred and purged with nitrogen for 5 minutes, and 4.0 g (.028 mmol, .15 eq) CuBr suspended in 1.0 mL DMF and a small piece of freshly cut copper wire were added. The reaction was then wrapped in aluminum foil and allowed to stir under nitrogen for four days. The cloudy solution was then precipitated into ether, and the solids isolated and dialyzed in using 3500 MWCO tubing in a 1:1 mixture of methanol and water to yield 371 mg (94 %) **G4(Boc)OH** as an off-white solid. ^{1}HNMR (D_2O, 600 MHz): δ 1.15 (s, 27); 1.31 (s, 20); 1.47 (s, 10); 3.18 (s, 2); 3.62 (s, 18); 3.69 (s, 23); 4.28 (br s, 13); 4.33 (br s, 15); 7.91 (s, 2). SEC: Mn: 29,300 PDI = 1.58. DLS: 29.8 nm diameter, PDI = 0.234.

G4(Boc)Gly: To a 25 mL flask containing 196mg (.0905 mmol) **G4(Boc)OH** in 2 mL DMF was added 7.6 g (43 mmol, 30 eq per dendrimer hydroxyl) of freshly distilled 2-(2-(ethoxy)ethoxy)acetic acid and 0.9 g (6.7 mmol, 4.5 eq per hydroxyl) HOBt. To this was then added 1.5 g (7.3 mmol, 5 eq) DCC dissolved in 3 mL DMF. The solution was then stirred for 48 hours and centrifuged to remove dicyclohexyl urea. The reaction solution was then precipitated into 100 mL cold ether, taken into 5 mL DCM, filtered and reprecipitated. The polymer was then dialyzed using 3500 MWCO dialysis tubing against water and lyophilized to give 288 mg (36 %) **G4(Boc)Gly** as an off-white solid. ^{1}HNMR (MeOD, 600 MHz): δ 1.15 (s, 9); 1.20 (s, 12); 1.31 (s, 18); 1.47 (s, 9); 3.34 (s, 24); 3.48 (s, 16); 3.66-3.71 (m, 70); 4.21-4.32 (m, 50); 7.91 (s, 3). THF SEC (PMMA standard): Mn: 21,200 Da, PDI = 1.39. DLS: 30.9 nm diameter, PDI = 0.640.

G4(Dox)Gly: To a 25 mL vial containing 25 mg **G4(Boc)Gly** was added 2 mL DCM. After approximately a minute of stirring, 2 mL TFA were added and the solution was stirred for two hours. The solvents were then removed *in vacuo*, and 1 mL MeOH buffered to pH 5 with 140 μL

of 1:1 Py:AcOH was added. To this was added 6.3 mg (3 eq) Doxorubicin and the solution was stirred at 60 ^{o}C overnight. The reaction was then filtered over glass wool and purified from free Doxorubicin using an LH 20 size exclusion column using methanol as the mobile phase. Methanol was then removed *in vacuo*, and the polymer was further purified using a PD 10 column. The product fraction was then lyophilized to give 22.3 mg (82 %) **G4(Dox)Gly** as a red solid. DLS: 29.4 nm diameter, PDI = 0.812. Doxorubicin content was 10.5 wt % as determined by UV Vis at 489 nm. DLS: 29.4 nm diameter, PDI = 0.812.

References

1) Pasut, G. and Veronese, F..M., Polymer-Drug Conjugation, Recent Achievements and General Strategies. *Progress in Polymer Science*, **2007**, *32*, 933-961.
2) Gulloti, E. and Yeo, Y. Extracellularly Activated Nanocarriers: A New Paradigm for Tumor Targeted Drug Delivery. *Molecular Pharmaceutics*, 2009, *6*, 1041-1051.
3) Matsumura, Y. and Maeda, H. A New Concept for Molecular Therapeutics in Cancer Chemotherapy: Mechanism of Tumoritropic Accumulation of Proteins and the Antitumor Agent SMANCS. *Cancer Research*, 1986, *46*, 6387-6392.
4) Uzgiris, E.,E. Role of Molecular Conformation on Tumor Uptake of Polymer Contrast Agents. *Investigative Radiology, **2004,** 39*, 131-137.
5) Kricheldorf, H. R., Polypeptides and 100 Years of Chemistry of α-Amino Acid N-Carboxyanhydrides, *Angew. Chem, Int Ed*. **2006**, *45*, 5752-5784.
6) Lee, C.C., Fréchet, J.M.J, Synthesis and Conformations of Dendronized Poly(L-Lysine), *Macromolecules*, **2005**, *39*, 476-481.
7) Yoshida, M., Fresco, Z., Ohnishi, S., Fréchet, J.M.J., Efficient Divergent Synthesis of Dendronized Polymers with Extremely High Molecular Weight: Structural Characterization by SEC-MALLS and SFM and Novel Organic Gelation Behavior. *Macromolecules*, 2005, *38*, 334-344.
8) Lee, C.C., Yoshida, M., Fréchet, J.M.J, Dy, E.E., and Szoka, F.C., In Vitro and in Vivo Evaluation of Hydrophilic Dendronized Linear Polymers. *Bioconjugate Chemistry*, **2005**, *16*, 535-541.
9) Murray, R.K, Granner, D.K., Mayes, P.A., Rodwell, V.W. *Harper's Illustrated Biochemistry*, Lange Medical Books/ McGraw-Hill: New York, *2003*. p20.
10) Lee, C.C., Gillies, E., R., Fox, M., Guillaudeu, S. J., Fréchet, JMJ., Dy, E.E., Szoka, F. C. A single Dose of Doxorubicin functionalized Bow-tie Dendrimer Cures Mice Bearing C-26 Colon Carcinomas. *PNAS*, **2006**, *103*, 16649-16654.
11) Fox, M. E., Szoka, F. C., and Fréchet, J. M. J., Soluble Polymer Carriers for the Treatment of Cancer, The Importance of Molecular Architecture, *Accounts of Chemical Research*, **2009**, *42*, 1141-1151.

Chapter 4: Effective Dendritic Delivery and Tumor Curing with a Synthetic Tubulysin Analogue

Introduction

The tubulysins, first isolated from myxobacterial cultures by the Höfle–Reichenbach group[1], are exceptionally potent cell-growth inhibitors that act by inhibiting tubulin polymerization and thereby inducing apoptosis. For this reason, the biosynthesis[2], mechanism[3], and anticancer activity[4] of the tubulysins have been intensively investigated. Tubulysin D (Figure 1), the most potent of the tubulysins, has activity that exceeds virtually all known tubulin modifiers, and in particular is 20 to 10000-fold more cytotoxic than the important, clinically approved anticancer drugs, the epothilones, vinblastine, and paclitaxel.[5,6]

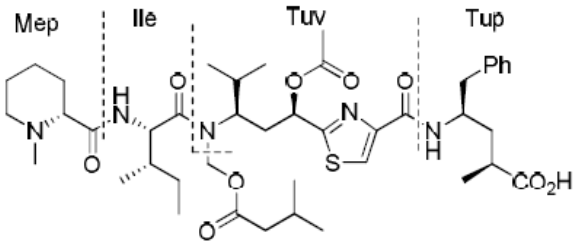

Figure 1. Tubulysin D structure and cytotoxicity.[8a]

Unfortunately, the extraordinary activity of the most potent tubulysins poses considerable complications for chemo- therapeutic applications due to toxicity against healthy cells and tissues. Moreover, the tubulysins are difficult to obtain in large quantities from the myxobacteria from which they are isolated, and total synthesis routes are prohibitively difficult due to the fragile and complex nature of the most potent of the naturally occurring tubulysins, which incorporate the labile N,O-acetal functionality.[7] Consequently, both academia and the pharmaceutical industry have focused on the synthesis and evaluation of simpler and more stable tubulysin analogues.[8] Similarly, significant efforts have been directed to pro- drug strategies for selective tumor delivery of tubulysin and its analogues in order to minimize toxicity[8r].

Macromolecular drug carriers have proven to be particularly promising for the selective delivery of drugs to tumors.[9] Carriers such as liposomes, particles, or polymer conjugates can improve drug delivery, and thus drug efficacy, by imparting the desirable properties of the carrier to the drug.[10] Bound or encapsulated drugs exhibit prolonged blood circulation[10j], increased tumor uptake due to the enhanced permeation and retention (EPR) effect[11], enhanced solubility[10i], and reduced systemic toxicity. Dendrimers, a class of highly branched polymers, are of particular interest as drug carriers. The stepwise synthesis of dendrimers allows for control over architecture and physicochemical properties while incorporating diversified functional handles for attaching different groups, such as solubilizing polyethylene glycol chains (PEG), drug molecules, or imaging agents.[12] Previous work by the Fréchet group focused on exploring polymer–drug delivery with different dendritic architectures[12c,e,s,u] and drug release mechanisms.[12a–c,s,t] In a seminal work by Fréchet and co-workers, doxorubicin (DOX), a

chemotherapeutic drug, was successfully attached to a dendrimer by an acyl hydrazone bond and evaluated in mice bearing C26 colon carcinomas.[9b]

Herein, we describe the synthesis of a novel synthetic tubulysin analogue that contains a ketone moiety for conjugation to a dendrimer via an acid labile hydrazone linker, which has previously been shown to form drug conjugates that are stable in the blood stream but release their payload in endosomal compartments.[13] The dendrimer conjugate has been characterized both in vitro and in vivo, and represents the first report of polymeric drug delivery vehicles using synthetic tubulysin analogues.[8r]

Experimental Section

General Information and Materials

Abbreviations: MTD: maximum tolerated dose, TEA: triethylamine, THF: tetrahydrofuran, TFA: trifluoroacetic acid, DMF: *N*,*N*-dimethylformamide. Unless otherwise noted, all reagents were obtained from commercial suppliers and used without purification. ^{1}H NMR and ^{13}C NMR spectra were obtained at room temperature with AVQ 400 MHz, AVB 400 MHz, DRX 500 MHz, or AV 600 spectrometers. ^{1}H NMR resonances are referenced to the residual solvent peak ($CDCl_3$, 7.26 ppm; methanol-d4, 3.34 ppm; D_2O, 4.79 ppm; DMSO, 2.50 ppm) and ^{13}C NMR resonances are referenced to the residual solvent peak ($CDCl_3$, 77.23 ppm; methanol-d4 49.01). Chemical shifts are reported in ppm, and coupling constants are reported in Hz. High-resolution mass spectra were obtained by the University of California at Berkeley Micro-Mass Facility. Toluene, THF, diethyl ether, 1,4-dioxane, and methylene chloride were dried over alumina under a nitrogen atmosphere. MeOH, MeCN, *i*-Pr_2NH, *i*-Pr_2EtN, and pyridine were distilled from CaH_2 immediately prior to use. DMF was dried and stored over 3 Å molecular sieves. Polymer-bound cyclohexylcarbodiimide (PS-CCD) was obtained from Biotage, Inc. Reactions were carried out in flame or oven-dried glassware under a N_2 atmosphere. Products were concentrated using a Buchi rotary evaporator under reduced pressure. Flash column chromatography was carried out either with Merck 60 230-240 mesh silica gel, or using a Biotage SP Flash Purification System with Flash+ 3 cartridges. Size exclusion chromatography was performed using either Biorad PD 10 or LH 20 sephadex columns (from GE Healthcare). Compounds **1**[8b], **2**[14], and **4**[12s] are known compounds and spectroscopic and analytical data are in good agreement with reported literature. Although the synthesis of **2** has previously been reported, due to insufficient information about its preparation and characterization, we have included its preparation and full characterization. ^{1}H NMR and ^{13}C NMR spectra are provided for known compounds to demonstrate purity. Compound **3** and [5] are new compounds and are fully characterized. UnPEGylated dendrimers were characterized by ^{1}H NMR with a 400 MHz AVB spectrometer (Bruker, Billerica, MS, USA) and MALDI-TOF mass spectrometry (PerSeptive Biosystems, Foster City, CA, USA). High molecular weight PEGylated dendrimers were characterized by ^{1}H NMR and size exclusion chromatography. The SEC system consisted of two SDV Linear S (5 μm) columns (Polymer Standards Service, 300 x 8 mm) using DMF with 0.2% LiBr as the mobile phase (1 mL/min) in series with a Waters 515 pump, 717 autosampler, 996 Photodiode Array Detector (210-600 nm), and 2414 differential refractive index detector.

Synthesis

1-(4-(2-Aminoethyl)phenyl)ethanone hydrochloride (**2**): To nitrobenzene (50 mL) was added portionwise $AlCl_3$ (20.00 g, 150.0 mmol), and the mixture was stirred for 15 min. After cooling to 20 °C (inner temperature), acetyl chloride (11.78 g, 150.0 mmol) was added to the mixture. To the resulting mixture was then added phenethylamine (6.06 g, 50.0 mmol) dropwise at a rate that maintained the inner temperature below 40 °C. After stirring at room temperature for 5 h, the

mixture was poured onto ice (100 g), and the resulting mixture was then stirred an additional 18 h. After washing with Et_2O (3 x 100 mL) then CH_2Cl_2 (5 x 100 mL) the aqueous layer was made basic with 6 N aqueous NaOH (ca. 300 mL) and extracted with CH_2Cl_2 (3 x 200 mL). The organic layer was then dried over sodium sulfate, filtered, and evaporated *in vacuo*. The residue was dissolved in EtOH (50 mL) and treated with concentrated hydrochloric acid (5 mL) at 0 °C. The precipitate was collected by filtration, washed with EtOH (3 x 10 mL), and dried *in vacuo* to give a solid (1.65 g). Concentration of the mother liquor to ca. 30 mL gave a second crop (0.54 g). The combined solid (1.65 + 0.54 = 2.19 g) was suspended in EtOH (15 mL), and the mixture was stirred at 100 °C for 20 min. After cooling to room temperature, the precipitate was collected by filtration, washed with EtOH (3 x 3 mL), and then dried *in vacuo* to give **2** (1.78 g, 18%) as a white solid. ^{1}H NMR (400 MHz, D_2O) δ = 2.57 (3H, s); 3.04 (2H, t, *J* = 7.4 Hz); 3.28 (2H, t, *J* = 7.4 Hz); 7.39 (2H, m); 7.89 (2H, m); ^{13}C NMR (100 MHz, D_2O) δ = 26.2, 32.7, 40.0, 129.1, 129.2, 135.3, 143.0, 203.4. HRMS (ESI) m/z Calcd for $C_{10}H_{14}NO$: 164.1070. Found 164.1079 (M + H+).

(1*R*,3*R*)-1-(4-(4-Acetylphenethylcarbamoyl)thiazol-2-yl)-3-((2*S*,3*S*)-*N*,3-dimethyl-2-((*R*)-1-methylpiperidine-2- carboxamido)pentanamido)-4-methylpentyl acetate (Tubulysin analogue **3**): To a stirred solution of **1** (108 mg, 0.20 mmol) and pentafluorophenol (74 mg, 0.40 mmol) in CH_2Cl_2 (6 mL) was added PS-carbodiimide (1.28 mmol/g, 469 mg, 0.60 mmol), and the mixture was stirred at room temperature for 18 h. The mixture was filtered and washed with CH_2Cl_2, and the filtrate was evaporated *in vacuo*. The residue was dissolved in DMF (4 mL). To the solution was added *i*-Pr_2NEt (0.139 mL, 0.80 mmol) followed by **2** (40 mg, 0.20 mmol) at 0 °C, and then the mixture was stirred at room temperature for 18 h. The mixture was evaporated *in vacuo*, and the residue was diluted with EtOAc and washed with 5% aqueous $NaHCO_3$ (3 x). The organic layer was evaporated *in vacuo*, and the residue was purified by silica gel column chromatography (EtOAc/MeOH 100:0 to 80:20) to give **3** (115 mg, 84%) as a colorless amorphous solid. ^{1}H NMR (400 MHz, CDCl3) δ = 0.79 (3H, d, *J* = 6.4 Hz); 0.92 (3H, t, *J* = 7.4 Hz); 0.98 (3H, d, *J* = 6.8 Hz); 1.01 (3H, d, *J* = 6.8Hz); 1.04-1.27 (2H, m); 1.28-1.41 (1H, m); 1.43-1.90 (7H, m); 1.95-2.07 (2H, m); 2.17 (3H, s); 2.22 (3H, s); 2.28-2.38 (1H, m); 2.47 (1H, dd, *J* = 11.0, 3.4 Hz); 2.60 (3H, s); 2.84-2.92 (1H, m); 2.98-3.05 (2H, m); 3.01 (3H, s); 3.68-3.76 (2H, m); 4.47-4.60 (1H, m); 4.78 (1H, dd, *J* = 9.6, 7.6 Hz); 5.65 (1H, dd, *J* = 11.4, 2.6 Hz); 7.04 (1H, d, *J* = 9.6 Hz); 7.36 (2H, d, *J* = 8.0 Hz); 7.40 (1H, t, *J* = 6.0 Hz); 7.92 (2H, d, *J* = 8.4 Hz); 8.06 (1H, s). ^{13}C NMR (100 MHz, CDCl3) δ = 10.9, 15.9, 19.6, 20.0, 20.8, 23.2, 24.4, 25.1, 26.6, 29.9, 30.4, 34.6, 35.9, 36.9, 40.3, 44.9, 52.9, 55.4, 69.4, 69.7, 123.5, 128.7, 129.0, 135.6, 144.5, 149.8, 160.8, 169.9, 170.1, 173.5, 174.2, 197.6. HRMS (ESI) m/z Calcd for $C_{36}H_{53}N_5O_6S$: 684.3789. Found: 684.3792 (M + H+).

PLL-G2-(Asp Glu(NNBoc)$_2$)PEG)$_8$ (**4**): Compound **4** was prepared according to the literature.[14] ^{1}H NMR (500 MHz, D2O): δ = 1.47 (br s, 180H); 1.6-1.9 (br m, 18H); 2.2 (br m, 8H); 2.4 (br m, 16H); 2.7-2.9 (br m, 18H); 3.21 (br s, 19H); 3.39 (s, 24H); 3.5-4.0 (br m, ~4300H); 4.24 (br m, 25H); 4.4-4.6 (br m, 15H). DMF SEC: *M*n = 34,000 Da, PDI = 1.06.

Tubulysin analogue-dendrimer Conjugate **5**: To a 100 mL round bottomed flask was added *N*-Boc protected poly-lysine dendrimer **4** (158 mg, 0.004 mmol dendrimer, 0.063mmol protected hydrazide). The polymer was then dissolved in CH_2Cl_2 (15 mL) and TFA (15 mL) was added. After two hours the solvents were removed under reduced pressure to provide the free hydrazide dendrimer as a white solid. To the flask was then added the tubulysin ketone derivative **3** (65 mg, 0.095 mmol), followed by MeOD (6.3 mL) and TFA (14.4 μL, 2.0 mmol). The reaction mixture was then placed under nitrogen atmosphere, warmed gently with warm water to dissolve any

residual solids, and stirred until the reaction was shown to be complete by ^{1}H NMR analysis. Reaction times were typically 24 h. At this time the reaction was quenched with TEA (144 μL, 1 mmol) and all volatiles were removed under reduced pressure. Final purification of the conjugate was carried out by centrifuging in water to remove solids followed by eluting through an aqueous PD 10 column and an LH20 column containing methanol as the mobile phase. Columns were repeated as necessary until the free tubulysin ketone was not detected by HPLC. The product was then dried *in vacuo* and lyophilized to give **5** (67.6 mg) as an off white solid. DMF SEC: *M*n = 37,053 Da, PDI = 1.10. ^{1}H NMR (400 MHz, MeOD): δ = .8-.99 (m, 92H); 1.8-2.05 (m, 108H); 2.06-2.56 (m, 65H); 2.57-3.03 (m, 97H); 3.36 (s, 24H); 3.63 (s, 3300H); 4.19-4.69 (m, 56H); 5.67 (br s, 8H); 7.28 (br s, 15H); 7.78 (br s, 15H); 8.18 (s, 7.5H).

Quantification of analogue 3 bound to conjugate 5

While ^{1}HNMR integrals of the aromatic peaks of analogue **3** provided a good indication of its loading on conjugate **5**, HPLC was used to support these measurements. Therefore, a calibration curve of **3** was made by running samples of this analogue in 1:2 ACN: pH 1 buffer (100 mM sodium citrate/HCl) at concentrations varying from 0.001 to 0.5 mg/mL under the HPLC conditions used to measure analogue release rates. A sample of conjugate **5** was then prepared by dissolving 3.5 mg in 200 μL of pH 1 buffer containing 15% ACN. The sample was then incubated at 40 °C for 1 hour to cleave analogue **3**, at which point the sample was analyzed by HPLC to obtain the peak integral for released **3.** The calibration curve was then used with this integral to extrapolate the loading of **3** in **5**, which was found to be 12% by weight, or 56% of the maximum theoretical loading of 16 analogues **3** per dendrimer molecule.

Release Rates

To quantify the hydrolysis of tubulysin from the dendritic polymer carrier in various buffers, the dendrimer was dissolved in either 1X PBS without Mg^{2+}/Ca^{2+} (pH 7.4) or acetate buffer (100 mM sodium acetate, pH 5.0) at a concentration of 5 mg of polymer/mL and incubated in the dark at 37 °C. At each time point, a 10 μL aliquot was injected into a RPHPLC system, which consisted of a C-18 Microsorb MV column (Agilent) in line with a Waters 996 photodiode array detector and a Waters 2414 refractive index detector, using an eluent of 1:1 distilled water (with 10 mM ammonium carbonate) and acetonitrile. All spectra were viewed at 254 nm. Release rates were determined by the rate of appearance of free tubulysin analogue **3**.

Animal and Tumor Models

All animal experiments were performed in compliance with National Institutes of Health guidelines for animal research under a protocol approved by the Committee on Animal Research at the University of California (San Francisco, CA) (UCSF). C26 colon carcinoma cells obtained from the UCSF cell culture facility were cultured in RPMI medium 1640 containing 10% FBS. Female BALB/c mice were obtained from Simonsen Laboratories, Inc. (Gilroy, CA).

Cytotoxicity Studies in Cells

The cytotoxicity of **3**, **5** and tubulysin D was determined by using the MTT assay with C26 cells. Cells were seeded onto a 96-well plate at a density of 5.0 X 10^3 cells per well in 100 μL of medium and incubated overnight (37 ^{o}C, 5% CO_2, and 80% humidity). An additional 100 μL of new medium (RPMI medium 1640, 10% FBS, 1% penicillin-streptomycin, 1% Glutamax) containing varying concentrations of **3**, **5** and tubulysin D were added to each well (performed in triplicate). After incubation for 72 h, 40 μL of media containing thiazolyl blue tetrazolium bromide (5 mg/ml) was added. The cells were incubated for 3 h, after which time the medium was carefully removed. To the resulting purple crystals were added 200 μL of DMSO and 25 μL of pH 10.5 glycine buffer (0.1 M glycine/0.1 M NaCl). Optical densities were measure at 570 nm

by a SpectraMAX 190 microplate reader (Molecular Devices, Sunnyvale, CA). Optical densities measured for wells containing cells that received neither dendrimer nor **3** were considered to represent 100% viability. IC50 values were obtained from sigmoidal fits of the data using Origin 7 8.0552 software (OriginLab, Northhampton, MA).

Maximum Tolerated Dose Study in Healthy Mice

Healthy female Balb/C mice (2 per group) were injected with **3** (10-30 mg tubulysin/kg) and **5** (10-165 mg tubulysin/kg). Mice were weighed and checked daily for two weeks. When a mouse lost > 20% of its initial weight or showed signs of toxicity, such as lethargy or rumpled fur, it was removed from the study.

Chemotherapy Experiments

While under anesthesia, female Balb/C mice were shaved, and C26 cells (3×10^5 cells in 50 μL) were injected subcutaneously in the right hand flank. At eight days post-tumor implantation, mice were randomly distributed into treatment groups of 8 animals. Mice were injected by means of the tail vein with **5** (165 mg tubulysin/kg) or **3** (10 and 20 mg tubulysin/kg) in approximately 200 μL of PBS buffer solution. Mice were weighed and tumors measured every other day. The tumor volume was estimated by measuring the tumor's length in three dimensions with calipers and calculated using the formula tumor volume = length x width x height. Mice were removed from the study when (i) a mouse lost 20% of its initial weight, (ii) any tumor dimension was > 20 mm, or (iii) the mouse was found dead. The mice were followed until day 60 post-tumor inoculation. Statistical analysis was performed as previously described[12t] using MedCalc 8.2.1.0 for Windows (MedCalc Software, Mariakerke, Belgium). The tumor growth delay was calculated based upon a designated tumor volume of 500 mm^3.

Results

The design and synthesis of a tubulysin analogue appropriate for dendrimer delivery was based on our work[8a] and that of others,[8m] which established that the synthetically challenging and highly labile N,O-acetal functionality of the most potent tubulysins could be replaced with a simple and highly stable N-methyl group with minimal reduction in cytotoxicity. Moreover, structure–activity relationship studies by us[8a] and others[8j] also established that the tubuphenylalanine (Tup) portion of tubulysin D (Figure 1) can be extensively modified or truncated with only modest decreases in activity. With this knowledge, we conceived and synthesized tubulysin analogue **3** (Scheme 1) from intermediate **1**, for which we had previously developed a synthetic route that proceeds in > 40 % overall yield from commercial materials.[8b] Analogue **1** was coupled with 4-acetylphenethylamine (**2**) using polymer-supported (PS) carbodiimide to give analogue **3** in 84 % yield (Scheme 1). Analogue **3** can readily be prepared in large quantities, is considerably more stable than the most potent tubulysin natural products that incorporate the N,O-acetal group, and also contains a ketone functionality to serve as a handle for coupling to a dendrimer carrier via an acyl hydrazone bond.

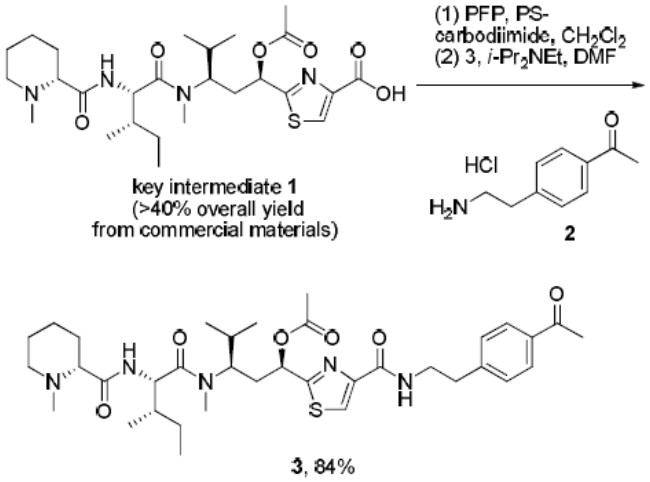

Scheme 1. Synthesis of tubulysin analogue **3** for dendrimer delivery from key intermediate **1** (> 40 % overall yield from commercial materials). Reagents and conditions: a) Pentafluorophenol (PEP), PS-carbodiimide, CH_2Cl_2 ; b) 3, iPr_2NEt, DME, 84 % (two steps).

The tubulysin analogue–dendrimer conjugate was prepared using dendrimer carrier **4**,[12s] which is a 40 kDa PEGylated dendrimer with a polypeptide core. This dendrimer scaffold is obtained in a total of ten high yielding steps, and the periphery is decorated with hydrazides for coupling the ketone of tubulysin analogue **3** to form the acyl hydrazone linkage (Scheme 2). Dendrimer **4**, after treatment with trifluoroacetic acid (TFA) to remove the N-Boc groups, is then coupled with tubulysin ketone **3** in methanol with TFA. The reaction progress was followed by ^{1}H NMR spectroscopy and was complete within 24 h, at which point the reaction was quenched by addition of triethylamine. Evaporation and subsequent purification by size exclusion chromatography resulted in pure tubulysin analogue–dendrimer conjugate **5** in 36 % yield as an off-white solid.

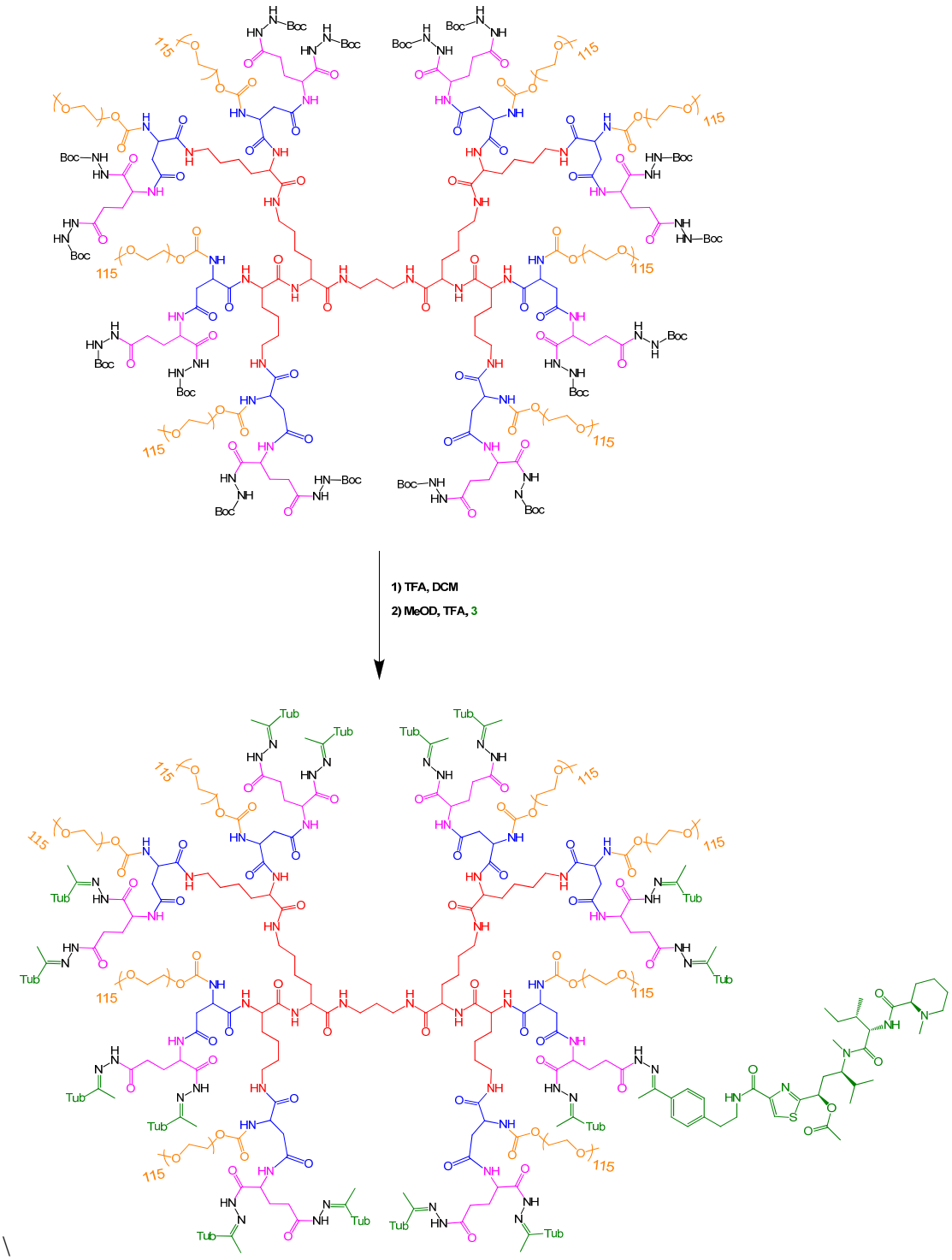

Scheme 2. Synthesis of conjugate **5** (12 wt % loading of tubulysin analogue **3**). Reagents and conditions: a) TEA, CH_2Cl_2 ; b) MeOD, TEA, **3**, 36 % (two steps).

The release rate of tubulysin analogue **3** from the tubulysin analogue–dendrimer conjugate **5** in blood and endosomal compartments is a critical parameter for the selective delivery of **3** to tumor tissue. The rate at which **3** was released from the carrier was therefore measured at both

pH 7.4 (1X phosphate-buffered saline (PBS) without Mg^{2+} /Ca^{2+}) and pH 5.0 (100 mM sodium acetate), which corresponds to the pH in blood and endosomal compartments, respectively. As shown in Figure 2, while **3** is released at pH 5.0, no observable release occurs at pH 7.4. These results support our original design of the carrier for release of the toxic tubulysin analogue after cellular endocytosis with little or no drug release during circulation in the blood.

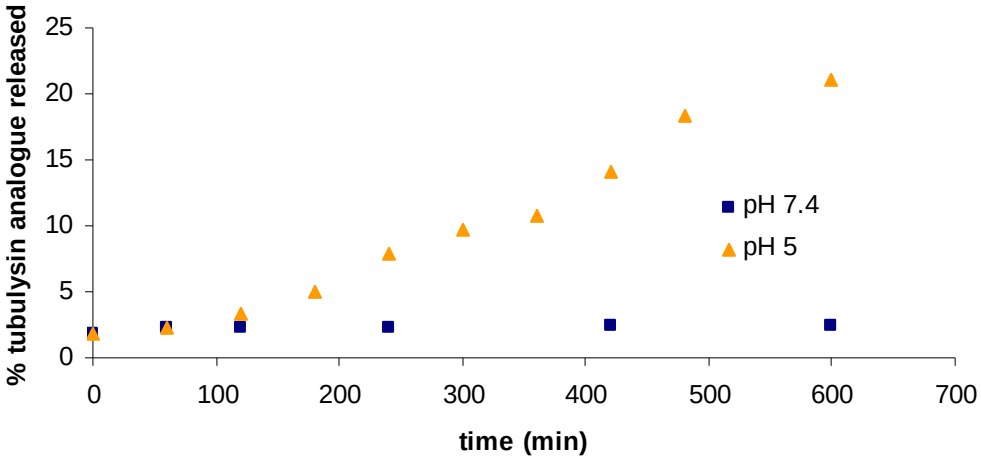

Figure 2. Selective release of tubulysin analogue **3**.

The cytotoxicities of tubulysin analogue **3** and conjugate **5** were next measured in C26 murine colon carcinoma cells. As a reference, the toxicity of tubulysin D was also determined and found to be 0.14 ± 0.3 nM. Tubulysin analogue **3** had a reduced toxicity (IC_{50} = 20 ± 7.4 nM) when compared to tubulysin D, which we anticipated would translate in vivo and allow for more favorable dosing conditions. Similarly, conjugate **5** exhibited a further reduction in toxicity (IC_{50} = 1.50 ± 0.01 mM), however, a significant increase in toxicity is expected upon endocytosis and hydrazone hydrolysis. It should be noted that while analogue **3** has limited water solubility, making in vivo application difficult, once appended to the dendrimer, conjugate **5** is readily water soluble.

To evaluate the toxicity of tubulysin analogue **3** and conjugate **5** in vivo, each compound was administered intravenously to healthy female Balb/C mice. The free analogue **3** was administered at 10 and 20 mg kg^{-1}. Immediate death resulted from higher doses; this is likely related to the low solubility of analogue **3** in aqueous systems, which leads to aggregation of **3** in the bloodstream with dire consequences. In contrast, soluble conjugate **5** could be administered at doses of up to 165 mg kg^{-1} of analogue **3**, without any sign of toxicity. Higher doses were not attempted for safety reasons after consideration of the viscous nature of highly concentrated polymer solutions.

The chemotherapeutic efficacy of tubulysin analogue **3** and conjugate **5** were next evaluated in C26 tumor bearing mice. Female Balb/C mice inoculated with C26 tumors were treated with a PBS control, analogue **3** (10 and 20 mg kg^{-1}), or conjugate **5** (165 mg kg^{-1} of **3**). Mice administered the free drug **3** exhibited signs of distress upon injection, again believed to be a side effect of compound aggregation. The injection proved fatal for two mice in the 20 mg kg^{-1} treatment group. In contrast, mice treated with **5** suffered no adverse effects during injection. Similarly, none of the treatment groups showed significant weight loss as a result of treatment-related toxicity. The free tubulysin analogue did not extend the lifetimes of tumor bearing mice or delay tumor growth (Figure 3 and Table 1). However, mice given the polymeric formulation of the tubulysin analogue showed a 172 % tumor growth delay (TGD) ($p = 0.001$) and a median

survival time of 38 days ($p < 0.0001$) with three of the eight mice tumor free at the conclusion of the study (Figure 4).

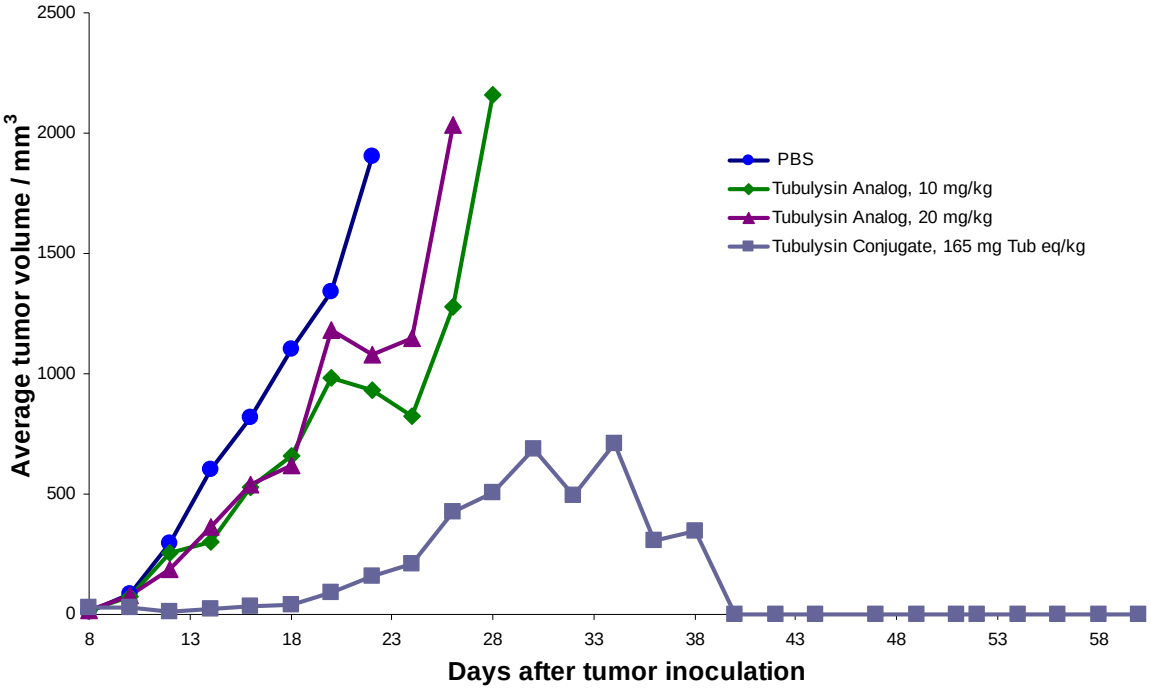

Figure 3. Effect on average tumor growth over time.

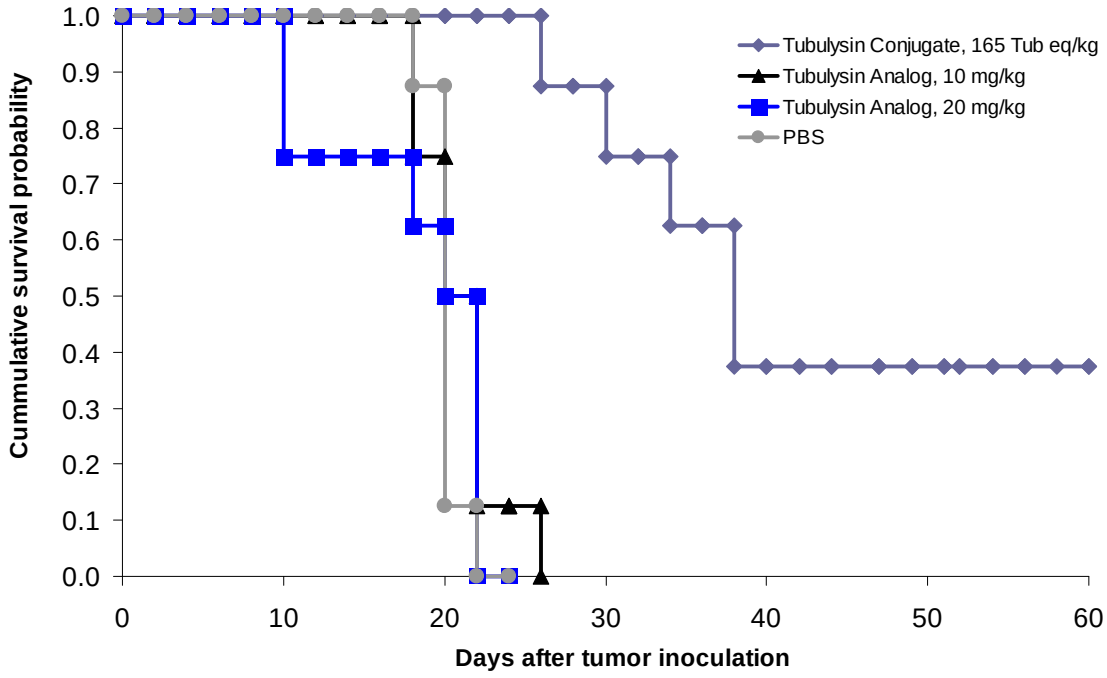

Figure 4. Antitumor efficacy in mice containing C26 colon carcinomas.

Table 1. Chemotherapeutic Efficacy of Tubulysin Ketone in C26 Colon Carcinoma

Treatment Group	No. mice	Dose (mg/kg)	Mean TGD (%)	Median survival time (days)	TRD	LTS
PBS	8	-	-	20	0	0
3	8	10	17	21	0	0
3	8	20	17	23	2	0
5	8	165	172[a]	38[b]	0	3

TGD- tumor growth delay, calculated from growth to 500 mm^3; TRD-treatment related deaths; LTS- long term survivors. [a]Compared to PBS, P = 0.001. [b]Compared to PBS, P < 0.0001

Table 1. Statistical significance of efficacy of **5** against tumors.

Conclusion

In conclusion, we have effectively delivered a novel, completely synthetic, tubulysin analogue **3** by conjugation to a dendrimer through an acyl hydrazone linkage. Although **3** did exhibit greater stability, lower toxicity, and could be synthesized more readily than naturally occurring tubulysins, solubility was a limiting factor for its in vivo use. In contrast, its dendrimer conjugate **5** is highly water soluble and contains a payload of over ten percent by weight of the tubulysin analogue. Tumor bearing mice treated with the maximum tolerated dose of analogue **3** suffered moderate to severe distress after injections and exhibited no therapeutic benefit compared to a PBS control. However, mice treated with a single dose of almost ten times the amount of polymer-bound conjugate **5** showed no signs of toxicity, exhibited a substantially longer lifespan (90 % increase on average), and showed a 37 % cure rate. While this high dose of the dendrimer–tubulysin conjugate was well tolerated, multiple dosing regimens at lower quantities, as well as investigation of more potent tubulysin analogues are currently being pursued. To the best of our knowledge, this is the first example of polymeric drug delivery using a synthetic tubulysin analogue.

References:

[1] F. Sasse, H. Steinmetz, J. Heil, G. Hofle, H Reichenbach, *J. Antibiot.* **2000***, 53*, 879-885.

[2] (a) A. Sandmann, F. Sasse, R. Muller, *Chem. Biol.* **2004***, 11*, 1071-1079. (b) S. C. Wenzel, R. Mueller, *Curr. Opin. Biotechnol*. **2005**,*16*, 594-606; (c) H. B. Bode, R. M_ller, *J. Ind. Microbiol.Biotechnol.* **2006**, *33*, 577-588; (d) S. C. Wenzel, R. Mueller, *Nat.Prod. Rep.* **2007**, *24*,

1211-1224. (e) Y. Chai, D. Pistorius, A. Ullrich, K. J. Weissman, U. Kazmaier, R. Mueller, *Chem. Biol.* **2010**, 17, 296-309.

[3] M. W. Khalil, F. Sasse, H. Lunsdorf, Y. A. Elnakady, H. Reichenbach, *ChemBiochem* **2006**, *7*, 678-683.

[4] G. Kaur, M. Hollingshead, S. Holbeck, V. Schauer-Vukasinovic, R. F. Camalier, *Biochem. J.* **2006**, *396*, 235-242.

[5] J. Howarth, P. Kenny, S. McDonnell, S. O'Connor, *Bioorg. Med. Chem. Lett.* **2003**, *13*, 2693-2697.

[6] (a) G. Hofle, N. Glaser, T. Leibold, U. Karama, F. Sasse, *Pure Appl. Chem.* **2003**, *75*, 167-178. (b) H. Steinmetz, N. Glaser, E. Herdtweck, F. Sasse, H. Reichenbach, *Angew. Chem. Int. Ed.* **2004**, *43*, 4888-4892. (c) A list of all approved cancer drugs can be found at http://www.fda.gov/cder/cancer/druglistframe.html.

[7] For total synthesis efforts see: (a) H. M. Peltier, J. P. McMahon, A. W. Patterson, J. A. Ellman, *J. Am. Chem. Soc.* **2006**, *128*, 16018-16019. (b) S. P. Sreejith, M. Sani, G. Terraneo, M. Zanda, *Synlett*, **2009**, *8*, 1341- 1345. (c) M. Sani, G. Fossati, F. Huguenot, M. Zanda, *Angew. Chem. Int. Ed.* **2007**, **46**, 3526-3529. (d) A. Doemling, B. Beck, U. Eichelberger, S. Sakamuri, S. Menon, Q-Z. Chen, Y. Lu, L. A. Wessjohann, *Angew. Chem. Int. Ed.* **2007**, *46*, 2347-2348. (e) A. Doemling, B. Beck, U. Eichelberger, S. Sakamuri, S. Menon, Q-Z. Chen, Y. Lu, L. A. Wessjohann, *Angew. Chem. Int. Ed.* **2006**, *45*, 7235-7239. (f) P. Wipf, T. Takada, M. J. Rishel, *Org. Lett.* **2004**, *6*, 4057-4060. (g) G. K. Friestad, J-C. Marie, A. M. Deveau, *Org. Lett.* **2004**, *6*, 3249-3252. (h) S. Handrasekhar, B. Mahipal, M. Kavitha, *J. Org. Chem.* **2009**, *74*, 9531- 9534. (i) O. Pando, S. Dorner, R. Preusentanz, A. Denkert, A. Porzel, W. Richter, L. Wessjohann, *Org. Lett.* **2009**, *11*, 5567-5569.

[8] For biological evaluation of the tubulysins and synthetic analogues, see: (a) A. W. Patterson, H. M. Peltier, F. Sasse, J. A. Ellman, *Chem. Eur. J.* **2007**, *13*, 9534-9541. (b) A. W. Patterson, H. M. Peltier, J. A. Ellman, *J. Org. Chem.* **2008**, *73*, 4362-4369 (c) A. Ullrich, J. Herrmann, R. Mueller, U. Kazmaier, *Eur. J. Org. Chem.* **2009**, *36*, 6367-6378. (d) J. A. Reddy, R. Dorton, A. Dawson, M. Vetzel, N. Parker, J. S. Nicoson, E. Westrick, P. J. Klein, Y. Wang, I. R. Vlahov, C. P. Leamon, *Mol. Pharm.* **2009**, 6, 1518-1525. (e) A. Ullrich, Y. Chai, D. Pistorius, Y. A. Elnakady, J. E. Herrmann, K. J. Weissman, U. Kazmaier, R. Mueller, *Angew. Chem. Int. Ed.* **2009**, *48*, 4422-4425. (f) T. Schluep, P. Gunawan, L. Ma, G. S. Jensen, J. Duringer, S. Hinton, W. Richter, J. Hwang, *Clin. Cancer Res.* **2009**, *15*, 181-189. (g) R. Balasubramanian, B. Raghavan, A. Begaye, D. L. Sackett, R. A. Fecik, *J. Med. Chem.* **2009**, *52*, 238-240. (h) C. P. Leamon, J. A. Reddy, M. Vetzel, R. Dorton, E. Westrick, N. Parker, Y. Wang, I. Vlahov, *Cancer Res.* **2008**, *68*, 9839-9844. (i) I. R. Vlahov, Y. Wang, P. J. Kleindl, C. P. Leamon, *Bioorg. Med. Chem. Lett.* **2008**, *18*, 4558-4561. (j) R. Balasubramanian, B. Raghavan, J. C. Steele, D. L. Sackett, R. A. Fecik, *Bioorg. Med. Chem. Lett.* **2008**, *18*, 2996-2999. (k) B. Raghavan, R. Balasubramanian, J. C. Steele, D. L. Sackett, R. A. Fecik, *J. Med. Chem.* **2008**, *51*, 1530-1533. (l) C. D. Richter, D. Nietlispach, R. W. Broadhurst, K. J. Weissman, *Nat. Chem. Biol.* **2008**, *4*, 75-81. (m) Z. Wang, P. A. McPherson, B. S. Raccor, R. Balachandran, G. Zhu, B. W. Day, A. Vogt, P. Wipf, *Chem. Biol.*

Drug Desig. **2007**, *70*, 75- 86. (n) G. Kaur, M. Hollingshead, S. Holbeck, V. Schauer-vukasinovic, R. F. Camalier, A. Doemling, S. Agarwal, *Biochem. J.* **2006**, *396*, 235-242. (o) D. Neri, G. Fossati, M. Zanda, *ChemMedChem* **2006**, *1*, 175-180. (p) A. Doemling, W. Richter, *Mol. Divers.* **2005**, *9*, 141-147. P. Wipf, Z. Wang, *Org. Lett.* **2007**, *9*, 1605-1607. (g) F. Sasse, D. Menche, *Nat. Chem. Biol.* **2007**, *3*, 87-89. (q) Tubulysin analogue delivery papers: (i) for the evaluation of folic acid coupling to tubulysins isolated from natural sources see: **ref 8h**. (ii) for the evaluation of polymers conjugates to tubulysins isolated from natural sourses see **ref 8f**.

[9] S.H. Medina, M.E.H. El-Sayed, *Chem. Rev.* **2009***, 109*, 3141–3157.

[10] (a) S. Liu, R. Maheshwari, L.L. Kiick, *Macromolecules.* **2009***, 42*, 3–13. (b) K. Kataoka, A. Harada, Y. Nagasaki, *Adv. Drug Delivery Rev.* **2001**, *47*, 113–131. (c) X. Guo, F.C. Szoka, *Acc. Chem. Res.* **2003**, *36*, 335–341. (d) D.A. Christian, S. Cai, D.M. Bowen, Y. Kim, J.D. Pajerowski, D.E. Discher, *Eur. J. Pharm. Biopharm.* **2009***, 71*, 463–474. (e) M.E. Fox, F.C.Szoka, J.M.J. Fréchet, *Acc. Chem. Res.* **2009***, 42*, 1141-1151. (f) M.H. Li, P. Keller, *Soft Matter* **2009***, 5*, 927-937. (g) J.J. Green, R. Langer, D.G. Anderson, *Acc. Chem. Res.* **2008***, 41*, 749–759. (h) R. Haag, F. Kratz, *Angew. Chem., Int. Ed.* **2006***, 45*, 1198-1215. (i) D. Peer, J.M. Karp, S. Hong, O.C. Farokhzad, R. Margalit, R. Langer, *Nat. Nanotechnol.* **2007***, 2*, 751-760.

[11] (a) L.W., Seymour, *Crit. Rev. Ther. Drug.* **1992***, 9*, 135–187. (b) Y. Matsumura, and H. Maeda. *Cancer Res.* **1986***, 46*, 6387–6392. (c) H. Maeda*, Bioconjugate Chem*. **1992**, *3,* 351-362.

[12] (a) E.R. Gillies, J.M.J. Fréchet, *Drug Discov. Today.* **2005***, 10*, 35–43. (b) C.C. Lee, J.A. MacKay, J.M.J. Fréchet, F.C. Szoka, *Nat. Biotechnol.* **2005***, 23*, 1517–1526. (c) C.C. Lee, E.R. Gillies, M.E. Fox, S.J. Guillaudeu, J.M.J. Fréchet, E.E. Dy, F.C. Szoka, *Proc. Natl. Acad. Sci. U.S.A.* **2006***, 103*, 16649–16654. (d) O.L.P De Jesus, H.R. Ihre, L. Gagne, J.M.J. Fréchet, F.C. Szoka. *Bioconjugate Chem.* **2002***, 13*, 453– 461. (e) M.C. Parrott, E.B. Marchington, J.F. Valliant, A. Adronov, *J. Am. Chem. Soc.* **2005***, 127*, 12081–12089. (f) E. Bellis, L. Hajba, B. Kovacs, K. Sandor, L. Kollar, G.J. Kokotos, *Biochem. Biophys. Meth.* **2006***, 69*, 151–161. (g) T.R. Krishna. S. Jain, U.S. Tatu, N. Jayaraman, *Tetrahedron.* **2005***, 61*, 4281–4288. (h) H.T. Chen, M.F. Neerman, A.R. Parrish, E.E. Simanek, *J. Am. Chem. Soc.* **2004***, 126*, 10044–10048. (i) J.D. Lim, E.E. Simanek, *Org. Lett. 2008, 10*, 201–204. (j) J. Lim, Y. Guo, C.L. Rostollan, J. Stanfield, J.T. Hsieh, X.K. Sun, E.E. Simanek, *Mol. Pharmaceut.* **2008***, 5*, 540–547. (k) R. Esfand, D. Tomalia, *Drug Discov. Today* **2001***, 6*, 427–436. (l) J.J. Khandare, S. Jayant, A. Singh, P. Chandna, Y. Wang, N. Vorsa, T. Minko, *Bioconjugate Chem.* **2006***, 17*, 1464–1472. (m) K. Kono, C. Kojima, N. Hayashi, E. Nishisaka, K. Kiura, S. Wataral, A. Harada, *Biomaterials.* **2008***, 29*, 1664–1675. (n) D. Bhadra, S. Bhadra, S. Jain, N.K. Jain, *Int. J. Pharm.* **2003***, 257*, 111–124. (o) A.K. Patri, A. Myc, J. Beals, T.P. Thomas, N.H. Bander, J.R. Baker, *Bioconjugate Chem.* **2004***, 15*, 1174–1181. (p) N. Malik, E.G. Evagorou, R. Duncan, *Anti-Cancer Drugs* **1999***, 10*, 767–776. (q) L.M. Kaminskas, B.D. Kelly, V.M. McLeod, B.J. Boyd, G.Y. Krippner, E.D. Williams, C.J.H. Porter, *Mol. Pharmaceut.* **2009***, 6*, 1190–1204. (r) T.L. Kaneshiro, X. Wang, Z.R. Lu, *Mol. Pharmaceut.* **2007***, 4*, 759–768. (s) T. Okuda, S. Kawakami, N. Akimoto, T. Niidome, F. Yamashita, M.J. Hashida, M. *J. Controlled Release.* **2006***, 116*, 330–336. (t) D. G. van der Poll, H. Kieler-Ferguson, W. C. Floyd, S. J. Guillaudeu, K. Jerger, F. C. Szoka, J. M. J. Fréchet, *Bioconjugate Chem.* **2010**, *21,* 764-773. (u) M. E. Fox, S. J. Guillaudeu, J. M. J. Fréchet, K. Jerger, N. Macaraeg, F. C. Szoka, *Mol. Pharmaceut*. **2009**, *6*, 1562-1572.

[13] K. Ulbrich, V. Subr V. *Adv. Drug Deliv. Rev*, **2004**, *56*, 1023-1050.

[14] B. Dubnick, E. W. Rucki, *Eur. J. Pharmacol.* **1970**, *12*, 280-288.

Chapter 5: Macromolecular Conjugation Effects on Gd(III) MRI Contrast Agents using Amide and Ester-amide Dendrimers

Introduction

In the last three decades, magnetic resonance imaging (MRI) has become one of the most prevalent medical imaging modality used in clinical radiology, with over 27.5 million MRI's performed in 2007. Paramagnetic gadolinium(III) contrast agents are used to enhance signal in about a third of these scans. This is done through the gadolinium's ability to slow the relaxation of water molecules after disturbance by a magnetic field, a parameter known as relaxivity (r1). Concern about gadolinium dosage and release has increased because of nephrogenic systemic fibrosis (NSF), an incurable thickening of tissue and skin seen in patients with late stage renal failure. This condition arises from the tendency for free gadolinium ions to bind to hydroxyapatite in bone tissue and transport across cellular ion channels.[1] Increasing the chelate stability, relaxivity and efficiency of contrast agents will allow for smaller doses and lower exposure to free gadolinium ions, improving their performance and lowering the risk for NSF.

All current commercial contrast agents use nitrogen donors to coordinate gadolinium and contain only one inner coordination water molecule *(q* = 1*)*. Previous research in this laboratory has developed oxygen donor chelators for gadolinium through hexacoordinate complexes containing either two 1-Me-3,2-hydroxypyridinonate (HOPO) or two 1,2-HOPO rings and an amine functionalized 2,3-dihydroxyterepthalamide (TAM) ring (Figures 1 and 2).[2-7] These tris(2-aminoethyl)amine (TREN)-capped ligands have at least two coordinated water molecules, with fast exchange rates, allowing a much larger theoretical relaxivity than the small molecule amine based chelators. These complexes exhibit high T_1 relaxivities (10-13 $mM^{-1}s^{-1}$) and thermodynamic complex stabilities (pGd ~ 17-18). The 1-Me-3,2-HOPO based ligands used in this study vary by the nature of the amine pendant to the TAM ring. Complex **1** has a short, rigid linker and a known *q* value of two.[2] Complex **2** has a longer, more flexible linkage incorporating a second ethylamine moiety, and complex **3** has a branched linkage with a third ethylamine group. Complex **4**, containing the 1,2-HOPO moiety varies from these by its nitrogen substitution within the HOPO rings.

MRI contrast agents can be further optimized for larger relaxivity and solubility through conjugation to a biocompatible macromolecule such as a protein,[3] polypeptide,[8] dendrimer,[9-14] or nanoparticle,[15,16] which lowers the molecular tumbling time of the gadolinium due to the reduced degrees of freedom of large molecules in solution.

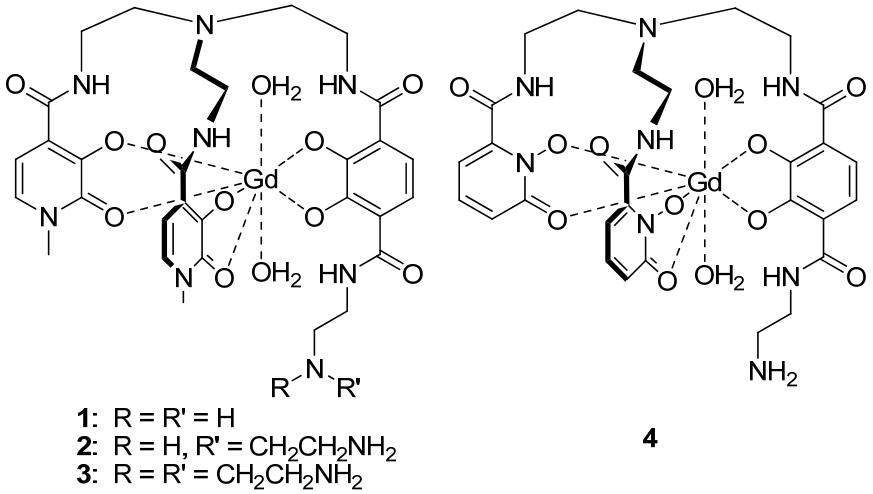

Figure 1. The Gd-TREN-bis(1-Me-3,2-HOPO)-TAM-ethylamine complexes **1-3** and Gd-TREN-bis(1,2-HOPO)-TAM-ethylamine complex **4**.

We anticipated that the previously reported easteramide (**EA**) and branched poly-L-lysine (**PLL**) based dendrimers[17] would be promising, as these degradable dendrimers offer a synthetically straightforward route to high molecular weight conjugates with facile renal clearance and low toxicity. We also anticipated that the densely packed core of the dendrimers would sterically inhibit the motion of the gadolinium complex, further increasing its relaxivity. The **EA** and **PLL** dendrimers developed by the Fréchet group have exhibited low toxicity *in vivo*, favorable degradation profiles (see supplementary information), and can be decorated with up to eight gadolinium complexes per dendrimer.[17, 18] These dendrimers have also been shown to increase half-life in blood serum and residence time of small molecule drugs, allowing for their improved drug delivery *in vivo.*[19] In addition to enhancing the relaxivity and blood half-life of contrast agents, polymeric carriers are also expected to significantly reduce the toxicity of these agents due to the much slower rates of endocytosis for macromolecules compared to lipophilic small molecule compounds such as nonpolymeric gadolinium complexes. This should reduce the amount of gadolinium entering cells, and thereby facilitate its eventual excretion through the renal system.

We report herein that **EA** and **PLL** dendrimers have been successfully conjugated to precomplexed Gd-TREN-bis-HOPO-TAM-Ethylamine based complexes. The conjugates exhibit high (up to 38 $mM^{-1}s^{-1}$) relaxivities (r1) under the clinically relevant conditions of 37 ^{o}C at 60 mHz, which is almost an order of magnitude higher than the relaxivities of many commercial contrast agents (Table 1).

Results and Discussion

The syntheses of the **PLL** and **EA** dendrimers[17], complexes **1-3**[2] and complex **4**[20] have been reported previously. Conjugates were obtained by peptide bond coupling between the carboxylic acid of the dendrimer and the amine of a Gd-TREN-bis-HOPO-TAM complex using carbodiimide coupling conditions (Scheme 1). Because the gadolinium introduced into the reaction is already tightly bound as a highly stable complex, this precomplexation of the metal before conjugation reduces the possibility that free gadolinium ions might bind to non-specific

coordination sites. Conjugates were purified by precipitation into ether followed by aqueous size exclusion chromatography using PD-10 columns.

When **1** was coupled to the **EA** dendrimer, (Scheme 1) ICP and DMF-SEC measurements indicate a loading of six gadolinium complexes per dendrimer. This conjugate, **5**, has a per gadolinium relaxivity of 38.14 ± 0.02 $mM^{-1}s^{-1}$, or 228 $mM^{-1}s^{-1}$ per dendrimer, at 37 ^{o}C. This value compares very favorably to other relaxivities measured under clinically relevant conditions, which are typically in the range of 3-5 $mM^{-1}s^{-1}$ for current commercial agents (Figure 3).

We further investigated **2** as a conjugate with the **EA** dendrimer (**6**) due to its high thermodynamic stability. This small molecule complex has a thermodynamic stability value three orders of magnitude larger than that of **1** or **3**.[2] This increased complex stability should reduce the amount of free gadolinium that can be leached from the conjugate *in vivo*, which may reduce toxicity concerns. However, due to the longer and more flexible linker, the molecular tumbling time and relaxivity were decreased compared to conjugate **5**, giving conjugate **6** a per gadolinium relaxivity of 31.9 ± 0.1 $s^{-1}mM^{-1}$. Although a lower complex loading per dendrimer was observed by ICP and SEC (2.8 complexes/dendrimer), conjugate **6** has the potential to be a safer option due to the higher thermodynamic stability of the gadolinium-chelate binding.

Given the success of the 1-Me-3,2-HOPO chelator, a variation on this moiety, a 1,2-HOPO chelator was evaluated. When conjugated to the **EA** dendrimer, relaxivity values of 20.2 ± 0.6 $mM^{-1}s^{-1}$ were obtained for conjugate **7**. In general the 1,2-HOPO complexes show lower relaxivity than their 1-Me-3,2-HOPO counterparts[4,21], and this trend appears to be conserved upon conjugation to the dendrimer.

We also investigated ligand conjugation to the **PLL** dendrimer to further test the versatility of this approach. Conjugate **8** has a per gadolinium relaxivity of 21.0 ± 0.6 $mM^{-1}s^{-1}$. While this result constitutes a significant increase over the small molecule complex, it is still significantly lower than that obtained with the **EA** dendrimer. We attribute this decrease to greater internal hydrogen bonding between the inner-sphere water coordination sites of the gadolinium and the more hydrophilic amide based **PLL** dendrimer core, or by increased tumbling of the gadolinium(III) complexes caused by the less branched and sterically crowded core employed in this dendrimer. This decreased relaxivity with the **PLL** dendrimer, combined with the more favorable biodegradability of the **EA** dendrimer, suggests that the **EA** dendrimer is a superior platform for this application.

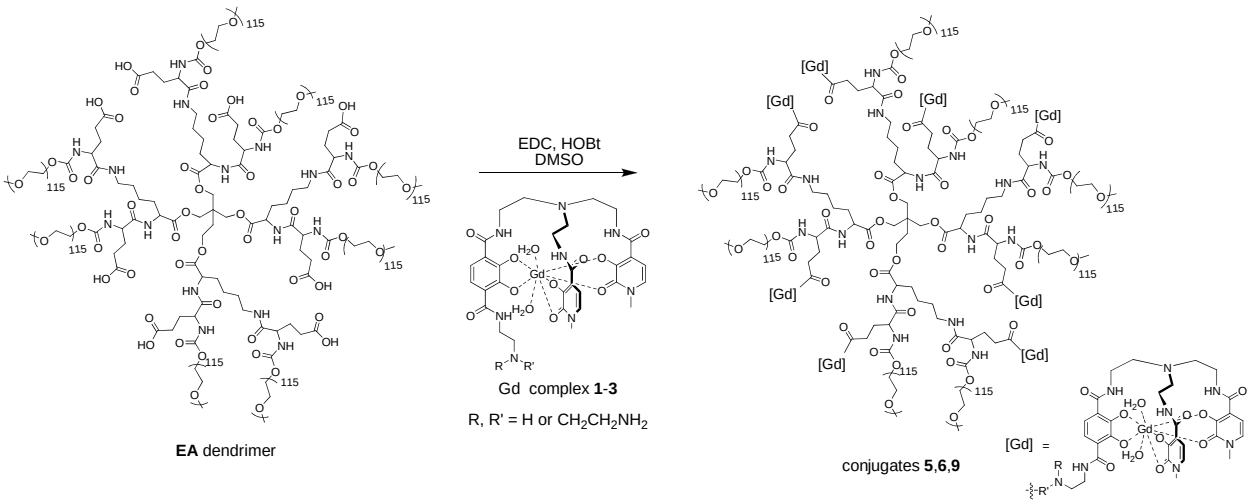

Scheme 1. The conjugation of Gd-TREN-bis(1-Me-3,2-HOPO)-TAM-Ethylamine complexes **1-3** to the **EA** dendrimer. Conjugates **7** and **8** were synthesized under identical conditions.

Finally, we investigated complex **3** with the **EA** dendrimer, but found that the extended linker and extra primary amine resulted in a conjugate, **9**, with a relatively low relaxivity of 7.19 ± 0.07 $s^{-1}mM^{-1}$.

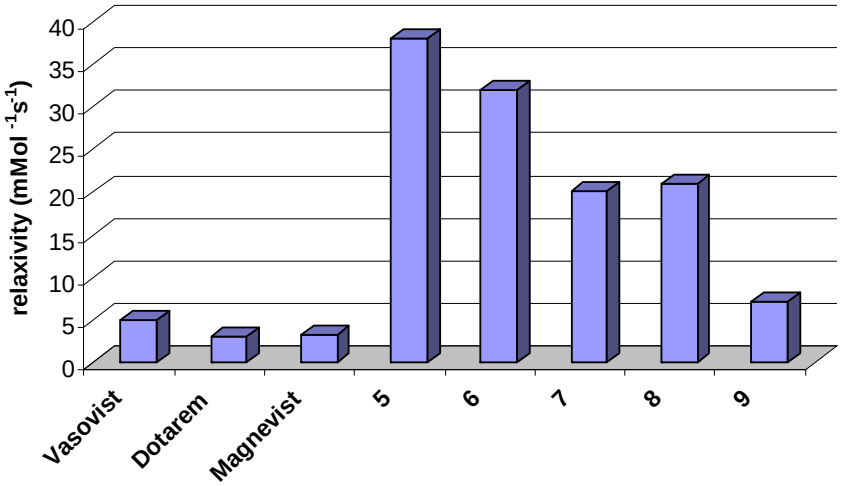

Figure 3. A comparison of the per gadolinium relaxivities of several clinical Gd(III) contrast agents and the dendrimer contrast agents investigated. Values measured at 37 ^{o}C at 60 mHz.

To evaluate the toxicity of these conjugates, cytotoxicity studies were carried out for 72h to determine their effect on cell viability using Gd-DTPA, **PLL**, and **EA** dendrimers as controls. While most MRI contrast agents are excreted within 24 hours, the macromolecules may be excreted more slowly, and cytotoxicity testing of 72 hours was performed to reflect this increased residence time. Each of the conjugates exhibited no evidence of cytotoxicity at 1.0 mg/mL concentrations of conjugates **5-9** (see Supplementary Information), indicating that these contrast agents have not acquired short term toxicity through their macromolecular conjugation. Through conjugation to highly biocompatible and readily synthesized dendrimers, the relaxivity of HOPO-based TREN capped Gd(III) complexes, relaxivity was improved over commercial agents without compromising clinical relevance and safety. The conjugates presented here

contain tightly bound gadolinium and give relaxivities of up to 38 $mM^{-1}s^{-1}$ under the clinically relevant conditions of 60 mHz and 37 ^{o}C, and were shown to be nontoxic to cells at mM concentrations.

Experimental Procedures

General Considerations: Unless otherwise noted, starting materials were obtained from commercial suppliers and used without further purification. All solvents were stored over 4 Å molecular sieves. Water was distilled and further purified by a Millipore cartridge system (resistivity 18.2 x 10^6 Ω). All organic extracts were dried over anhydrous $MgSO_4$ and solvents removed *in vacuo* by a rotory evaporator or vacuum pump evacuation. Flash chromatography was performed on Merck Silica Gel (40-7 Mesh). Ion exchange chromatography was done on Phenomenex Strata X-C prepacked columns (pore size 85 Å, particle size 33 μm). ^{1}H and ^{13}C NMR spectra were recorded on a Bruker AVQ600 at 600 MHz, AVQ 400 at 400 MHz and 100 MHz or a Bruker AVB 400 at 400 MHz and 100 MHz, respectively; the residual solvent peak was used as an internal reference. Elemental analysis and mass spectra (LR = low resolution; HR = high resolution; FAB MS = fast atom bombardment mass spectrometry; EI MS = electron ionization mass spectrometry; ES MS = electrospray mass spectrometry) were performed by the Microanalytical Laboratory and Mass Spectrometry Laboratory, respectively, at the College of Chemistry at the University of California at Berkeley. Matrix Assisted Laser Desorption Ionization mass spectra (MALDI-MS) were recorded on an Applied Biosystems Voyager System 6322. Applied Biosystems, USA). MALDI measurements were recorded using a 25:1 α-cyano-hydroxycinnamic acid: sample ratio, using positive linear ion detection, with accelerating voltage = 20kV, grid voltage = 94%, and delay time of 100ns. Prep-HPLC was done on a Varian Prep HPLC system using a Varian super-prep C18 column (Dynamax C18, 41.4 x 250 mm, 10 μm particle size). Electrospray LC/MS analysis was performed using an API 150EX system (Applied Biosystems, USA) at standard instrument settings equipped with a Turbospray source and an Agilent 1100 series LC pump. All synthetic reactions were performed in an atmosphere of nitrogen, unless otherwise noted. The esteramide (EA) and PLLG2(Asp(COOH)$PEO)_8$ Polylysine (PLL) dendrimers were Synthesized as was previously reported.[17]

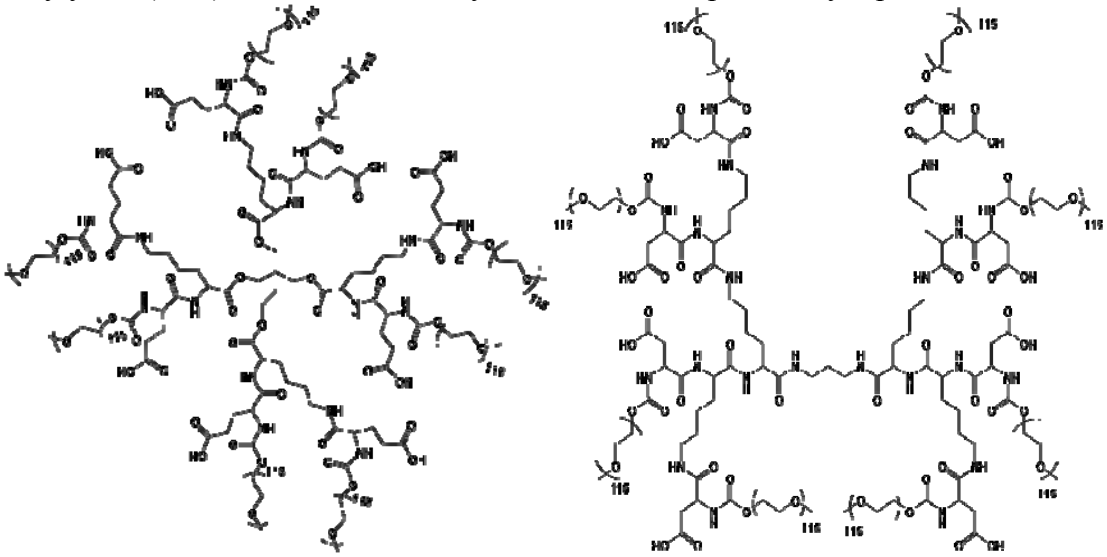

Figure 1. The esteramide (**EA**) dendrimer (left) and polylysine dendrimer (**PLL**) (right).

Gd-TREN Complex Synthesis: Gd-TREN-bis(1-Me-3,2-HOPO)-TAM-Ethylamine (**1**), Gd-TREN-bis(1-Me-3,2-HOPO)-TAM-Ethylamine-ethylamine (**2**) and Gd-TREN-bis(1-Me-3,2-HOPO)-TAM-Ethylamine-bisethylamine (**3**) were synthesized as previously reported. See Pierre, V.; Botta, M.; Aime, S.; Raymond, K. N. *Inorg. Chem.* **2006**, *45,* 8355-8364. Gd-TREN-bis(1,2-HOPO)-TAM-Ethylamine (**4**) was synthesized as previously reported. See Werner, E.J.; Kozhukh, J.; Botta, M.; Moore, E.G.; Avedano, S.; Aime, S.; Raymond, K. N. *Inorg. Chem.* **2009**, *48,* 277-286.

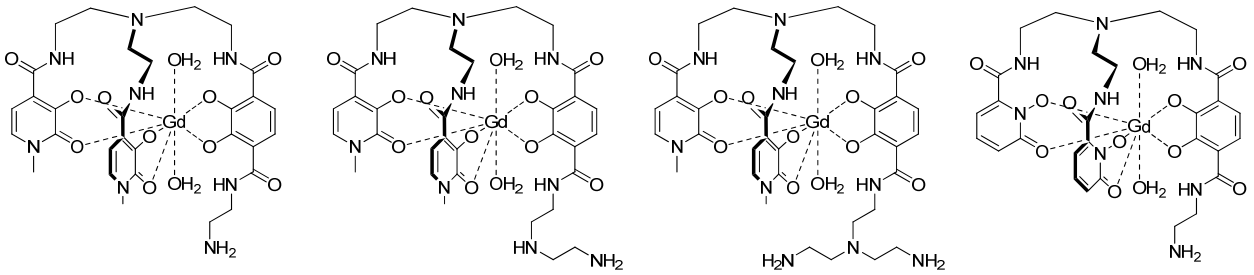

Figure 2. The gadolinium chelators used for macromolecular conjugation.

Size Exclusion Chromatography (SEC): The SEC system consisted of two SDV Linear S (5 µm) columns (Polymer Standards Service, 300 x 8 mm) using DMF with 0.2% LiBr as the mobile phase (1 mL/min) in series with a Waters 515 pump, 717 autosampler, 996 Photodiode Array Detector (210-600 nm), and 2414 differential refractive index (RI) detector. Sample volumes were 100 µL and UV spectra were viewed at 350 nm. Molecular weight calibrations for RI spectra were made using linear polyethylene glycol standards with toluene as a reference peak. Gadolinium loading was quantified by comparing polymer peak integrals in UV spectra with a calibration curve obtained from spectra of known concentrations of gadolinium complexes run under identical conditions.

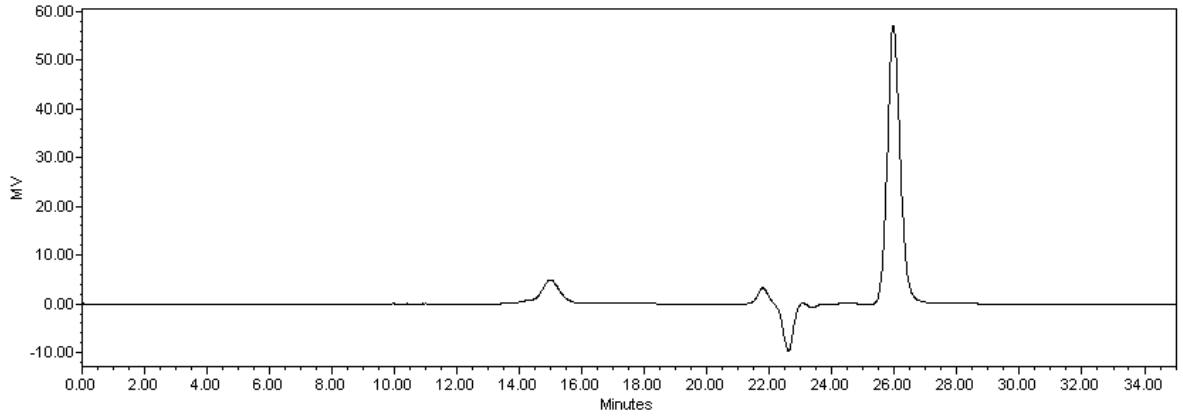

Figure 4. Reference refractive index (RI) SEC trace of the **EA** dendrimer. The 40 kDa dendrimer appears at 15 minutes, residual 5 kDa PEG will appear at 18 minutes, and the toluene reference peak appears at 26 minutes. The oscillation in the baseline at 21-23 minutes is a system peak present in all traces. Prior to conjugation the **EA** dendrimer does not appear in the UV trace at 350 nm.

Inductively Coupled Plasma- Optical Emission Spectroscopy (ICP-OES): ICP-OES was performed on a Perkin Elmer Optima 700 DV. Samples for analysis were diluted in 2% (v/v) nitric acid in Millipore water. Gd(III) standards were prepared in 2% (v/v) nitric acid/Millipore

water with concentrations between 0.01 and 40.0 μg/mL. Using a weighed sample, a percentage Gd (III) of the sample could be calculated and therefore quantify Gd (III) per dendrimer (μm).

Conjugate	Complex loading (Gd/dendrimer)
5	6.0
6	2.9
7	8.0
8	4.5
9	3.0

Table 1. Complex loadings of conjugates as measured by ICP. The theoretical maximum loading is eight Gd complexes per dendrimer.

Dynamic light scattering (DLS): DLS determined hydrodynamic size and was performed at 25 °C by dissolving samples in 1X PBS buffer to a concentration of approximately 0.5-1 mg/mL. After brief vortexing the samples were filtered over 0.45 μm PTFE filters to remove dust and added to a 0.45 μL quartz cuvette and analyzed using a Zetasizer Nanoseries ZS (Malvern Instruments, UK). Results were repeated in triplicate with averages reported.

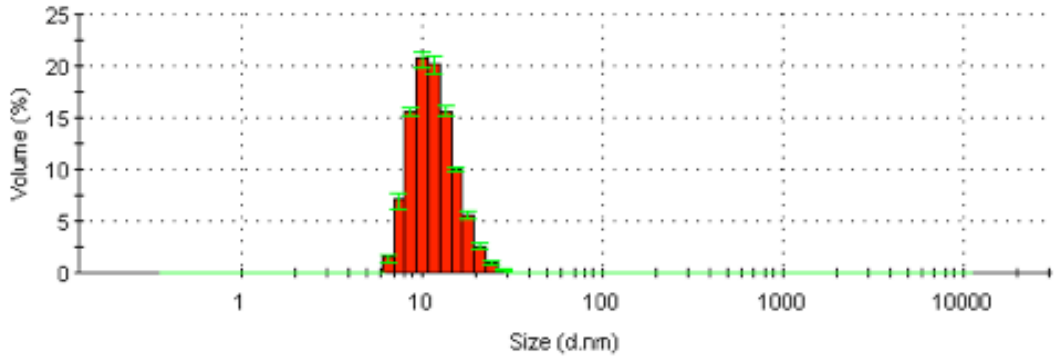

Figure 5. DLS of Esteramide dendrimer at 1.0 mg/mL (filtered) showing a 10 nm diameter particle with no aggregation.

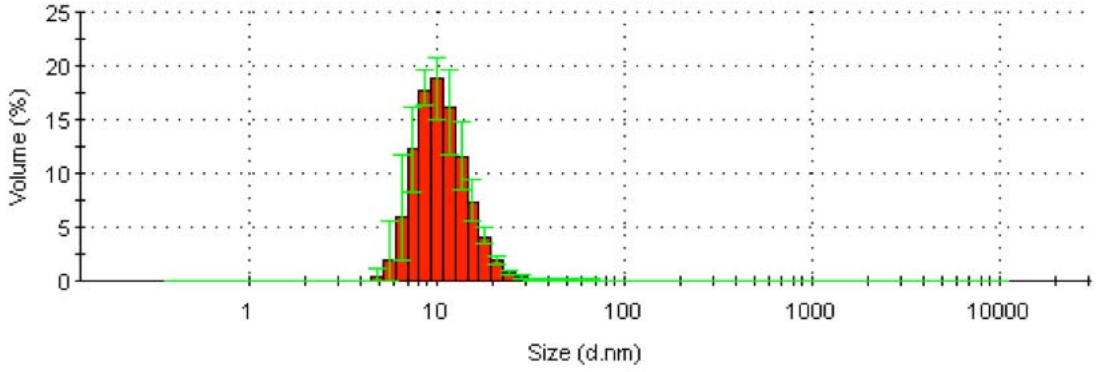

Figure 6. DLS for the PLL dendrimer at 0.5 mg/mL showing a 10 nm diameter polymer with no aggregation.

Dendrimer-Complex Conjugation

8: To a 25mL scintillation vial containing 15 mg (0.017 mmol, 1.3 eq.) of gadolinium complex **1** was added 70 mg (0.014 mmol by carboxylic acid) of **PLL** dendrimer. To this was added 11 mg

(0.11 mmol, 7 eq.) each of N-hydroxysuccinimide (NHS) and hydroxybenzotriazole (HOBt). The solids were dissolved in 0.5 mL DMSO and 3.5 mg (0.018 mmol, 1.3 eq.) of EDC (EDAC or EDCI, 1-ethyl-3-(3-dimethylaminopropyl) carbodiimide) were added and the reaction was allowed to stir overnight at room temperature under nitrogen atmosphere. After overnight stirring, the solvent was removed *in vacuo* and solids were taken into 5 mL DCM. After filtering solids through a 0.45 μm PTFE (polytetrafluoroethylene) filter the solution was precipitated by addition to 100 mL diethyl ether (anhydrous) to give a light yellow solid. The solids were isolated by centrifugation and residual impurities were removed using a PD-10 size exclusion column to give 35 mg (50.%) of conjugate **8** as a yellow solid. SEC: Mn = 38,000 Da, PDI = 1.11. ^{1}H NMR (D_2O, 500 MHz): δ (ppm) = 0.97 (br s 4), 1.20 (br s, 10), 1.36 (br s, 10), 1.56 (br s, 10), 1.74 (br s, 3), 2.4-2.7 (br m, 20), 2.73 (s, 7), 2.79 (br s, 7), 3.01 (br s, 25), 3.23 (s, 24), 3.4-3.8 (br m, ~3500), 4.24 (br s, 25).

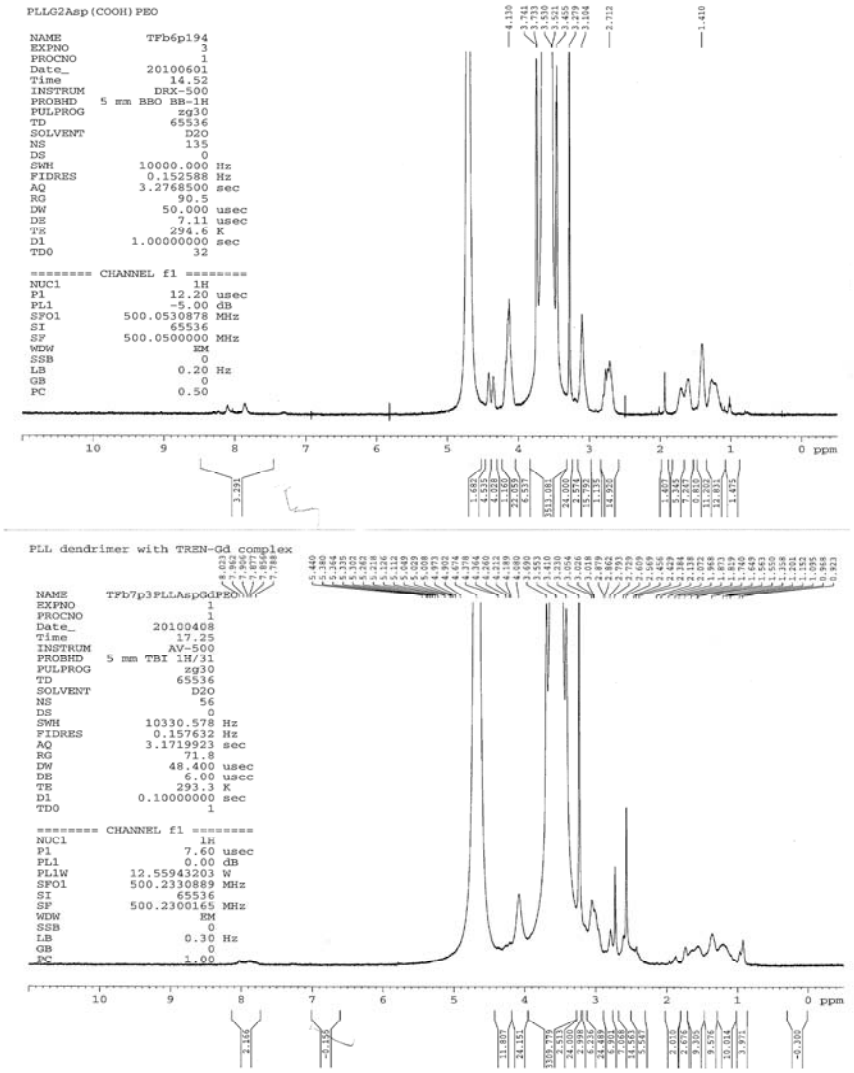

Figure 7. ^{1}HNMR of **PLL** binding to **1**. Top: PLL dendrimer before conjugation. Bottom: Conjugate **8**, PLL dendrimer with complex **1** attached. The peaks are broadened by the seven unpaired electrons of the gadolinium interfering with the NMR signal.

5: To a 25mL scintillation vial containing 7.5 mg (0.0090 mmol, 1.7 eq.) of complex **1** was added 27 mg (0.005 mmol by carboxylic acid) of **EA** dendrimer. To this was added 4 mg (0.03

mmol, 5 eq.) each of HOBt and DMAP. The solids were dissolved in 1 mL DMSO and 8 mg (0.04 mmol, 8 eq.) of EDC were added and the reaction was allowed to stir overnight at room temperature under nitrogen atmosphere. After 14 hours the solvent was removed *in vacuo* and solids were taken into 5 mL DCM. After filtering solids through a 0.45 µm PTFE filter the red solution was precipitated with the addition of 100 mL ether to give a pink fluffy solid. The solids were isolated by centrifugation and residual ligand was removed using a PD-10 size exclusion column to give 20 mg (70%) of conjugate **5** as a pink solid. SEC: Mn = 44,000 Da, PDI = 1.36.

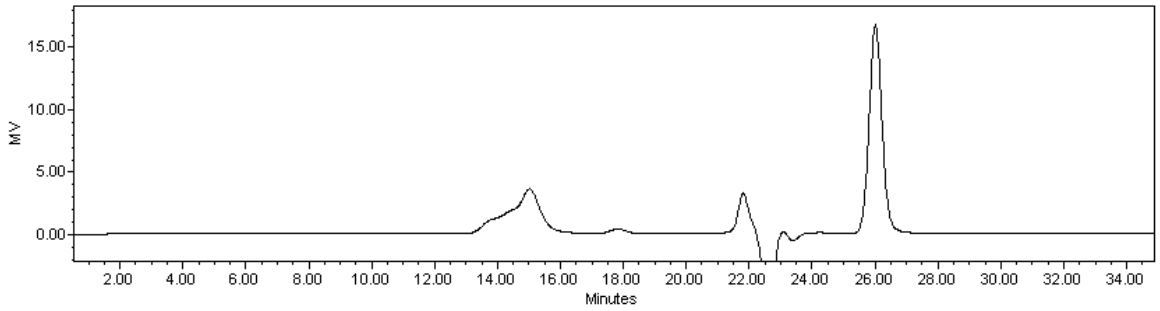

Figure 8. SEC RI Trace **5**. The high molecular weight shoulder at 14 minutes indicates that the conjugate partially aggregates in DMF.

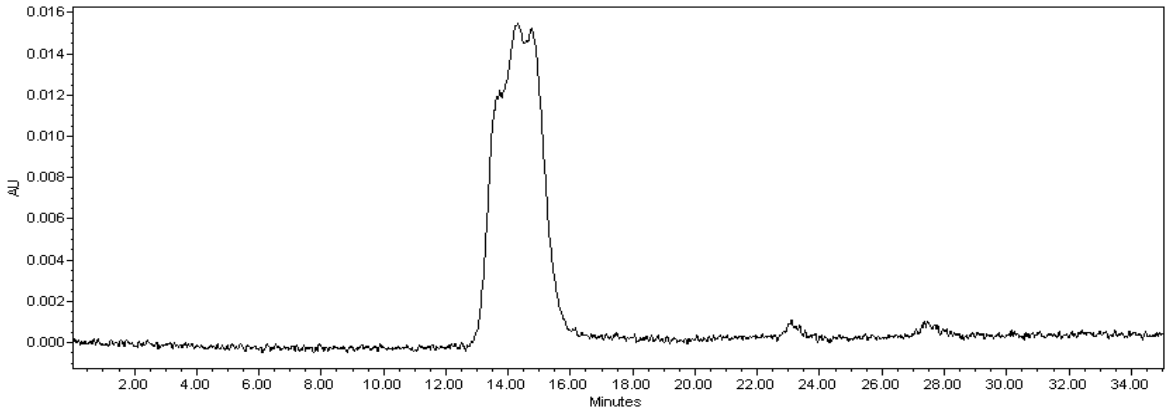

Figure 9. SEC UV-Trace of **5**. The 40 kDa polymer present at 13-16 minutes is now UV active, indicating conjugation of the HOPO-TAM ligands to the dendrimer. Free Gd chelates will appear in the small molecule region of 25-30 minutes.

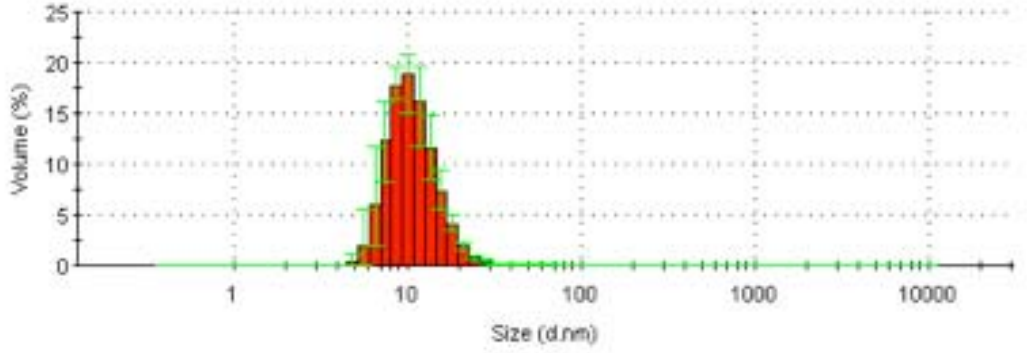

Figure 10. DLS of conjugate **5**, showing a polymer with a 10nm diameter. While SEC showed aggregation in DMF, no aggregation is present in aqueous DLS samples.

6: To a 25mL scintillation vial containing 5.9 mg (0.0070 mmol, 1.7 eq.) of complex **2** was added 20 mg (0.004 mmol by carboxylic acid) of **EA** dendrimer. To this was added 3 mg (0.02 mmol, 5 eq.) each of HOBt and DMAP. The solids were dissolved in 0.5 mL of a 1:1 mixture of DMSO and 2.6 mg (0.013 mmol, 3 eq.) of EDC were added and the reaction was allowed to stir overnight at room temperature under nitrogen atmosphere. After 14 hours the reaction was precipitated with the addition of 100 mL ether to give a brown solid. The solids were isolated by centrifugation and taken into 5 mL DCM and filtered over a 0.45 µm PTFE filter. After evaporation residual ligand was removed using a PD-10 size exclusion column to give 18 mg (85%) of conjugate **6** as a pale yellow solid. SEC: Mn: 30,900 Da, PDI: 1.18.

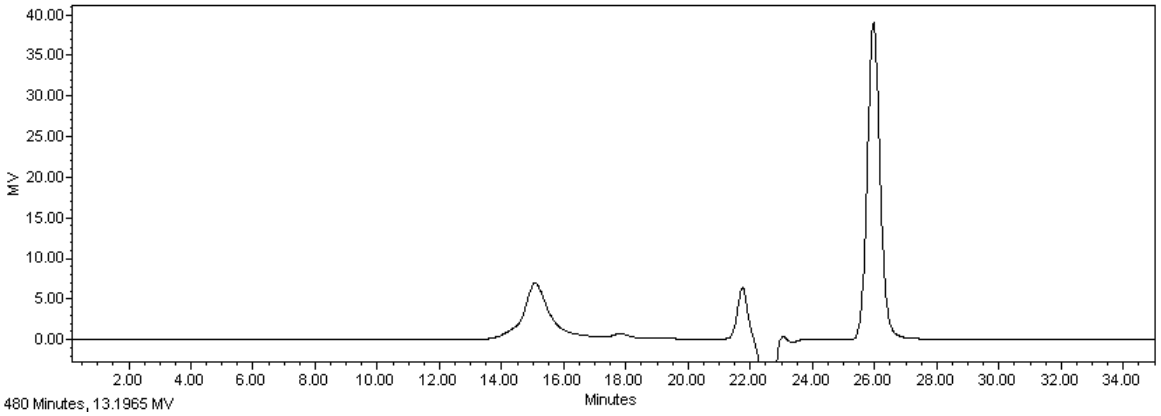

Figure 11. SEC RI trace of **6**.

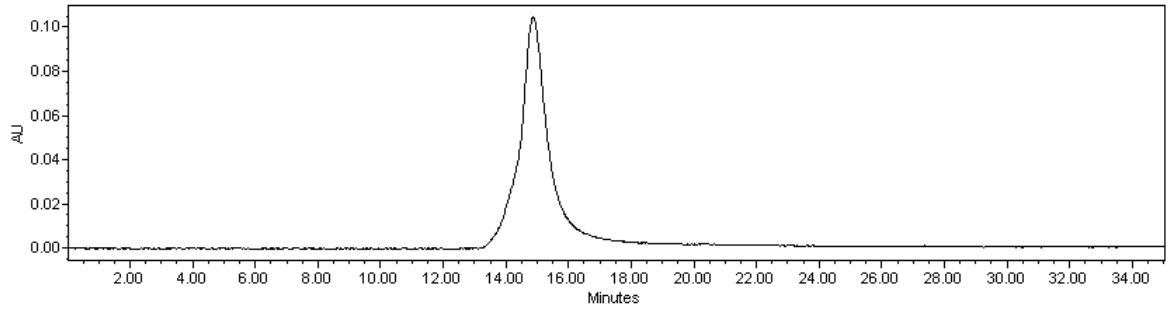

Figure 12. SEC UV trace of **6**, showing a uv active macromolecule.

.

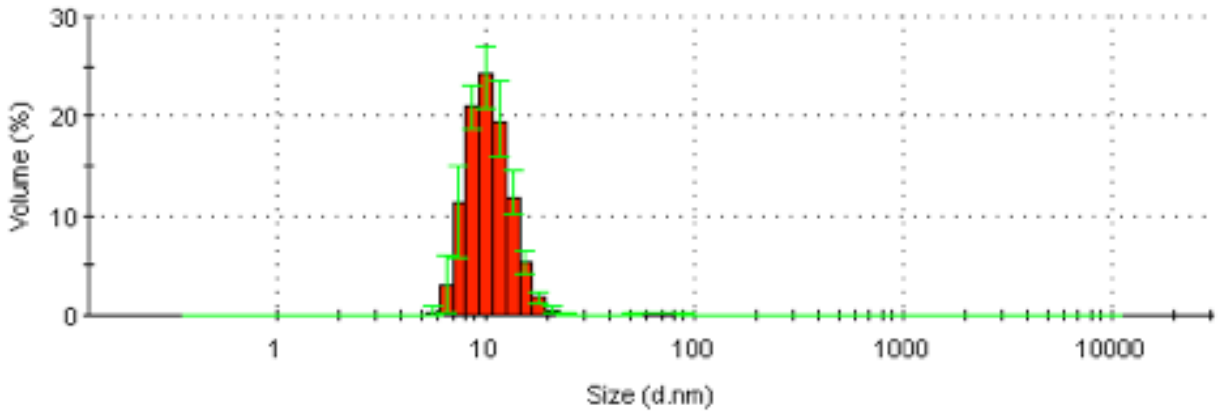

Figure 13. DLS of **6** at 0.5 mg/ml.

9: To a 25mL scintillation vial containing 10.5 mg (0.00197 mmol by carboxylic acid) of **EA** dendrimer was added 3 mg (0.03 mmol, 10 eq.) of NHS. To this was added 0.5 mL of DMF and the solution was vortexed briefly to dissolve solids. To this was added 2 mg (0.01 mmol, 5 eq.) of EDC and the reaction was stirred for 5 minutes. To this solution was then added 3.5 mg (0.0041 mmol, 2 eq.) of complex **3** and the reaction was allowed to stir overnight at room temperature under nitrogen atmosphere. After 14 hours the reaction was precipitated with the addition of 15 mL ether and centrifuged to give a brown solid. The solids were then taken into 5 mL DCM and filtered over a 0.45 µm PTFE filter. Solvent was removed under reduced pressure to give 9.5 mg (86%) of conjugate **9** as a clear film. SEC: Mn: 37,400 Da, PDI: 1.12

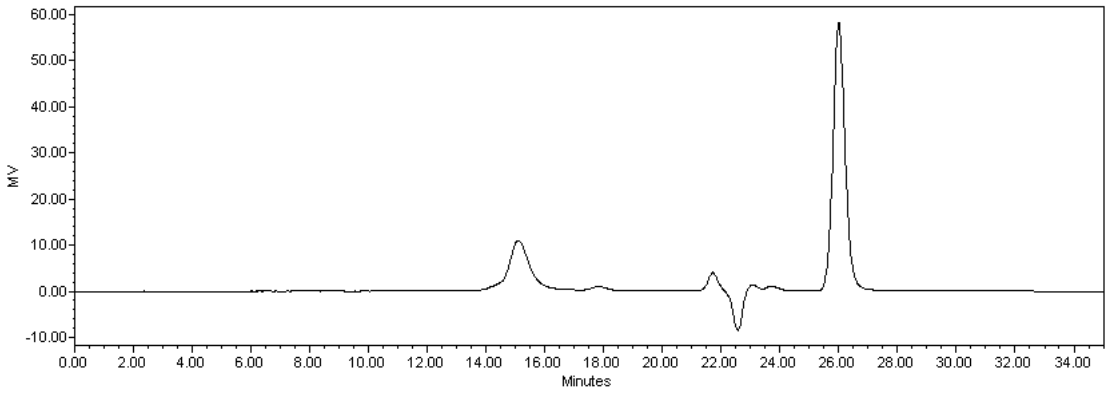

Figure 14. SEC RI trace of **9**.

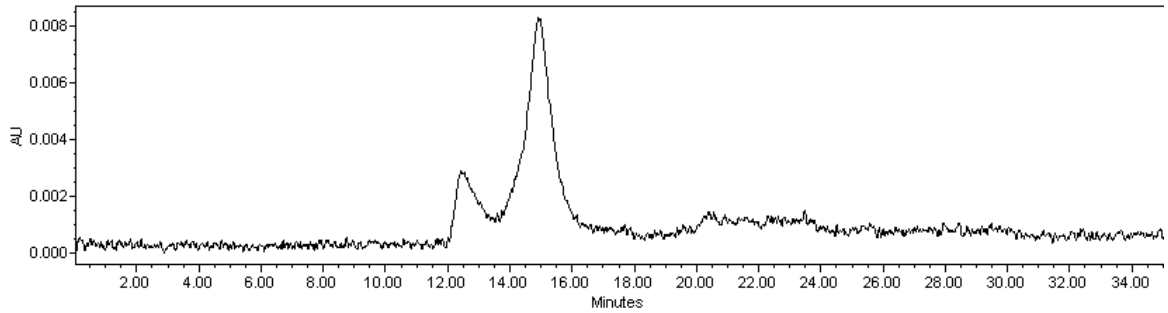

Figure 15. SEC UV trace of **9**. Two peaks in this trace indicate that the ligand is in two unique environments on the dendrimer, suggesting aggregation.

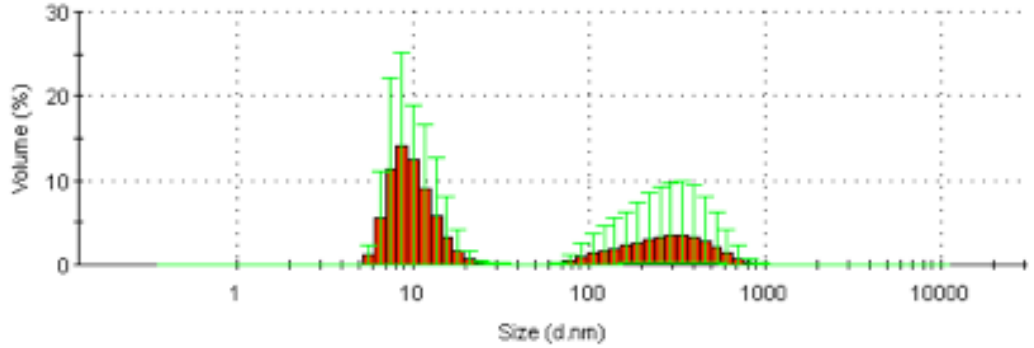

Figure 16. DLS of **9**, showing significant aggregation.

7: To a 2 mL vial containing 2.0 mg (0.0024 mmol, 2.2 eq) of **4** was added 5.5 mg **EA** dendrimer (0.0011 mmol COOH), 0.75mg DMAP (0.0058 mmol, 5.3 eq), and 0.75mg HOBt (0.0065 mmol, 6.9 eq) in 200 µL DMF. This was stirred and vortexed until a homogeneous

solution was obtained, and 1.9 mg EDC (0.0099 mmol, 9.0 eq.) was added in 200 µL DMF and the reaction was allowed to stir overnight at room temperature under nitrogen atmosphere. After 14 hours the solvent was removed *in vacuo* and the solids were purified by precipitation in ether from DCM followed by PD-10 size exclusion columns and filtration of the product fraction over 0.45 µm PTFE filters. Lyophilizing gave **7** (6.3 mg, 98%) as a white fluffy solid. SEC: Mn: 38,400 Da, PDI: 1.22

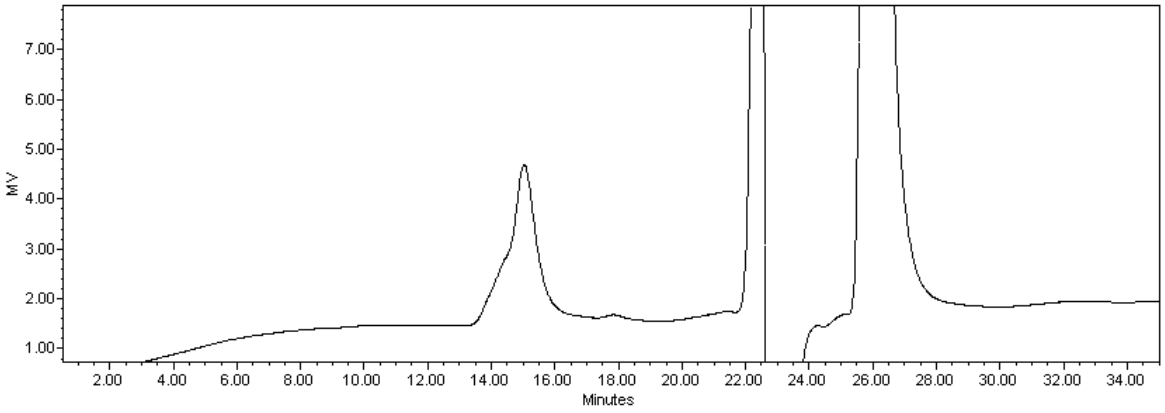

Figure 17. RI trace of **7**.

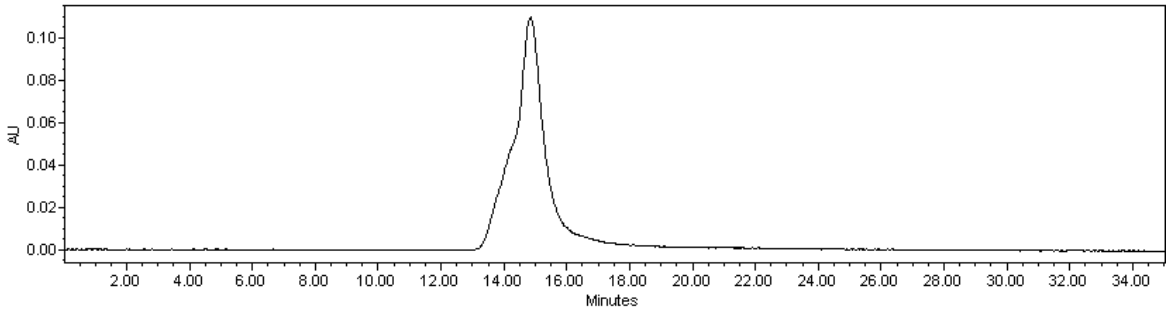

Figure 18. UV-Vis trace of **7** at 350 nm. All UV active material is bound to the polymer.

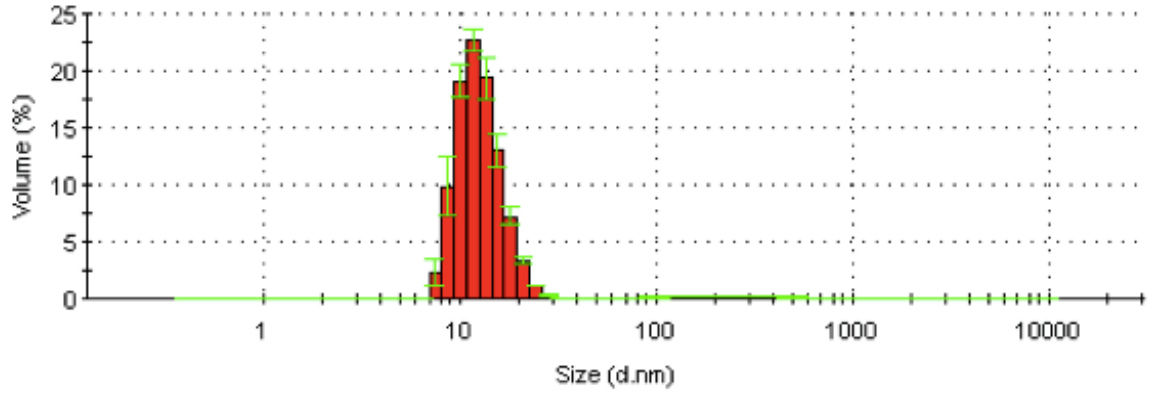

Figure 19. DLS of conjugate **7**.

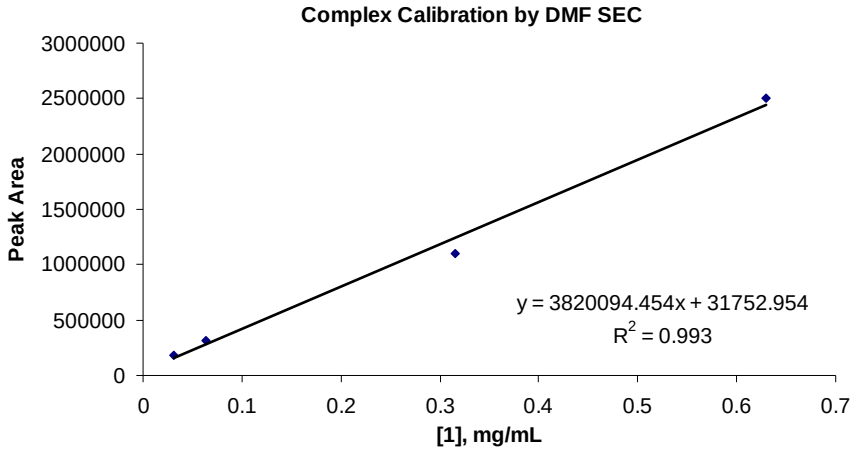

Figure 20. SEC-UV data calibration plot. Plotting peak area versus complex **1** concentration, a sample's Gd concentration could be determined from the SEC's peak area. A preliminary loading of 4.5 gadolinium complexes/dendrimer (55% of theoretical max) for **8** was calculated in this way .

Cell Culture by MTT Assay for Conjugates: HeLa cells were purchased from American Type Culture Collection (ATTC) and plated by the Molecular and Cell Biology Cell Culture Facility at University of California, Berkeley, to 10,000 cells per well. All conjugates were evaluated, as well as control samples used were the esteramide dendrimer, the polylysine dendrimer, and Gd-DTPA, a commercial MRI contrast agent.

Solutions were made in the concentration of 1.0 mg/mL in Dulbecco's modification of Eagle's Media (DMEM, with glucose and 10% fetal bovine serum (FBS). Dilutions were made on one plate at the rate of two-fold per well, for eight total dilutions and a final concentration of 0.05 mg/mL of sample. These solutions were transferred in 100 µL dilutions onto HeLa cells, which were already in 100 µL of media. These samples were incubated for 72 h at 37 °C and 5% CO_2. After 24 hours, 40 µL of thiazolyl blue tetrazolium bromide (98% TLC) was added for a MTT assay at 2.9 mg/mL. These samples were incubate for 30 min at 37 °C and 5% CO_2. After 30 min, the cells were aspirated and 200 µL of DMSO added, followed by 25 µL of pH 10.5 glycine buffer (100 mmol glycine and 100 mmol salt). Absorbance was measured at 570 nm on a Molecular Devices plate reader and cytotoxicity determined based on blank live cells and starved cells (terminated by denying media). All results repeated in triplicate and averaged reported.

Complex: Dendrimer (if applicable)	% Viability (After 72 hours)
Esteramide Control	99.44 ± 0.04
PLL Control	99.9 ± 0.2
Gd-DTPA (Commercial MRI Contrast Agent) Control	99.6 ± 0.1
Conjugate **5**	99.7 ± 0.3
Conjugate **8**	99.6 ± 0.2
Conjugate **6**	99.8 ± 0.1
Conjugate **9**	99.7 ± 0.2
Conjugate **7**	99.8 ± 0.21

Table 2. Cytotoxicity results for over 72 hours at 1.0 mg/mL concentrations.

Relaxivity Studies: T_1 measurements were performed on a Bruker mq60 minispec relaxometer. T_1 was determined at 60 MHz (1.5 T) using an inversion recovery pulse sequence. Temperature controlled at 37 °C using a Julabo F25 circulating water bath. Each sample was analyzed by ICP-OES for exact Gd(III) concentration. The inverse of the longitudinal relaxation time of each sample ($1/T_1$, s^{-1}) was plotted against Gd(III) concentration (μM) and fit by linear regression (R^2 > 0.99). Relaxivity analyses were performed in triplicate (three samples). Samples vortexed prior to analysis to break up potential aggregation of complexes. 37°C instrument (36 °C water bath). Instrument Parameters: Scans: 4; Recycle Delay: 18.5 s; Gain: 53; Dummy Shots: 0; Detection mode: real; Bandwidth: Broad, 20,000 kHz; Monoexponential Curve Fitting, Phase Cycling. First Pulse Separation: 5 ms; Final Pulse separation: 18,500 ms, Number of data points for fitting: 20; Delay sample window: 0.05 ms; Sampling Window: 0.02 ms; Time for Saturation Curve Display: 6 s.

References

1. Caravan, P. *Chem. Soc. Rev*. **2006**, *35*, 512-523.
2. Pierre, V. C.; Botta, M.; Aime, S.; Raymond, K. N. *Inorg. Chem.* **2006**, *45*, 8355-8364.
3. Datta, A.; Raymond, K. N. *Accts. Chem. Res.* **2009**, *7*, 938-947.
4. Werner, E. J.; Avedano, S.; Botta, M.; Hay, B. P.; Moore, E. G.; Aime, S.; Raymond, K. N. *J. Am. Chem. Soc*. **2007**, *129*, 1870-1871.
5. Doble, D. M. J.; Botta, M.; Wang, J.; Aime, S.; Barge, A.; Raymond, K. N. *J. Am. Chem. Soc.* **2001**, *123*, 10758-10759.
6. Cohen, S. M.; O'Sullivan, B.; Raymond, K. N. *Inorg. Chem.* **2000**, *39*, 4339-4346.
7. Raymond K. N.; Pierre, V. C. *Bioconj. Chem*. **2005**, *16*, 3-8.
8. Mishra, R.; Su, W.; Pohmann, R.; Pfeuffer, J.; Sauer, M. G.; Ugurbil, K.; Engelmann, J. *Bioconj. Chem.* **2009**, *20,* 1860-1868.
9. Pierre, V. C.; Botta, M.; Raymond, K. N. *J. Am. Chem. Soc*. **2006**, *127*, 504-505.
10. Ali, M. M.; Woods, M.; Caravan, P.; Opina, A. C. L.; Spiller, M.; Fettinger, J. C.; Sherry, A. D. *Chem.- Eur. J.* **2008**, *14,* 7250-7258.

11. Weiner, W.C., Konda, S., Shadron, A. Brechbeil, M. Ganswo, O., *Invest. Radiol.*, **1997**, *32*, 748-754
12. Chen, Z, Thorek, D. L. J., Tsourkas, A., *Angew. Chem. Int. Ed*., **2010**, *49*, 346-350
13. Nwea, K., Bernardo, M., Regino, C. A. S., Williams, M., Brechbiel, M. W. *Bioorg Med Chem*, **2010**, *18*, 5925-5931.
14. Bumb, A., Brechbeil, M. W., Choyke, P., *Acta Radiol*, **2010**, *51*, 751-767.
15. Manus, L. M,; Mastarone, D. J.; Waters, E. A.; Zhang, X-Q.; Schultz-Sikma, E. A.; MacRenaris, K. W.; Ho, D.; Meade, T. J. *Nano Lett.* **2010**, *10,* 484-489.
16. Song, Y.; Xu, X.; MacRenaris, K. W.; Zhang, X-Q.; Mirkin, C. A.; Meade, T. J. *Angew. Chem. Intl. Ed.* **2009**, *48,* 9143-9147.
17. van der Poll, D. G.; Kieler-Ferguson, H. M.; Floyd, W. C.; Guillaudeu, S. J.; Jerger, K,; Szoka, F. C.; Fréchet, J. M.J. *Bioconj. Chem.* **2010**, *21,* 764-773.
18. Fox, M. E.; Szoka, F. C.; Fréchet, J. M. J. *Acc Chem Res.* **2009**, *42*, 1141-1151.
19. Lee, C.C.; Gillies, E.R.; Fox, M.E.; Guillaudeu, S.J.; Fréchet, J. M. J.; Dy, E.E.; Szoka, F.C. *Proc. Nat. Acad. Sci.*, **2006**, *103*, 16649-16654.
20. Werner, E. J.; Kozhukh, J.; Botta, M.; Moore, E. G.; Avedano, S.; Aime, S. Raymond, K. N. *Inorg. Chem.* **2009,** *48*, 277-286.
21. Xu, J. Franklin, S. J.; Wisenhunt Jr., D. W.; Raymond, K. N. *J. Am. Chem. Soc.* **1995,** *117,* 7245-7246.

Chapter 6: Targeted Dendrimers for Imaging Applications

Introduction

While dendrimers appear to be promising agents for the binding and delivery of various drugs and imaging agents, these applications still don't utilize their full potential as delivery agents. One primary interest in the improvement of PEGylated dendrimers is the elaboration to include targeting groups, which may aid in the specific accumulation of the carrier in a targeted area, such as a tumor or arterial plaque. This has obvious advantages for disease treatment and imaging, as many drugs are toxic when exposed to healthy tissues, and false positives and negatives are obtained when an imaging agent either accumulates in nontargeted areas or fails to accumulate in the region of interest. As discussed previously, macromolecular carriers have an innate advantage over small molecules for accumulation in well formed tumors due to the well known EPR effect. However, this effect is only noticeably manifested in well formed tumors, and cannot be relied on for delocalized or metathesized tumors. Due to the imperfect nature of this passive targeting mechanism, it would be highly advantageous if the periphery of the carrier displayed a specific targeting molecule capable of actively binding to an area of interest. Two potential candidates for this targeted imaging are tumors and atherosclerotic tissue, as these comprise two of the most difficult current therapeutic challenges.

One popular targeting compound to receive a high degree of attention in the selective delivery to tumors is folic acid (Figure 1), as the folate receptor has been found to be overexpressed in many tumor cell lines.[1]

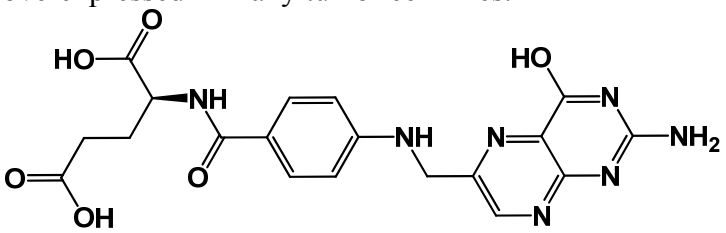

Figure 1. Folic acid, a commonly employed targeting group for chemotherapeutic drug delivery.

However, effective delivery using folate is not entirely straightforward. Folic acid is generally bound to a carrier through one of its carboxylic acids, and some carrier systems, such as the PEGylated dendrimers described above, lack peripheral amines or other nucleophiles that would allow for this conjugation. Furthermore, addition of a large excess of folate to a carrier can bring about adverse effects such as decrease blood circulation times[2] and increased accumulation in the spleen and kidneys[3], possibly due to an increased influence of weak nonspecific binding at high folate concentrations. For these reasons, it's important that the carrier not only be synthetically competent for folate conjugation, but also that the degree of folate coverage be controlled. This requirement may put many carriers lacking specific structures, such as nanoparticles and liposomes, at a disadvantage due to their random distributions of peripheral sites. Depending on the desired structure, however, dendrimers can be synthesized to display specific numbers of targeting groups, allowing elucidation of trends in the numbers and densities of displayed ligands, and thus their optimization. While tumors comprise a primary goal for targeted carrier studies, arterial plaques are also of high interest.

Cardiovascular disease is the leading cause of death worldwide[4], making the development of improved treatment and diagnostic capabilities a high priority. Increased diagnostic

capabilities would not only enable early detection and treatment of these diseases, but also increased understanding of their mechanisms, causes, and preventative measures.[5] One emerging approach to accomplishing this is through the use of natriuretic peptides as targeting groups for imaging agents. These peptides selectively bind to receptors commonly over expressed in arterial plaques, and play a crucial role in regulation of blood pressure and other cardiovascular functions.[6] A recognized portion of one of these peptides, a cyclic pentadecapeptide known as C-ANF (C-type atrial natriuretic factor, Figure 2), is currently under active investigation for the imaging of cardiovascular disease.[7]

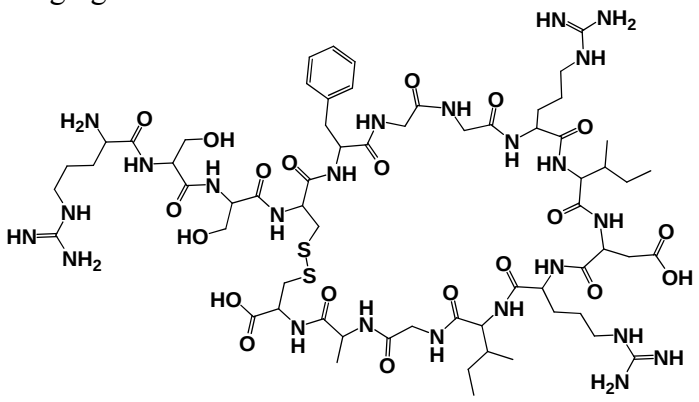

Figure 2. C-ANF targeting peptide for cardiovascular disease.

As apparent from the structure of C-ANF, selective coupling to a carrier without the use of protection chemistry may be challenging. One approach to coupling C-ANF to a dendrimer carrier would be through the use of the copper (I) catalyzed 1,3-dipolar Huisgen cycloaddition (aka, azide-alkyne cycloaddition, the click reaction) to achieve this coupling. However, this would involve selective functionalization of both the carrier and C-ANF to include an azide and an alkyne, which involves additional steps. This reaction also introduces Cu(I) ions, which can be toxic if not completely removed from the reaction. Because introduction of an alkyne usually comes from reacting an amine or acid with pentynoic anhydride or propargyl amine, respectively, it may be more straightforward to use similar amide bond formation to bind a carrier and C-ANF. Like folic acid, it contains two carboxylic acids which may be bound to a carrier through an amide bond. However, one of these acids is crucial for substrate binding[7], and differentiating between these two acids is not apparently possible. Perhaps more importantly, upon activation of an acid one of the nucleophiles present in the peptide could react with these acids before a nucleophile present on a carrier, which would yield C-ANF oligomers rather than targeted carriers. C-ANF contains eight potentially nucleophilic groups: an amine end terminus, three guanidines, two alcohols, and two thiols. However, guanidines are generally protonated *in vivo*, greatly reducing their nucleophilicity, and alcohols made only moderate nucleophilicity. The thiols are bound as a disulfide bridge, which prevents them from undergoing nucleophilic attacks as well, leaving only the amine end of the peptide to act as a potent nucleophile under physiological conditions. A further complication arises from the presence of the two aforementioned carboxylic acids, which necessitates preactivation of a carrier's carboxylic acid to prevent C-ANF oligomerization.

With these requirements in mind, a PEGylated dendrimer capable of targeted delivery can be designed. For a model system, an imaging dendrimer was sought, although introduction of orthogonal chemistries at the core could allow for addition of drug or alternative imaging molecules. We envisioned using this carrier for imaging using Positron Emission Tomography

(PET), which detects the location of origin of an alpha particle emitted by decaying nuclei such as ^{124}I.[8] To incorporate ^{124}I into a carrier structure, phenols are generally used, as their iodination is a synthetically straightforward process. While previous work in our group has incorporated an all ester core[9], and current work predominantly incorporates an ester amide hybrid core (see chapter 2), an all amide core was sought in this case for a more general platform, as it shows greater tolerance to a wider variety of synthetic conditions. In order to bind both nucleophile and electrophile containing targeting groups, dendrimer peripheries containing both acids and amines were sought.

Results and Discussion

Synthesis

Beginning with a second generation polyester dendrimer (Scheme 1, black), phenols were introduced by successive coupling reactions to commercially available N-Boc-O-benzyl ether protected tyrosine (**1**). This iteration of the tyrosine addition was done to double the PET imaging signal obtained from the final PEGylated dendrimer, as preliminary results suggested that eight labeled phenols on a 40 kDa dendrimer may be insufficient for imaging purposes. This yields a dendrimer core (**2**) containing sixteen protected phenols (blue) for radiolabeling and a protected amine for PEGylation.

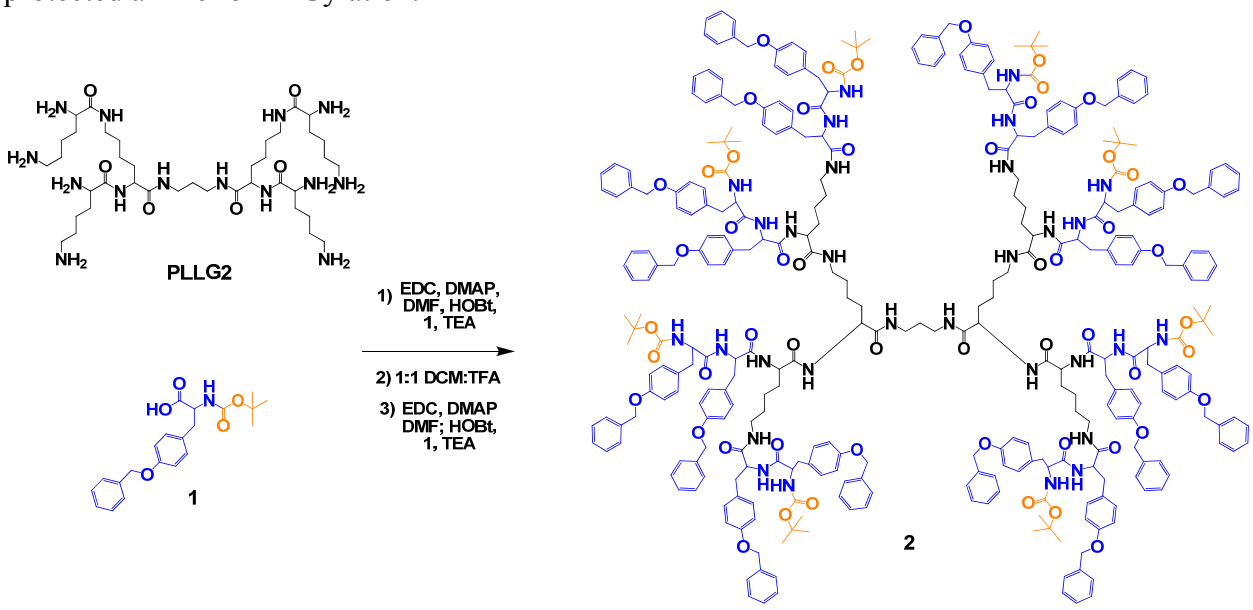

Scheme 1. Synthesis of a polyamide dendrimer containing protected phenols and PEGylation locales.

While dendrimers described here for previous work incorporated monofunctional PEG containing a methyl ether on one end, PEGs employed for imaging purposes must contain synthetically useful moieties on each end. Because the dendrimer core contains an amine, one of these end groups should be an electrophile such as a carboxylic acid. If the targeting group to be attached contains a carboxylic acid for coupling, such as folate, the other PEG end would appropriately contain an amine. However, if the targeting group contains a nucleophile such as an amine, the PEG will ideally end in an electrophile such as an isocyanate or carboxylic acid. Due to the similarities of these coupling reactions, one end group of the PEG must also be

protected. To obtain a suitable PEG, commercial 5 kDa amine and acid functionalized PEG was reacted with di-tert-butyldicarbonate to afford Boc protected PEG carboxylic acid (Scheme 2).

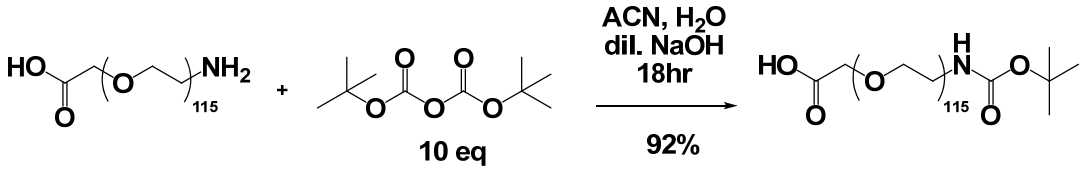

Scheme 2. Protection of bifunctional PEG.

In addition to Boc protection of the PEG amine, the conversion of the carboxylic acid to the methyl ester using trimethylsilyl diazomethane in methanol was also attempted. While the monoprotected PEG obtained in this fashion appeared promising, SEC analysis of acid terminated dendrimers PEGylated with this material were shown to contain high molecular weight shoulders and 10 kDa PEG dimers (Data not shown). It is suspected that the amine terminus of the PEG is capable of addition into the methyl ester to yield these dimers. Due to this drawback, the Boc protected PEG shown in Scheme 2 was used in all syntheses. Reaction of this Boc protected PEG with dendrimer core **2** afforded the protected PEGylated dendrimer **3** (Scheme 3).

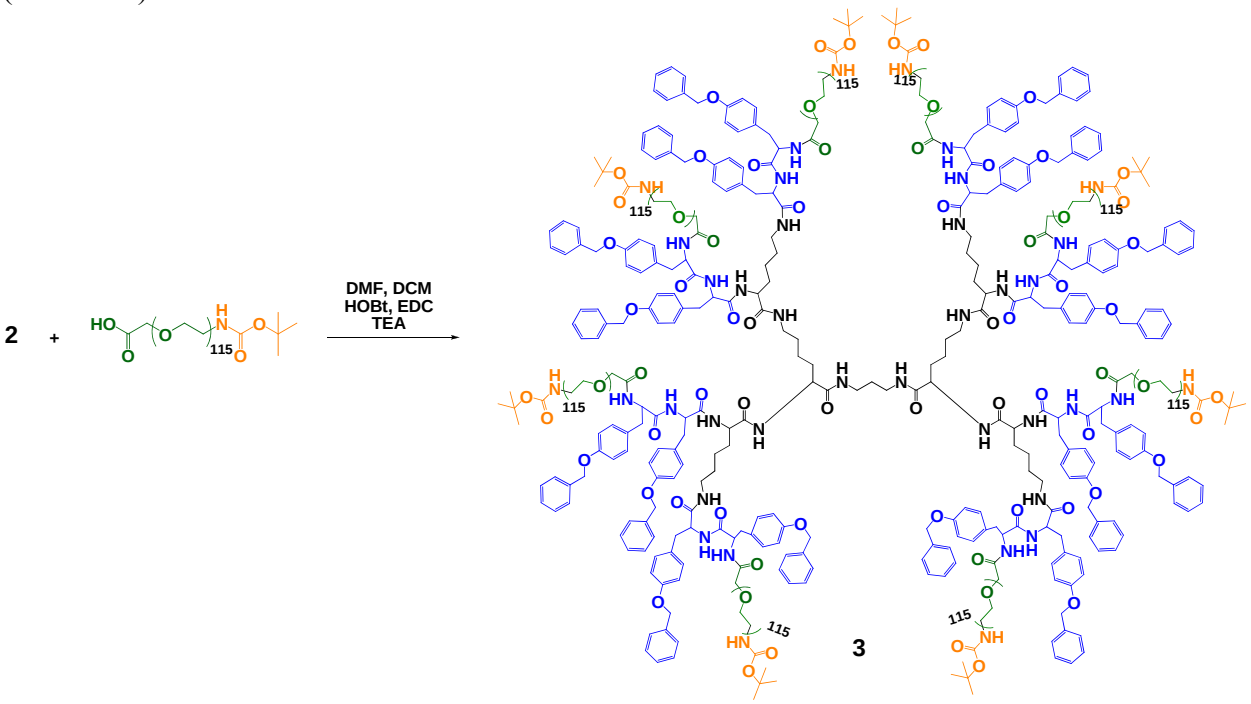

Scheme 3. Synthesis of PEGylated dendrimer **3**, containing protected phenols (blue), 5 kDa PEG chains (green) and a Boc protected amine periphery (orange).

Deprotection of the amines using trifluoroacetic acid affords an amine terminated dendrimer capable of conjugation to electrophile containing targeting groups such as folic acid. For conjugation to nucleophile containing targeting moieties such as C-ANF, this deprotected dendrimer can be further reacted with glycolic anhydride to yield acid functionalized dendrimer **4** (Scheme 4).

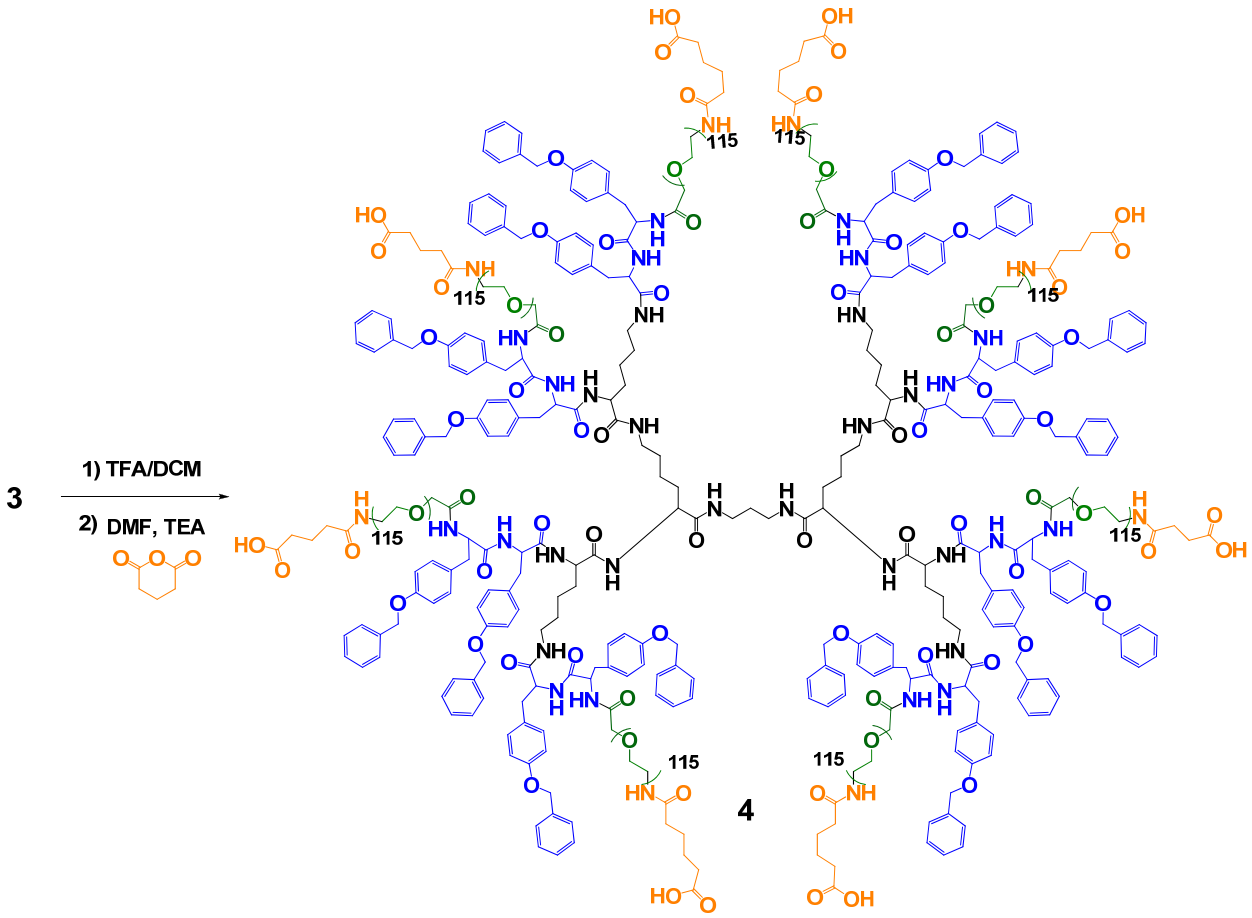

Scheme 4. Synthesis of an acid functionalized dendrimer for conjugation to nucleophile containing targeting groups.

As a proof of concept, dendrimer **4** was bound to a test nucleophile, benzylamine, to show coupling competency. The resulting conjugate contains approximately eight benzylamines attached to each dendrimer by preliminary ^{1}HNMR analysis, suggesting that this platform may serve as a promising targeted carrier for future work.

Despite this optimistic beginning, however, the attempted coupling between C-ANF and this dendrimer proved ineffective. This reaction was attempted using two routes. The first used preactivation of the dendrimer acid using an excess of CDI (1,1-carbonyldiimadzole) to form the acyl imidazole, which was then isolated by precipitation in ether. This activated dendrimer was then combined with 1.1 eq of C-ANF peptide in DMF and TEA. After 24 hours, DMAP was added to accelerate the reaction (It was not added sooner as it also accelerates the side reaction of hydrolysis by residual water in the solvent). HNMR in DMSO –D6 indicated no reaction had occurred. Deprotection of the benzyl ethers using TFA/DCM/Thioanisole/pentamethylbenzene at approximately 1:1:1:.5 overnight yielded a polymer soluble in D2O, but no expected product peaks were observed. Reactions using 1.1 equivalent each of EDC and C-ANF with an excess of HOBt in DMF were similarly unsuccessful. Interestingly, the duplicity of C-ANF's nucleophiles, while an obvious concern, does not appear to be an issue, as this would still result in C-ANF bound somehow to the dendrimer. C-ANF oligomerization also does not appear to be occurring, as C-ANF oligomers would likely not be separated by the precipitation and PD-10 purification methods and would thus be expected to appear in the HNMR spectra were this to be occurring.

It appears to be more of an issue of a slow reaction rate, as the C-ANF and dendrimer are used in 1:1 ratios owing to the valuable nature of the C-ANF, and the reaction must be carried out dilute with respect to the active nucleophile and electrophile in order to solubilized the remainder of the polymers. Furthermore, reactions between two polymers are known to occur slowly due to the low statistical probability of favorable interactions along the reaction coordinate. Finally, the amine terminus of the C-ANF peptide is a relatively weak nucleophile compared to most amines, as it is both secondary, which increases steric effects, and contains a nearby electron withdrawing amide group, which decreases its nucleophilicity.

Conclusion

Due to the complex and hindered nature of the polymers used in this study, conjugation through amide bond formation has proved elusive. Alternatives for favoring a high yielding reaction include simple adjustments such as large excesses of C-ANF or the targeting moiety of choice or incorporation of a superior nucleophile such as a primary alkyl or benzyl amine. Alternative "click" chemistries such as the Huisgen cycloaddition used in Chapter 3 may also be pursued, as the successful monoacylation of C-ANF with the anhydride of pentynoic acid has been observed (Welch group, private communication.), and functionalization of dendrimer PEG end groups with azides is expected to be straightforward.

Experimental Procedures

Materials. Materials were used as obtained from commercial sources unless otherwise noted. Poly(ethylene glycol) was purchased from Laysan Biosciences Inc. Amino acid derivatives were purchased from Bachem. Dimethylformamide (DMF), pyridine, and CH_2Cl_2 for syntheses were purged 1 h with nitrogen and further dried by passing them through commercially available push stills (Glass Contour). Solvents were removed under reduced pressure using a rotary evaporator or by vacuum pump evacuation. The second generation Polylysine dendrimer was published according to literature procedure.[10]

Characterization. NMR spectra were recorded on Bruker AV 300, AVB 400, AVQ 400, DRX 500 or AV 600 MHz instruments. Spectra were recorded in $CDCl_3$, DMSO-D6 or D_2O solutions and were referenced to TMS or the solvent residual peak and taken at ambient temperature. MALDI-TOF MS was performed on a PerSeptive Biosystems Voyager-DE using 2,5-dihyroxybenzoic acid (DHB) as a matrix. Samples were prepared by diluting dendrimer solutions (~1 M) 40-fold in 100 mM matrix solutions in tetrahydrofuran and spotting 0.5 μL on the sample plate. Size exclusion chromatography (SEC) was performed using a Waters 515 pump, a Waters 717 autosampler, a Waters 996 Photodiode Array detector (210-600 nm), and a Waters 2414 differential refractive index (RI) detector. SEC was performed at 1.0 mL/min in a PLgel Mixed B (10 μm) and a PLgel Mixed C (5 μm) column (Polymer Laboratories, both 300 x 7.5 mm), in that order, using DMF with 0.2% LiBr as the mobile phase and linear PEO (4,200-478,000 MW) as the calibration standards. The columns were thermostated at 70 °C.

$PLLG_2((Tyr(Bn))_2Boc)_8$, **2**: Boc deprotected second generation polylysine dendrimer (**1**) (100 mg .48 mMol amine) was added to a 20 mL reaction vial and dissolved in DMF (2 mL). 1-hydoxybenzotriazole (HOBt) (35 mg, 5 eq) and N,N-dimethylaminopyridine (DMAP) (39 mg, 5 eq), and TEA (42 μL, 5 eq), were added and the mixture was stirred to give a homogeneous solution. Boc-O-Benzyl-L-tyrosine (**1**) (217 mg, 1.2 eq per dendrimer amine) was added, followed by 1-Ethyl-3-(3-dimethylaminopropyl)carbodiimide (EDC) (58 g, 5 eq) and the reaction was stirred overnight. After confirming reaction completion by MALDI-Tof analysis,

the reaction solution was diluted with ethyl acetate (150 mL) and washed with 1 M NaOH (5 X 50 mL), 1M HSO_4^- (3 X 50 mL), H_2O (2 X 50 mL) and brine (1 X 50 mL). DMF was occasionally added as needed to maintain solubility. The organic phase was dried over $MgSO_4$, filtered, concentrated to a volume of approximately 10 mL, and precipitated into diethyl ether (150 mL). Isolation of solids by centrifugation gave $PLLG_2((Tyr(Bn)Boc)_8$ (180 mg, 80%) as a white solid. Deprotection of 30 mg (.065 mMol amine) of this dendrimer by 1:1 TFA:DCM (5 mL) followed by iteration of this process gave dendrimer core **2** as a pale yellow solid (53 mg, 84 %). Calc $[M]^+$ ($C_{335}H_{386}N_{30}O_{54}$) *m/z* = 5696.8. Found MALDI-ToF $[M+Na]^+$ *m/z* = 5705. ^1H NMR (500 MHz, DMSO-D6): δ 1.20-1.80 (br m, 124H), 2.78 (m, 14 H) 3.00 (br s, 21H), 3.08 (m, 25H), 4.05 (s, 7H), 4.20 (s, 4H), 4.25 (s, 2H), 4.40 (s, 4H), 4.55 (s, 4 H), 5.00 (s, 32H), 6.85 (br s, 40H), 7.06-7.17 (m, 33 H), 7.35 (m, 82 H), 7.8-8.3 (br m, 21 H).

$PLLG_2((Tyr(Bn))_2PEOBoc)_8$, **3**: Compound **2** (4.45 mg, .01 mMol amine) was deprotected in 1:1 TFA:DCM (1 mL) and reagents were removed *in vacuo*. To the remaining solid was added DMF (.8 mL), TEA (10 μL), HOBt (6 mg) and DMAP (6 mg). To this solution was added N-Boc protected carboxylic acid functionalized 5 kDa PEG (scheme 2) (59 mg, 1.2 eq) in DCM (3 mL). The DCM was then removed by rotary evaporation, and EDC (12 mg) was added. Because Boc functionalized PEG streaks slightly in SEC, the reaction was monitored by DMF SEC until polymer growth was observed to reach a maximum. The reaction was then quenched with acetic anhydride (30 μL) and N,N-dimethylethylene diamine (60 μL) and precipitated in ether (100 mL) and dialyzed in 100,000 MWCO dialysis tubing in water to remove free PEG. Lyophilization gave **3** (40 mg, 67%) as an off-white solid. DMF SEC: 32,000 Da. DPI: 1.18. . ^1H NMR (500 MHz, DMSO-D6): δ 1.20-1.80 (br m, 124H), 3.00 (br s, 12H), 3.08 (m, 25H), 3.40-3.90 (br m, ~3,400H), 4.00-4.40 (br m, ~36H), 5.00 (s, 32H) 6.77 (br s, 8H), 6.85 (br s, 34 H), 7.08 (m, 38 H), 7.35 (m, 82 H), 7.57 (br s, 7 H).

$PLLG_2((Tyr(Bn))_2PEOCOOH)_8$, **4**: Compound **3** (30 mg, .006 mMol) was dissolved in 1:1 TFA:DCM (1 mL) and stirred for two hours. After removal of volatiles, the residual solid was dissolved in acetonitrile (2 mL) and glutaric anhydride (10 mg) and TEA (20 μL) were added. After 24 hours the reaction was precipitated into ether (20 mL). Solids were collected by centrifugation and further purified by PD-10 size exclusion chromatography. After lyophilizing compound **4** (30 mg, 100%) was obtained as a white solid. ^1H NMR (500 MHz, DMSO-D6): δ 1.20-1.74 (br m, 124H), 1.75 (m, 20H), 2.17, (m, 16 H), 2.25 (14H), 3.00 (br s, 12H), 3.08 (m, 25H), 3.40-3.90 (br m, ~3,700H), 4.00-4.40 (br m, ~36H), 5.00 (s, 32H) 6.77 (br s, 8H), 6.85 (br s, 34 H), 7.08 (m, 38 H), 7.35 (m, 82 H), 7.57 (br s, 7 H).

References

1) Leamon, C. P., Reddy, J. A., Folate Targeted Chemotherapy, *Advanced Drug Delivery Reviews*, **2004**, *56,* 1127– 1141.

2) McNeeley, K. M., Annapragada, A., Bellamkonda, R. V. Decreased Circulation Time Offsets Increased Efficacy of PEGylated Nanocarriers Targeting Folate Receptors of Glioma, *Nanotechnology*, **2007**, *18*, 385101-385112.

3) Ohguchi, Y., Kawano, K. , Hattori,Y., Maitani, Y., Selective Delivery of Folate-PEG-linked, Nanoemulsion-loaded Aclacinomycin A to KB Nasopharyngeal Cells and Xenograft: Effect of Chain Length and Amount of Folate-PEG Linker, *Journal of Drug Targeting*, **2008**, *16*, 660-667.

4) World Health Organization. The Top 10 Causes of Death. Available at: http://www.who.int/mediacentre/factsheets/fs310/en/index.html. Accessed November 17, 2010.

5) Sinusas, A, Multimodality Cardiovascular Molecular Imaging: An Overview, *Journal of Nuclear Medicine*, **2010**, *51*, 1S-2S.
6) Levin, E. R., Gardner, D. G., Samson, W., K., Natriuretic Peptides, *New England Journal of Medicine*, **1998**, *339*, 321-328.
7) Liu, Y., Abendschein, D., Woodard, G.E., Raffaella Rossin, R., McCommis, K., Zheng, J., Welch, M. J., Woodard, P. K., Molecular Imaging of Atherosclerotic Plaque with ^{64}Cu-Labeled Natriuretic Peptide and PET, *Journal of Nuclear Medicine*, **2010**, *51*, 85-91.
8) Erdi, Y.E., The use of PET for Radiotherapy, *Current Medical Imaging Reviews*, **2007**, *3*, 3-16.
9) Almutairi, A., Rossin,, R., Shokeen, M., Hagooly, A., Ananth, A., Capoccia, B., Guillaudeu, S., Abendschein, D., Anderson, C. J., Welch, M. J., Fréchet, J. M. J. Biodegradable Dendritic Positron-Emitting Nanoprobes for the Noninvasive Imaging of Angiogenesis, *PNAS*, **2009**, *106*, 685-690.
10) Fox, M. E., Guillaudeu, S., Fréchet, J. M. J., Jerger, K., Macaraeg, N., and Szoka, F. C. Synthesis and In Vivo Antitumor Efficacy of PEGylated Poly(L-lysine) Dendrimer-Camptothecin Conjugates. *Molecular Pharmaceutics*, **2009**, *6*, 1562-1572.